Aalto University
School of Engineering

Sampsa Timo Johannes Ranta

Electrical and mechanical integration of polymer electrolyte membrane fuel cell into electric bus test platform

Thesis submitted for examination for the degree of Master of Science in Technology.

Espoo 12.11.2018
Thesis supervisor: Professor Kari Tammi
Thesis instructor: D.Sc. (Tech) Antti Pohjoranta

Aalto-yliopisto
Insinööritieteiden
korkeakoulu

Aalto-yliopisto, PL 11000, 00076 AALTO
www.aalto.fi

Diplomityön tiivistelmä

Tekijä Sampsa Timo Johannes Ranta		
Työn nimi Electrical and mechanical integration of polymer electrolyte membrane fuel cell into electric bus test platform		
Koulutusohjelma Master's Programme in Mechanical Engineering		
Pää-/sivuaine Konetekniikka	**Koodi** 3001	
Työn valvoja Professori Kari Tammi		
Työn ohjaaja(t) D.Sc. (Tech) Antti Pohjoranta		
Päivämäärä 12.11.2018	**Sivumäärä** 110	**Kieli** Englanti

Tiivistelmä Työ kattaa taustaa ja käytännön työn esittelyn kaupallisen polttokennon integroimiseksi osaks liikkuvaa laboratoriota, VTT Muuli-bussia. Integroitava kokonaisuus sisältää Hydrogenics Inc valmistaman polttokennon, sekä DCDC muuntimen Prisma Ecotechiltä. Käytännön työn tavoitteena on rakentaa itsenäinen siirrettävissä oleva modulaarinen polttokennopohjainen range extender bussiin. Range extenderin on tarkoitus olla ohjattavissa bussin CAN-laiteväylän kautta. Integraatiota lähestytään aluksi teknologian kuvauksella, tämän kattaen teknisiä vaatimuksia sekä laitteen liitäntöjä. Integroinnin osalta kuvataan otettuja askeleita yksittäisten komponenttien käyttöönottotestauksesta aina laitteen testaukseen Muuli-bussissa. Työn tavoitteena on dokumentoida rakennettu laitteisto, sekä laitteistoratkaisun integrointiin liittyvä työ. Osana integrointityötä, jokaiseen kehitysiteraation kuului funktionaalista testausta, jolla laitteen toiminnallisuutta varmistettiin. Integroinnin ja testauksen tulokset esitellään omassa osuudessaan, tässä osuudessa esitellään myös kerättyä mittaustietoa. Mittaustietoa on myös jalostettu niin, että sen avulla työssä pystytään esittelemään laitteen toimintaa graafeina ja siten käyttämään visualisoituja tuloksia polttokennon toiminnan esittelyssä. Työn viimeisessä yhteenveto osuudessa työn tuloksia analysoidaan, sekä esitetään mahdollisuuksia laitteen yhteydessä tehtäville jatkotutkimusaiheille .

Avainsanat PEM polttokenno hybridi linja-auto DCDC muunnin vety CAN

Aalto University
School of Engineering

Aalto University, P.O. BOX 11000, 00076 AALTO
www.aalto.fi

Abstract of master's thesis

Author Sampsa Ranta		
Title of thesis Electrical and mechanical integration of polymer electrolyte membrane fuel cell into electric bus test platform		
Degree programme Master's Programme in Mechanical Engineering		
Major/minor Mechanical Engineering		**Code** 3001
Thesis supervisor Professor Kari Tammi		
Thesis advisor(s) D.Sc. (Tech) Antti Pohjoranta		
Date 12.11.2018	**Number of pages** 110	**Language** English

Abstract This thesis covers background and practical work on electrically and mechanically integrating a commercial fuel cell power module into VTT EMule prototyping bus. The integrated components include power module from Hydrogenics Inc and DCDC converter from Prisma Ecotech. Target apparatus is a reasonably movable modular fuel cell power module based range extender, controllable over the vehicle CAN bus. Literature part of the work provides background on research with focus on defining the environment, terminology and technology behind to understand the experiment. The integration experiment begins with establishing understanding the technology, by its requirements and interfaces. Integration steps are described from commissioning the relevant independent components to integration testing the apparatus in the actual EMule vehicle. Goal of this work is to document the apparatus and work done while integrating it. During the integration, each increment on implementing the range extender functionality was verified by test runs. In results section of this work, the findings and data collected from experiments is processed and visualized as basis of understanding the operations of the hydrogen powered range extender unit. Final discussion overviews and analyses the findings and path towards further research with the apparatus.

Keywords PEM Fuel Cell Hybrid Bus HV DCDC converter hydrogen CAN

Foreword

This master thesis is result of co-operative work at VTT in a project for deployment of hydrogen powered PEM fuel cell range extender on the research bus platform.

The thesis topic is following current trend on alternative powertrain research with heavy vehicles. Fuel cell hybridizing and operating a heavy electrical vehicle on an emission free alternative energy source provides alternative method of extending the bus operating range compared to increasing battery size. The energy to weight factor as well as other characteristics differ with the solution compared to fully electrical battery based vehicle.

This thesis focus is on working towards hybridization of VTT multidimensional energy test platform on wheels, eMULE bus. The eMULE bus is VTT owned prototyping bus, which has the characteristics similar to typical public transportation bus. VTT is engaged on fuel cell technology research and is continuously engaged on developing testing and demonstration platforms. Implementing a modular hydrogen fuel power module based range extender onboard the vehicle can enable practical approach research on the topics related to energy conversion, control strategies and economy related.

The solution demonstrated on this thesis is focusing on commercial PEM fuel cell power module and DCDC converter mechanical and electrical integration, together forming a range extender into the electrical bus. This thus enables the vehicle on having the hydrogen fuel cell hybridization demonstration capabilities. For fuel cell technology, PEM technology based fuel cell is the current de-facto early commercialization solution for in-vehicle operations.

The scope and focus on this master thesis is to document the steps taken towards the solution, including the experimental results gained during the process. The thesis will also give additional literature background on the research field and technology used, while the primary focus remains on the process towards integration.

I would like to thank you VTT, my supervisors, instructor and collegues for the guidance and on the opportunity to join the research team during this work. I would also like to thank Hydrogen on providing support for the project, Czech Technical University of Praque for hosting me as exchange student while writing this thesis, as well as to all the people who contributed by supporting me on the work.

Espoo 12.11.2018

Sampsa Ranta

Sampsa Ranta

Table of contents

Abbreviations

bps	bits per second
CO	carbon monoxide (molecule)
CC	constant current (operating mode)
CV	constant voltage (operating mode)
DI-water	deionized water
DC	direct current
FC	fuel cell
FCPM	fuel cell power module
FCREX	fuel cell range extender
H_2	hydrogen (gas)
ICE	internal combustion engine
kbps	kilobits per second (1000s of bits per second)
PEM	proton exchange membrane (fuel cell technology)
PHEV	A plug-in hybrid electric
SOC	state of charge (for a battery)
Vac	voltage, alternating current
Vdc	voltage, direct current

1 Introduction

This thesis is a result of authors work at VTT towards fuel cell related research and development with-in context of heavy vehicle fuel cell hybridization. Fuel cell technology falls into category of sustainable alternative energy solution. The key benefit of the fuel cell hybridization discussed is the fact it does not emit any harmful emission. A PEM fuel cell uses hydrogen and oxygen as reactants and the process exhaust is water.

The research was carried out at VTT fuel cell research facility at Otaniemi. The practical work is of fuel cell hybridization of VTT on wheels research platform, eMULE. Picture of eMule can be seen in Figure 1.The work effort was put towards enabling use of commercial polymeric electrolyte fuel cell power module (PEM FCPM) as in the bus as range extender, together with the electrical power train. This will enable operating eMule as series fuel cell hybridized vehicle prototyping platform.

Alternative energy solutions are part of ongoing research towards more sustainable energy economy beyond fossil fuels. The hybridized demonstration platform will enable further research on the fundamental technology, as well as working with the actual solutions, solution providers and customers on the field requiring the expertise.

This thesis will first cover the literature to support as background for the terminology used. And as experimental part, actual mechanical and electrical build of range extender into reasonably transporable frame that can be deployed into eMule. In analysis part, the data collected during integration is processed and further analyzed, this also provides illustration on the apparatus control and behavior.

Figure 1. eMULE test platform in the assembly hall for testing. The access ramp is providing a path to hydrogen tanks on top of the vehicle.

1.1 Goal of the work

For this master thesis, the topic was chosen per the practical research work of the author, to provide added value for the work by means of scientific writing and documentation. The background and mechanical and electrical solutions towards hybridization of eMule are covered in this master thesis.

In the next section, the background for the eMule, hybridization and related technologies are discussed with goal of introducing the terminology and principles for the following work. The actual work towards hybridization and integrating the apparatus are explain in section 3, the experiment. The experiment part level of detail goal both to preserve documentation for the apparatus, as well to duplicate the experiment. Section 4 discusses the results and findings during the experiments, and the tools pipeline to process the results is also given. Final conclusions and future work ideas are in section 5.

In short, the goal for this thesis is to provide a coherent package of understanding the background of the work, together with how and why the eMule electrical and mechanical integration took place. As for the results part, the control and behavior are discussed to understand operations of the resulting range extender apparatus as mechatronic device.

Last but not least, the thesis goal is to demonstrate professional and safe engineering practice in the field of mechatronics within given research environment.

1.2 Scope of the work

The scope of this work is to work towards fuel cell hybridization of eMule. This includes explaining the background and the actual implemention of the PEM fuel cell power module and DC/DC converter together as fuel cell range extender. The fuel cell range extender is to be considered a subsystem in the vehicle and thus needs to be interconnected with eMule vehicle. Due, the establishing electrical interconnect towards eMule control and electrical powertrain is also within the scope of this work.

Per this work, the fuel cell power module and DC/DC converter used are considered as commercially available mechatronics devices to be integrated. Thus technologies behind are introduced with level of details relevant to the reader in order to understand the terminology used within work. The internal details of integrated technologies are not the focus of the work. The overall research field related to electrical powertrain, fuel cells, fuel cell hybridization of a vehicle and relevant technologies is broad.

The practical work focus is on the electrical and hybridized bus technology as experiment in the specific case. The work does not attempt to generalize the solution discussed, the focus on this thesis is on the sole specific solution.

1.3 Motivation for work

Working at VTT fuel cells allowed a rare opportunity to take part in interdisciplinary research on fuel cell hybridization of a bus. Regardless the approach and focus taken in this work does not highlight the full extents of the technology factors involved, contribution of the several technological

trends could be observed. Such trends include for example research and commercial fuel cell technology, hydrogen economy, electrical and hybrid automotive powertrains.

For VTT, EMule is a full size electrical bus test vehicle “test mule”, a prototyping and research platform. EMule incorporates technologies related to research of electric bus technologies. The eMule provides testing capabilities for partners and customers as well as internal demand. The implementation of fuel cell hybridization is driven by customer demand. The fuel cell hybridization will further enable the vehicle to be used as case example on research in the technology trends mentioned before. The technology solutions follow the industry trends, PEM fuel cells are the industry standard de-facto generation commercial solution on fuel cell of the day.

Motivation for thesis author towards the topic is to extend the understanding of power conversion and control over hydrogen powered alternative energy system. Author had prior experience over CAN communications, as well as, for power conversion and alternative energy solutions mainly on solar panels. Joining the research on hybridizing the eMule presents example of mechatronic environment with interesting but challenging aspects. For example, the fuel cell component selected for fuel cell range extender is quite powerful and run with flammable gas. The fuel cell power module enable output power rating high enough to drive 4 average sauna stoves, and the device was to be operated from high pressure hydrogen supply. Within the job description, the given experimental goals presented unique opportunity to work on interesting piece of hardware configuration and gain firsthand experience on current state of the hydrogen economy.

2 Background

The background section provides technology introduction and literature research part in this thesis. The section introduces the established concepts and terminology. The experimental section following this section bases on the background laid out.

The work is towards electrical and fuel cell hybrid buses. The eMule electrical bus is the platform for integration and this provides ground for some of the requirements. For example, the power requirements follow a suburb last mile bus route providing feed traffic backbone route such as metro. Such requirements would change if the bus route characteristics were different.

Fuel cell and DC/DC converter technologies are in main focus of the experiment, as the mechanical and electrical integration mainly concerns these technologies. Further, the CAN bus and VCU are introduced is the communications bus and control point in the automotive concept.

This background section backs on literature references covering the relevant fields and technologies more in depth.

2.1 Trend on electrification of automobile powertrains

The solutions based on these electrical automotive powertrains have recently made a commercial breakthrough and are becoming more popular. The electrical powertrain in vehicle also enables improving goals on improving efficiency and thus reducing emission. This is when compared to traditional powertrains operated directly by internal combustion engine. Electrical powertrain can work standalone on batteries, or it can be used as hybrid solution.

In the electrical powertrains, an electrical propulsion system is used to generate the torque needed to drive wheels. The electrical motor can be used both to generate torque for driving, as well as, to convert the kinetic energy back to electrical when braking. The process of converting kinetic energy back to electrical is known as regenerative braking. The electrical motor can also provide good torque over range of rotational speeds enabling realization of simplified design, as for example transmission with gear shift is not necessarily needed. Figure 2 shows typical configuration of vehicle with a series hybrid electrical powertrain, the arrows present the energy flow directions. The figure highlights range extender generator, which only supports energy flow in one direction. Electrical storage can further support bidirectional energy flows, and thus allows aforementioned regenerated braking energy to be recovered.

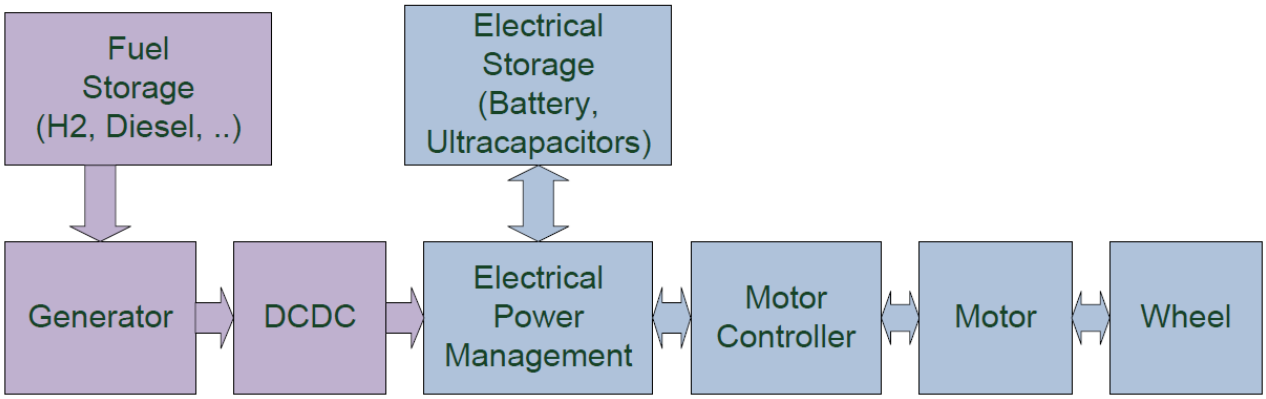

Figure 2. Typical main components in vehicle with series hybrid electric powertrain

With hybrid solutions, the electrical powertrain allows decoupling of generator from the torque required by drivetrain. A series hybrid solution uses energy storage together in series with the generator. Decoupling of the generator allows more flexibility on the generator usage, thus allow optimizing the requirements and operating conditions for improved efficiency. For example, the electrical storage can compensate for transient power demands, while the generator can be driven at constant operating point at its optimal range. This can be used improve solution overall efficiency, thus reducing emissions and reducing operating cost.

For terminology, plain hybrid powertrain solution term typically refers to configuration of electrical powertrain, battery and internal combustion engine. Fuel cell hybrid solution refers to electrical powertrain solution with configuration of fuel cell and battery. Figure 3 highlights the operating principles of fuel cell, battery and internal combustion engine technologies.

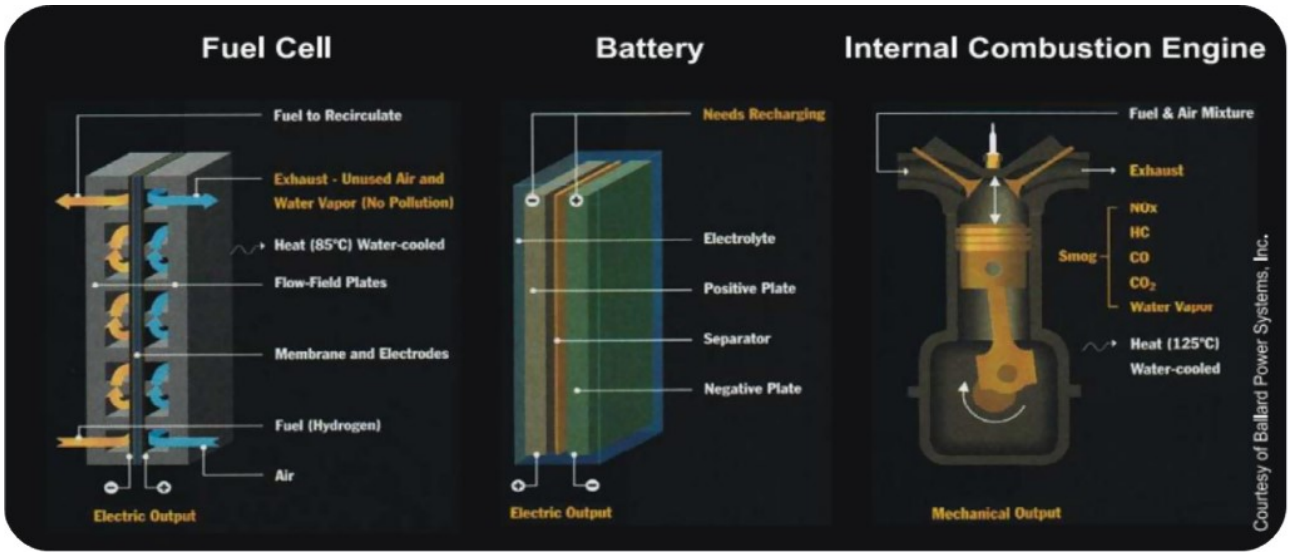

Figure 3.Structure of FC, battery and ICE [1]

2.2 Alternative energy hydrogen-hybrid/FC-hybrid powertrains

Hydrogen based fuel cell solutions fall under sustainable alternative energy solutions and are such solutions are also referenced together with hydrogen economy terminology. In hydrogen economy, hydrogen is used as fuel. Hydrogen based fuel cells are used together with electrical powertrain and this is called fuel cell powertrain or hydrogen hybrid powertrain. Main advantage over fuel cell hybrid solution to internal combustion engine-based hybrid solution is the emission free operations as exhaust is plain water. [2]

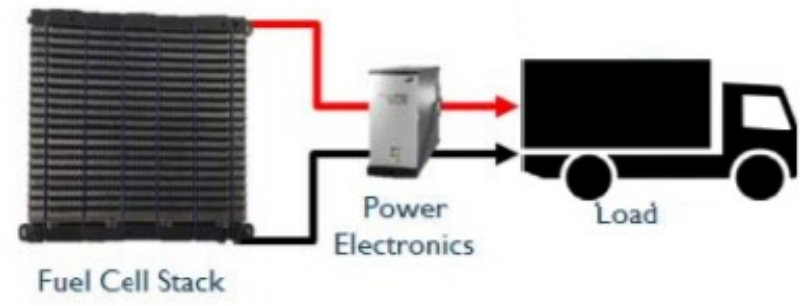	Fuel Cell Powertrain (Non hybrid)
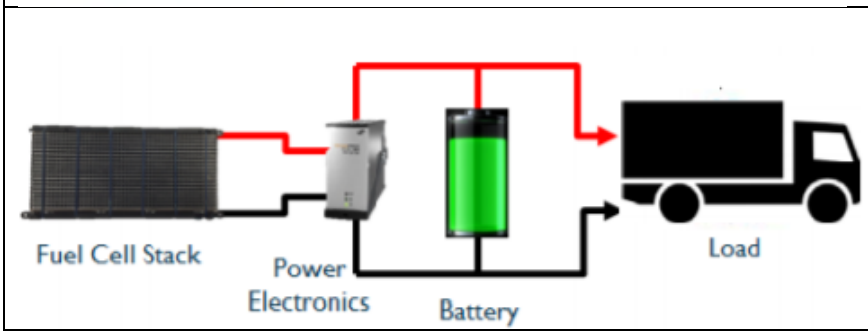	Hybrid Fuel Cell Powertrain (Series Hybrid)

Table 1. Fuel cell and series hybrid fuel cell vehicle [3]

A fuel cell can be used as standalone configuration to feed the powertrain. However, fuel cell systems have typical disadvantages on cost, slow response and no regenerative energy recovery option during braking. [4] Thus, actual solutions are often realized as fuel cell series hybrid powertrains, having a configuration with energy storage such as battery in series as buffering electrical energy storage. The difference on series hybrid fuel cell powertrain solution versus fuel cell power train solution is illustrated in Table 1. The hydrogen hybrid series powertrain solutions in literature are divided to soft and hard hybrid solutions. In the hard hybrid solution, the solution is designed so that the energy storage, such as battery, is considered very small buffer and the fuel cell mostly meets the energy requirements of the vehicle. On soft hybrid solution, the energy storage is considered to store more energy and will manage the higher transient power demand, for example during acceleration. To generalize, with series hybrid solutions, the vehicle power requirements can be decoupled from the power output requirements of the fuel cell.

The fuel cell hybridization point of interest to using different modes of generators and energy storages is related to the economical performance and operational features. Such as characteristics of the energy storages, including costs, expected life cycle, weights and related emissions. Range and charging time are key features when operating fleet of vehicles. [5]

For hydrogen operated vehicles, the storage tank technologies also contribute to the total vehicle economics, gasoline used by ICE engine is as liquid well suited for traditional tank, but hydrogen storage requires more careful consideration. For hydrogen operations, the hydrogen tank increases weight and volume of the solution. Hydrogen tank solutions are illustrated per weight to volume ratio in Figure 4. [2] In the experimental part of this work, the solution is high-pressure hydrogen gas tank with pressure is up to 200bar, equivalent to 20MPa.

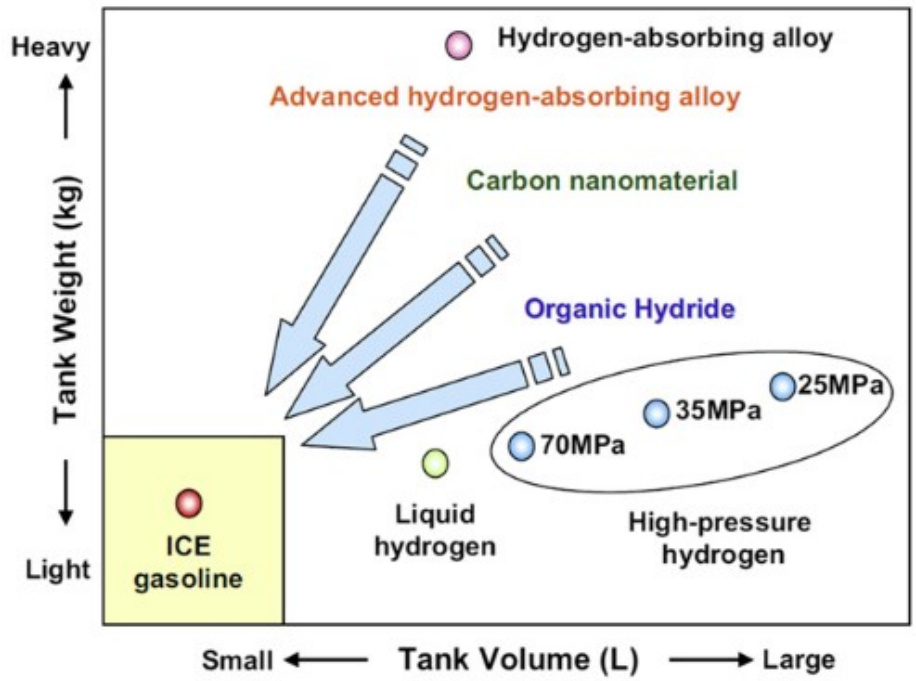

Figure 4. Hydrogen storage tank solutions by weight and volume ratio [2]

This work focus is on fuel cell series hybrid solution. Benefits for the series hybrid solution come in solutions with following conditions, [6]

- the system load is cyclic
- the system load includes many transient conditions
- the system includes many auxiliary devices using power

The literature also uses term primary energy source, this refers to the actual source of energy. This is important when the overall environmental effect is evaluated. For example, the battery can be charged by wind energy, and the source of hydrogen used can be natural gas. Hydrogen and electricity used can be considered intermediate products used for power storage and transmission.

2.3 Electric and fuel cell hybrid electric buses

Using latest advanced battery technologies, the battery solutions as energy storage allows storing and releasing the energy to the storage and the good response to dynamic changes of the power requirements are good in when driving. Yet, battery solutions are still heavy by weight to stored energy ratio. Also the charging speed is related to electrochemical reaction speed, and can be considered an limiting factor together with the weight ratio.

For fuel cell based solution, the characteristics are different. For hydrogen based fuel cell solution, the cylinder contains pressurized hydrogen and the ratio of weight to energy on the fuel is less when compared to weight/energy ratio of battery solutions available. The PEM fuel cell power module used as base of this work does not allow bi-directional energy conversion process, and cannot for example recover the braking energy.

In order to refill the hydrogen storage on bus, the hydrogen cylinder needs to be refilled or replacement, and this process can be related more as similar process to refilling fossil fuel gas tank. In general, the gas transfer is more related to piping and mass transfer process than as electrochemical process. As follows, the rate of refill can be rapid compared to battery solution, as well as the hydrogen fuel tank can designed following similar principles as fossil fuel tanks.

The PEM FC hybrid solution in public transportation bus platform is a realistic approach on enabling pilot cases for hydrogen enabled solutions. This allows the mass transport companies to take active role on addressing concern on the environment and driving the industry providing the solutions. The hydrogen powered solution also requires hydrogen distribution infrastructure to support the fleet operations. Public transport centralized depots can be used to enable controlled test ground for the hydrogen enabled solutions. The infrastructure concerned would cover for example the solutions required to refill the vehicle hydrogen storage. For typical public transport bus operations, the internal combustion engine solution can be operated so, the gasoline tank only needs to filled once per day. If the fuel cell hybrid bus could similarly also drive the day on single charge / fuel cycle, this would support the current fleet operations model.

A typical end mile bus drive discussed in this thesis has a driving cycle in suburban, consisting of low average speed and many braking cycles. Thus, the advantage of series hybrid solution improves the energy efficiency by being able to reuse the kinetic energy recovered on regenerative braking. Also sizing the fuel cell to full peak power requirement would also present more significant cost factor on the fuel cell technology. In series hybrid solution, the fuel cell solution can be optimized for the average consumption while battery manages the transient demand. The research and actual data gathered from test vehicles allows further research on optimizing the combination of the battery and fuel cell solutions.

2.4 VTT eMule test and research platform

The VTT eMule, a test mule prototyping platform discussed here is an established test and research prototyping platform with system configuration similar to public transport vehicles. The eMule can be used to study multiple aspects on public transport vehicle configuration. eMule provides prototyping and testing services to meet internal, partner and customer demands.

The eMule is also used as part of larger concept of electric city bus and infrastructure demonstration environment in Finland. [7] For example, to provide basic reference drive, there also exists an established bus route that is used as reference route for comparison. City line 11 is typically used as reference driving line for eMule when evaluating the performance, the route can be seen in Figure 5. Within the research community, similar established routes can also be found in other major cities that are used for reference comparison as these provide characteristics distinct to the city and route. Such routes provide ground for understanding the feasibility and study on different environments.

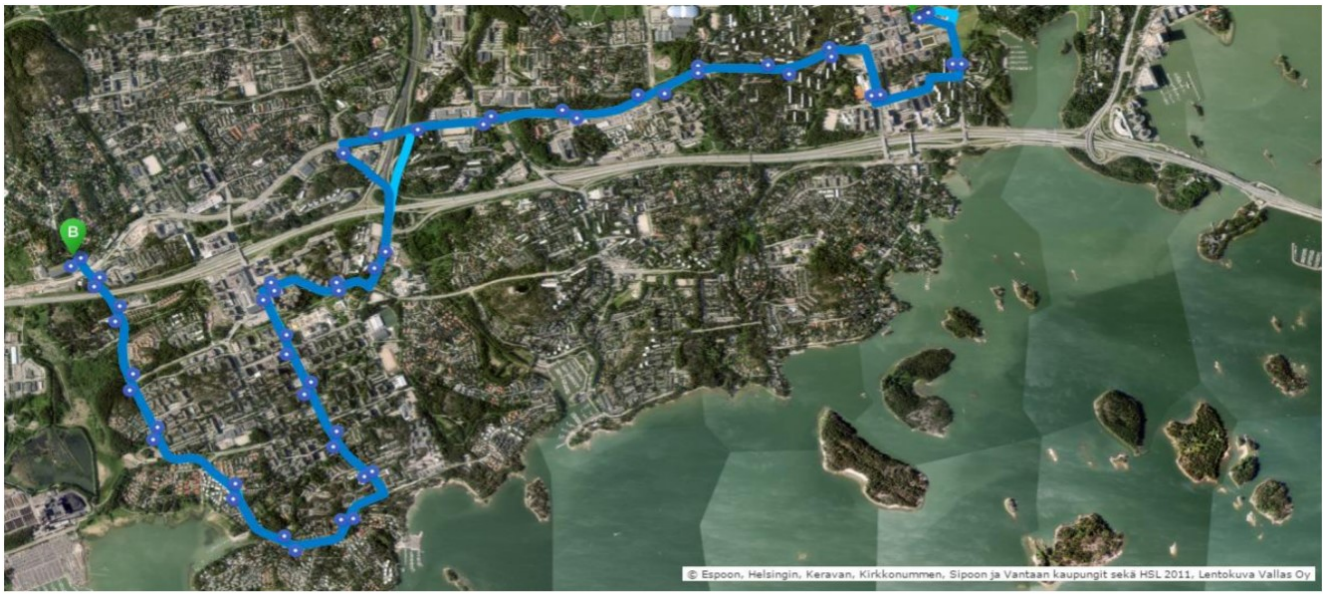

Figure 5. Map plot of Line 11. [7]

The eMule bus has previously provided the base platform for other auxiliary devices used for research, such as internal combustion engine based range extender and pantograph device for rapid charging the battery from grid. The data collected from previous research also provides as reference valuable data that can be compared when new solutions are evaluated. The prototype bus is used for both for VTT internal research as well as for customers and partners demand.

The base platform to be fuel cell hybridized, is thus an electrical bus with electrical propulsion system. The battery bank is typically used the main energy source powering the locomotion. The fuel cell technology hybridization is introduced to the bus as independent modular auxiliary testing device, that can be used to extend the energy availability beyond the capacity of battery bank energy storage, and thus increase operating range of the vehicle.

2.4.1 eMule electrical power system

The eMule platform configuration on electrical power systems and power trains are visualized in Figure 6. eMule vehicle power systems considered are high voltage DC bus (HV DC BUS) and auxiliary 24V battery system. For the range extender integration perspective, both power systems are relevant, as 24Vdc is used to provide system power for range extender components. As well as the vehicle common ground is tied to 24Vdc negative potential.

The eMule HV battery configuration is illustrated in Table 2. The battery is based on LTO lithium battery technology. The eMule integrates two existing options for the battery charging, onboard 3 phase grid charger and pantograph interface on roof used to interface rapid charging station. The LTO batteries onboard can accept up to 5C charge current, this translates into charge current up to 450A, with nominal voltage of 590V, this would translate to charging with power of P=U*I=590V*450A=265,5kW. Actual voltage and power might vary.

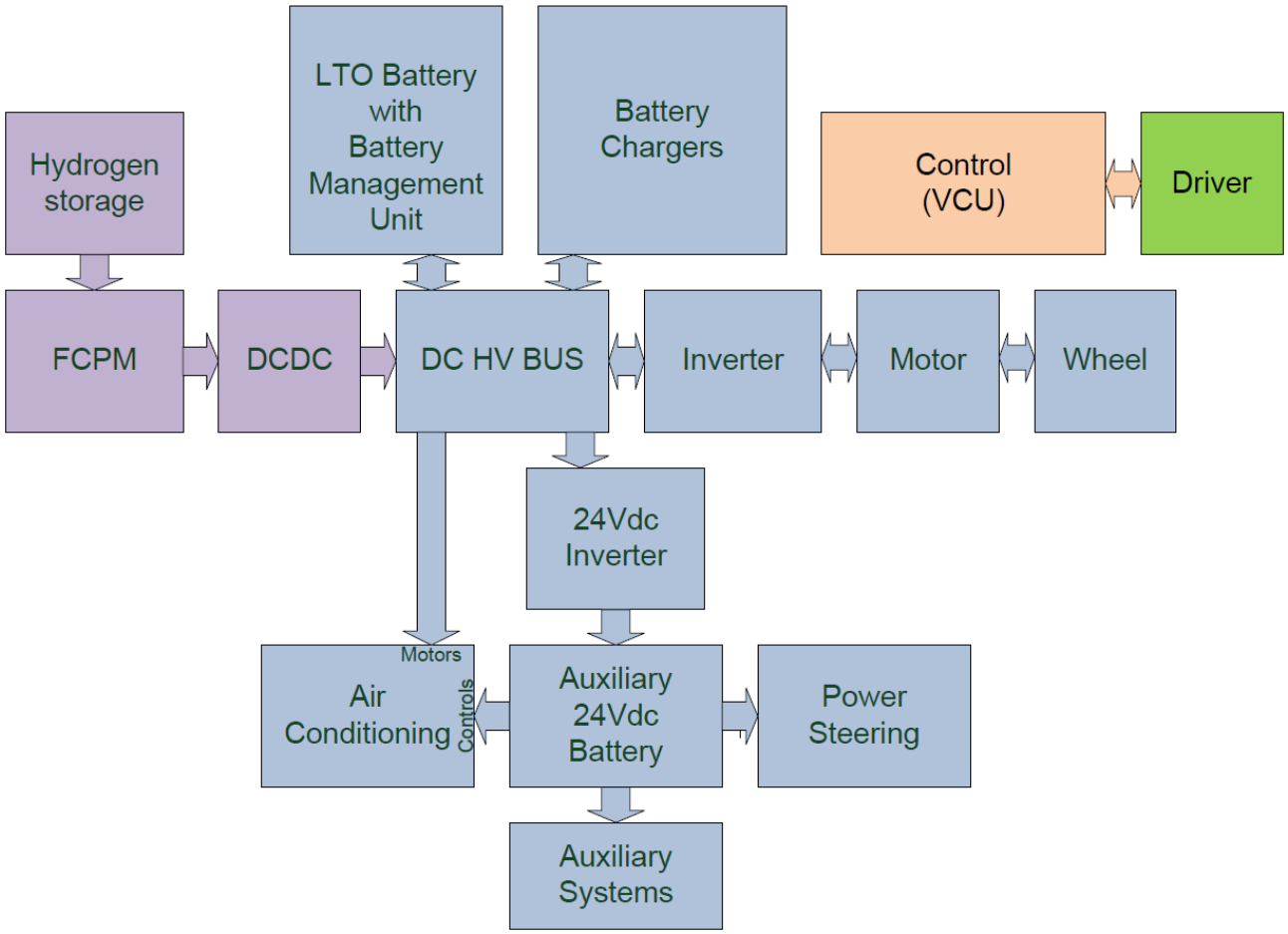

Figure 6. eMule power systems and powertrain main components

Battery technology	LTO
Energy store	53kWh / 90Ah
Nominal voltage	590V
Weight	1500kg
Battery configuration	32 water cooled modules in 6 separate enclosures

Table 2. eMule HV battery configuration

In Figure 7 is picture of the eMule DC HV BUS, the high voltage interconnect rail, this consists of copper plate power distribution plates that are interconnected with high voltage isolation relays. Positive and negative potential both have separate power rails, and the rail consists of three separate sections. Outermost sections are called DRIVEBUS, and these are used to connect the power inverters to the bus. The middle section is BATTERYBUS, this is the section connected to the battery terminals through main switch. The center section is CHARGEBUS, this is used for connecting the battery chargers. The actual devices are connected through fuses. The configuration seen in figure already includes connection towards FCPM range extender.

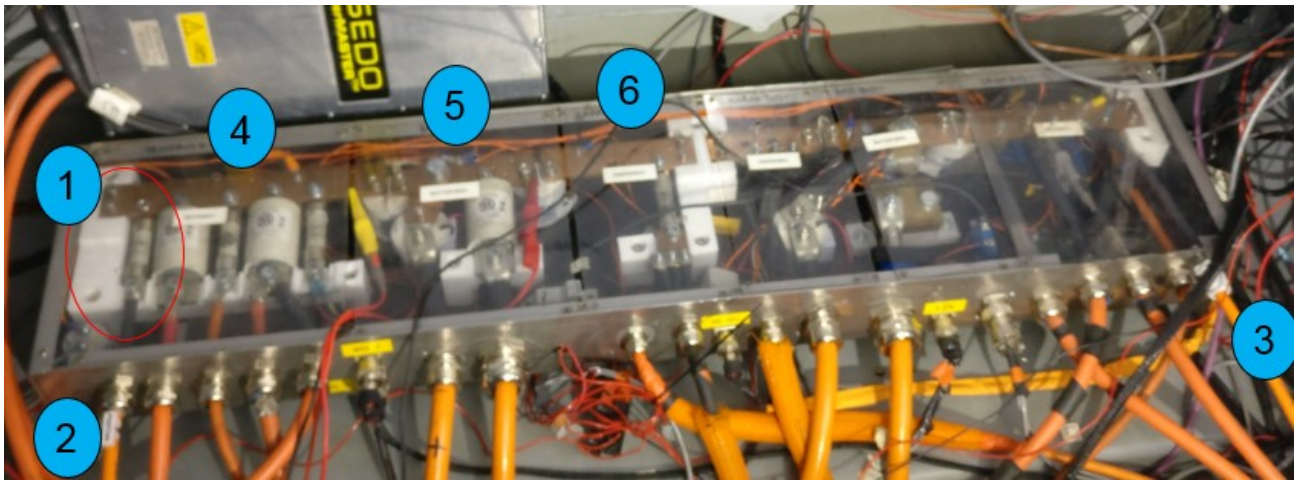

Figure 7. DC interconnection bus bar, with contactors, fuses. Right side is for negative and left side is for positive bus voltage interconnect. Numbered items, 1. 50A fuse for connection towards DC/DC converter 2. Positive voltage cable towards FCPM range extender 3. Negative cable towards FCPM range extender 4. DRIVEBUS 5. BATTERY BUS 7. CHARGEBUS

2.4.2 eMule power consumption

As for eMule, previous established research literature also provides understanding of energy requirements on route. For the reference line 11, average vehicle speed and in-service energy consumption can be seen in Figure 8. Previous research also has characterized the power usage from the point where the platforms batteries are charged from grid to the actual consumption or loss, so the energy usage and distribution is already charted and understood. The battery energy distribution is presented in Figure 9. As the average energy consumption over time is established, it was also used as design criteria for the components used in this work. The average energy consumption of eMule vehicle on line 11 is shown in Figure 9.

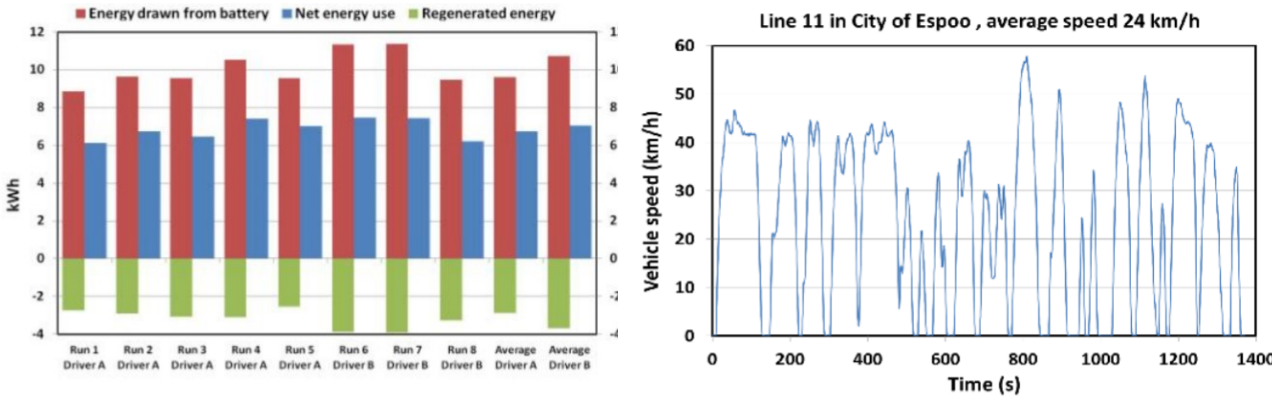

Figure 8. Average vehicle speed and in service electric energy consumption of test bus running on Line 11. [7]

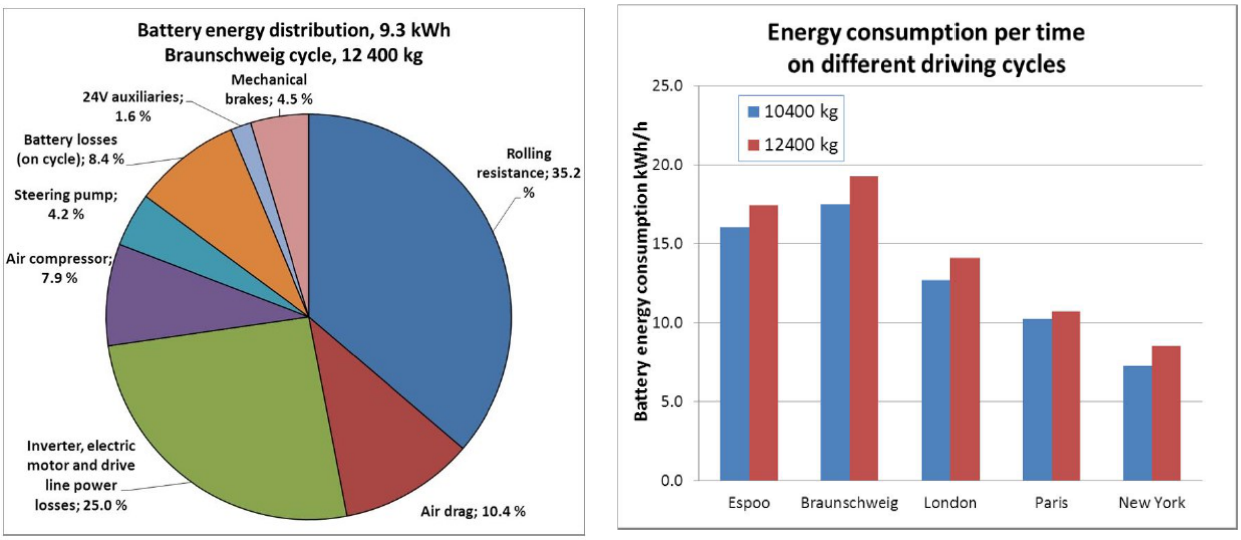

Figure 9. eMule battery energy distribution and bus energy consumption over time [8]

2.5 Fuel Cells

Fuel cell is an electrochemical device that transforms the energy contained by fuel directly into electrical energy without intermediate steps. This energy conversion process is more direct than compared to typical method of internal combustion engine, which is heat engines where the energy is first transformed into heat before mechanical energy.

Fuel cell research is interdisciplinary science, including fields of electrochemistry, thermodynamics, engineering economics and electrical engineering. Fuel cell solutions exists with different approaches, some technologies include reconditioning stages enabling use of different fuel sources where the hydrogen is extracted from. In this thesis, the polymer electrolyte membrane (PEM) is introduced, as fuel cell power module introduced and integrated later in the work is based on this technology.

2.5.1 PEM Fuel Cell (PEMFC)

A PEM fuel cell operating principle is illustrated in Figure 10. In the center is electrolyte membrane. The electrolyte membrane separates the electrodes, the anode and the cathode. The fuel cell inputs are hydrogen and oxygen, and the products are electricity, heat and water. For electricity, the output voltage V_{FC} (voltage towards load) of single fuel cell depends of the actual membrane solution and material, as well as the operating conditions. Theoretical output voltage of single fuel cell is 1.2, but under load closer to 0.7V. [9]

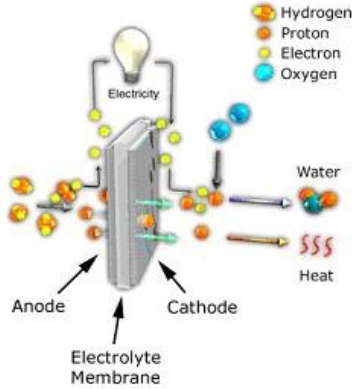

Figure 10. PEM fuel cell operating principle [9]

The characteristics of this fuel cell technology are such, that it works in low temperature, provides high efficiency and high performance in wide working conditions. PEM fuel cells utilize hydrogen as fuel and oxygen from air as oxidizer. The reaction outlets are water, heat and electric energy. Operating temperature of PEM fuel cell is limited between freezing and boiling of water since the electrolyte membrane needs humification for the process. Typical operating temperature below 80º.

Basic equations for hydrogen oxidation are, [10]

$$H_2 \rightarrow 2H^+ + 2e^- \quad (1)$$

$$\frac{1}{2}O_2 + 2H^+ + 2e^- \rightarrow H_2O \quad (2)$$

Total overall reaction of actual PEM fuel cell reaction realizes such that the reaction produces water, electricity and heat:

$$\frac{1}{2}O_2 + H_2 \rightarrow H_2O + \mathrm{W_{ele}} + Q_{heat} \quad (3)$$

As the process primary product is water and the process does not generate other particles, there are no harmful emissions generated. Lack of emissions are particularly important issue compared for example internal combustion engines. The proton exchange membrane fuel cell power module introduced is a commercially available technology, and current de facto technology solution for portable applications. The fuel cell process is well suited for in-vehicle applications.

In PEM FC operations, the excess by-products, water and heat must be managed in such way the isothermal conditions for optimal operations are maintained as well as the moisture rate of the electrolyte is optimal. Due to this, the heat and water management are important key areas of stable fuel cell operations. [10]

2.5.2 PEM Fuel Cell stack (PEMFC stack)

For practical applications, the output power and voltage levels of single fuel cell are low. Scaling up a single fuel cell is possible, but might not be feasible. Many of the actual losses in fuel cell energy equation are in function of current, and as power is defined as function of voltage times current, thus increasing the power would require higher current or voltage. Increasing the current would also increase the losses as increased current will also cause negative impact on voltage.

Typical approach to scale up the power is to stack more cells into series, and in this configuration the stack voltage is sum of the cells in stack. Typical fuel cell stack consists of multiple layers of fuel cells, together with channels for fluids and gasses, as well with the electrical series connections of the membranes. Typical stack also has end plates that include the connection ports into the system. Principal of the stack is illustrated in Figure 11.

$$V_{stack} = \sum_{1}^{n} V_{FC_x} \quad (4)$$

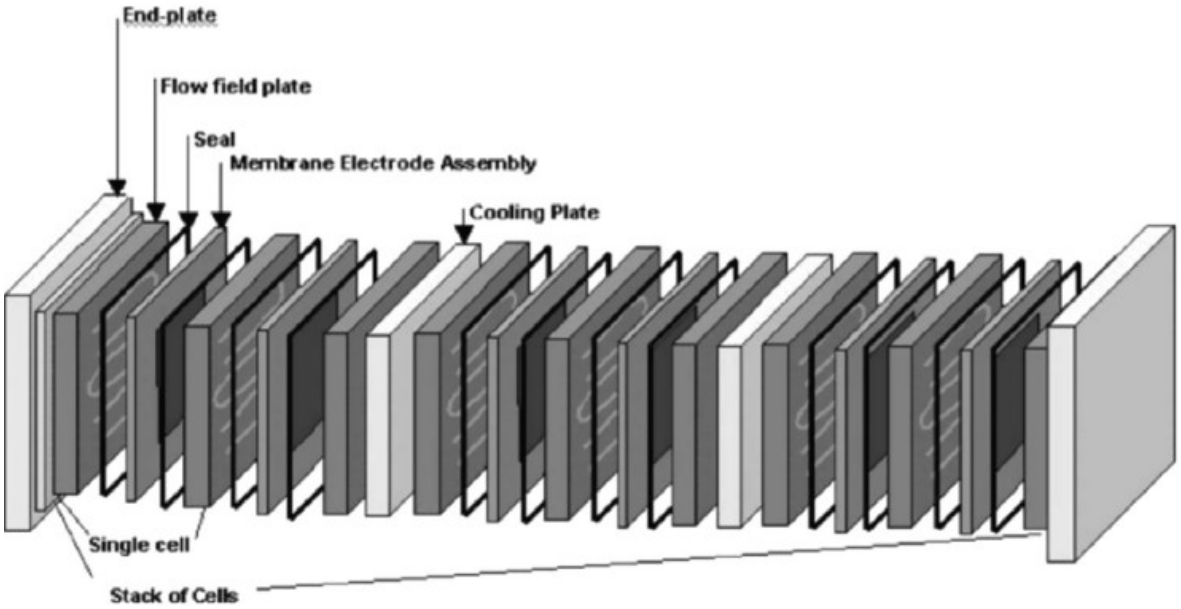

Figure 11. Stack of fuel cells [1]

2.5.3 Hydrogenics PEM Fuel Cell Power Module (PEM FCPM)

The PEM Fuel Cell Power Module (FCPM) concept introduced here is a commercial fuel cell solution from Hydronics Inc. The concept consists of fuel cell stack solution with integral balance of plant solution. The FCPM solution provides fuel cell technology as proven integration ready bundle. Such solution is focused as an easy approach into PEM fuel cell technology for parties interested enabling fuel cell solution powered solutions, such as integrators, fleet owners and OEMs.

The FCPM concept is a part of Hydrogenics Inc commercial fuel cell value chain products. Figure 12 illustrates the vendor products portfolio on fuel cell technologies. The figure also highlights the features of the solution.The figure illustrates a single PEM fuel cell is the basic building block of which the FCPM consists of, integrated with required auxiliary components and control. The portfolio also includes futher refined solution that includes energy storage such as hydrogen tank and cooling solutions as a kit.

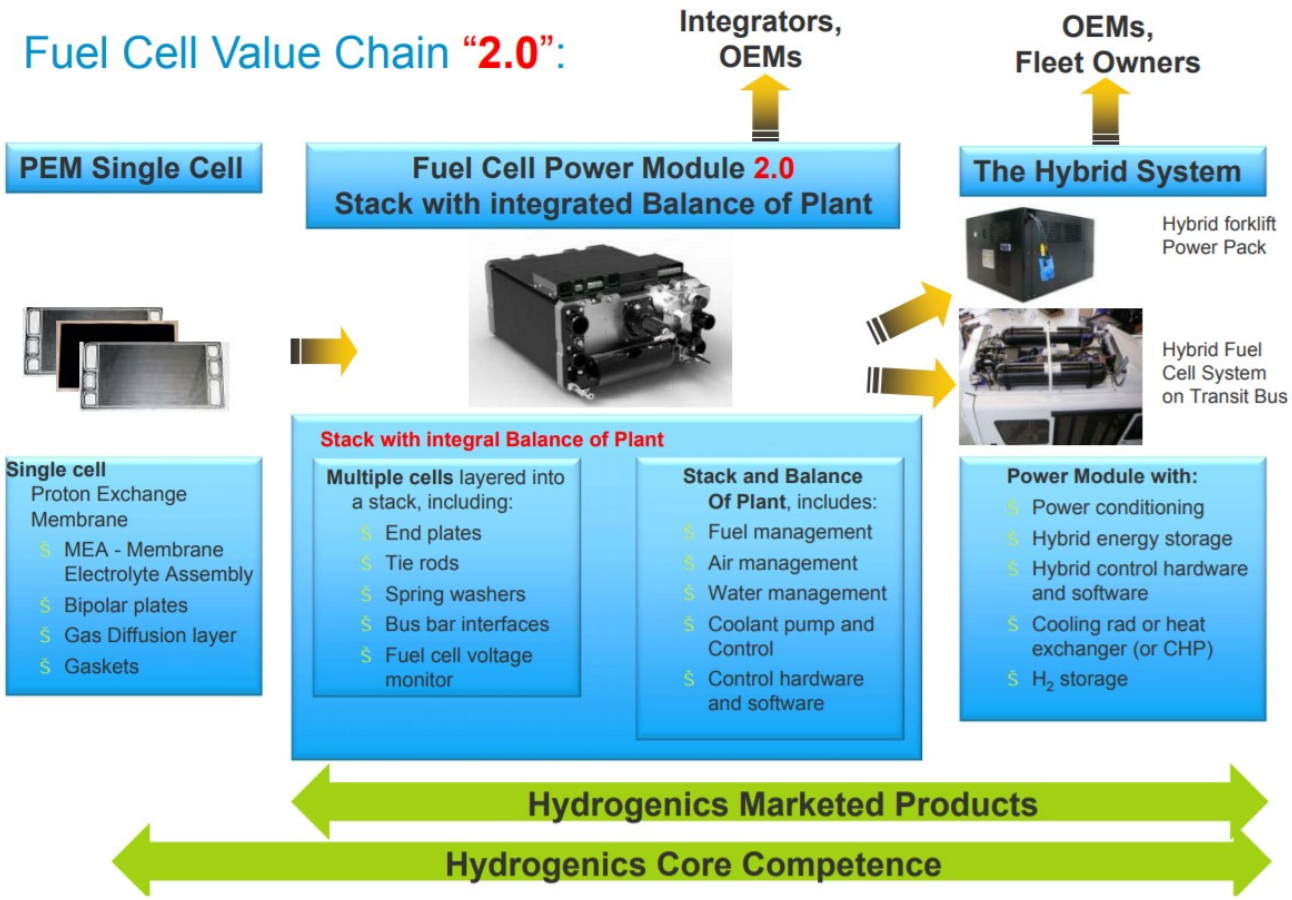

Figure 12. Hydrogenics Fuel Cell Power Module 2.0 solution. [11]

The fuel cell power module used in this thesis presents the latest generation of the PEM HyPM power module products provided by Hydronics Inc. During the development cycle of the FCPM product, number of major components has reduced. Also other functional improvements have been made to enable more straightforward integration, for example the fuel cell operations no more require external water supply for humidification. Recent in house development history of the HyPM power module is illustrated in Figure 13.

The features of FCPM used in this thesis include liquid cooled, system has onboard controls and diagnostics, the system has rapid start-up and dynamic response, unlimited start-stop cycling, the system is robust, rugged and reliable, and no water is required for humidification. Also according to the material provided by Hydrogenics Inc, the FCPM manufacturer can provide basis for system safety certification related matters. Such safety certifications would be required to show the final product to confirms the requirements meeting the criteria for UL and CE product approvals and safety certifications.

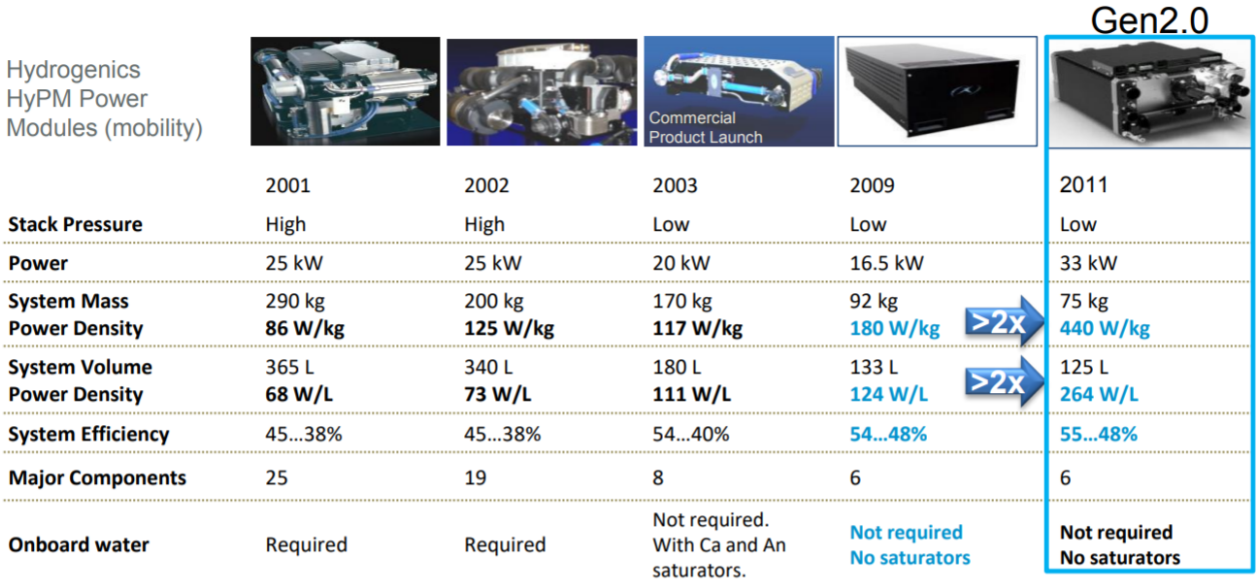

	2001	2002	2003	2009	2011
Stack Pressure	High	High	Low	Low	Low
Power	25 kW	25 kW	20 kW	16.5 kW	33 kW
System Mass **Power Density**	290 kg **86 W/kg**	200 kg **125 W/kg**	170 kg **117 W/kg**	92 kg 180 W/kg	75 kg 440 W/kg
System Volume **Power Density**	365 L **68 W/L**	340 L **73 W/L**	180 L **111 W/L**	133 L 124 W/L	125 L 264 W/L
System Efficiency	45...38%	45...38%	54...40%	54...48%	55...48%
Major Components	25	19	8	6	6
Onboard water	Required	Required	Not required. With Ca and An saturators.	Not required No saturators	**Not required** **No saturators**

Figure 13. Hydrogenics fuel cell development history regarding the FCPM [12]

2.6 DC/DC converter

A DC/DC converter here is introduced as an concept, as it is used to match the electrical output of FCPM into the voltage and current levels required by the bus. In addition, it provides a control method over the power transfer. In other words, a DCDC converter provides as power electronics to boost the voltage from the FCPM power output into level required to feed the vehicle HV DC bus bar. The voltage level on the HV DC bus varies when the bus is operated, as well as the power requirement is not constant. The output voltage level of FCPM is directly tied to the fuel cell stack output and confirms to the electro-chemical process within the PEM FCPM. The DC/DC converter discussed provides means to control the characteristics of the electrical power coupling.

In this work, the focus is given to the DC/DC converter technology aspects related to the application in hand. Following the solution components, an isolated full bridge switching boost circuit is introduced as high level concept. Isolated circuit means galvanic isolation of the voltage rails, there is no common ground between the input and load of the DCDC voltage rails. Following the isolation nature, a single wire would between input and output rails, would not cause current flow between, as the potentials are isolated..

The DCDC converter topology is discussed also, as the FCPM requirements state there should be reverse-current protection diode in case the fuel cell load can feed current back to FCPM. If needed, reverse protection diode should be installed as can be seen per Figure 14. The topology operating principle of the the DCDC type used is described in next section.

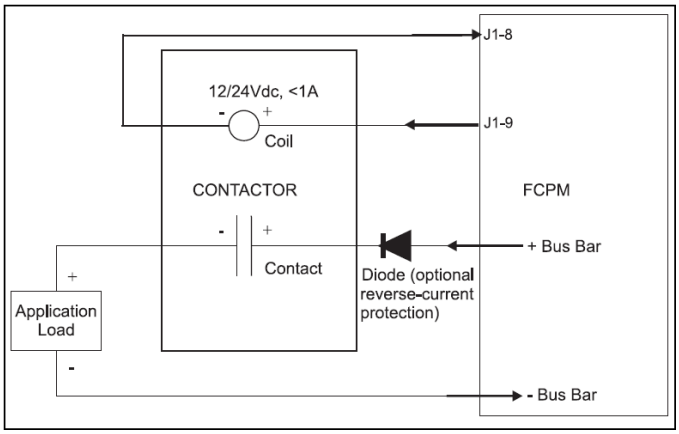

Figure 14. FCPM application load installation per FCPM operations manual [13]

2.6.1 Isolated full bridge DC-DC converter

Isolated full bridge DC-DC converter explained consists of input side and output side, isolated by transformer. The transformer provides galvanic isolation between the two sides, thus the input side and output side do not share common ground and are floating. [14]

The components of full bridge DC-DC converter are shown in Figure 15. The transistors, T1-T4 provide means to alternate the current towards the transformer, as alternating current is used to energize the transformer. The transformer can also provide gain by different winding ratios on primary and secondary side. On the secondary side, there is a diode bridge rectifier, choke and capacitor that rectify the alternating current back to direct current. [14]

The DC-DC internally drives the switches in full bridge in phase shifted mode, driving the full bridge in four steps. Two switches on left or right side cannot be forwarding current same time as this would short circuit the input power rails, thus there must be a gap between the two forwarding states. The frequency of switching can be variable or fixed, depending on the actual DC-DC converter implementation. Duty cycle between the current forwarding and not forwarding states depend on how much energy is to be transferred during the cycle.

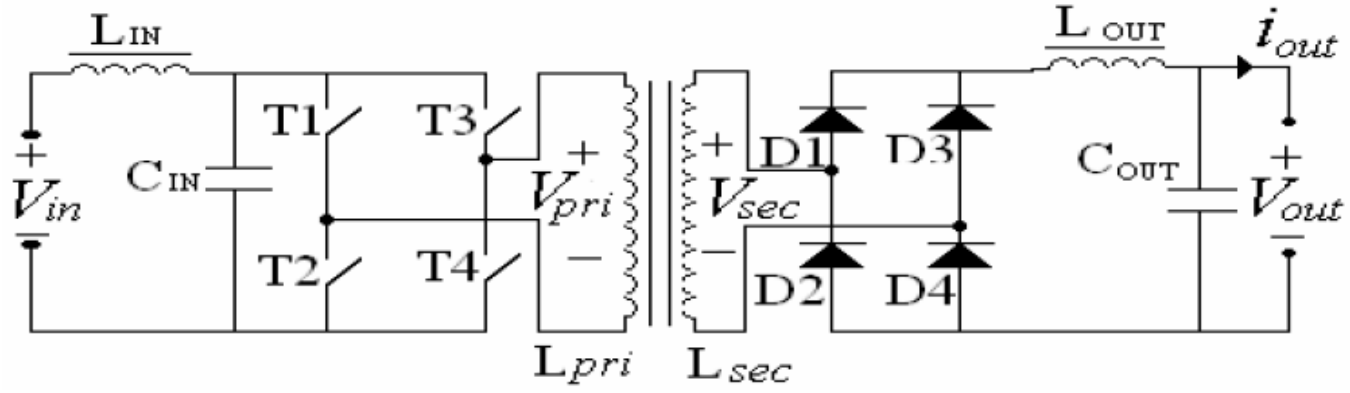

Figure 15. Full bridge DC-DC converter component layout [14]

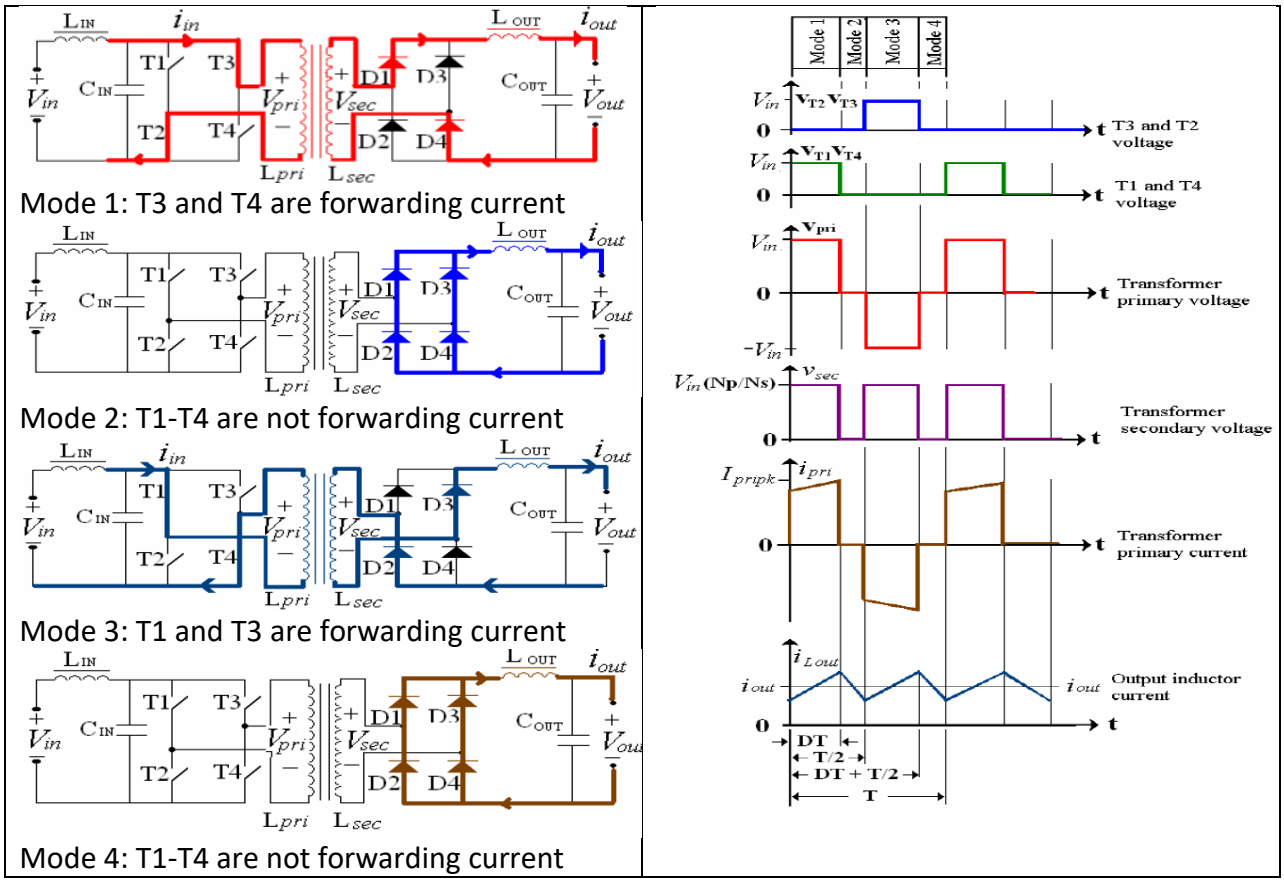

Figure 16. DC/DC converter phase shifted PWM mode operations [14]

2.7 CAN bus

A Control Area Network bus (CAN) is a message based communication protocol, commonly used in automotive communication purposes. The CAN development started during 1983, and as current the CAN bus specification has been standardized and widely adopted into automotive industry. The specification is separated two to parts, one defining the communications protocol on Data Link Layer, this is standardized into ISO 11898-1. Underneath this, the Data Link Layer defines the physical media layer, this is standardized into ISO 11898-2,3. [15]

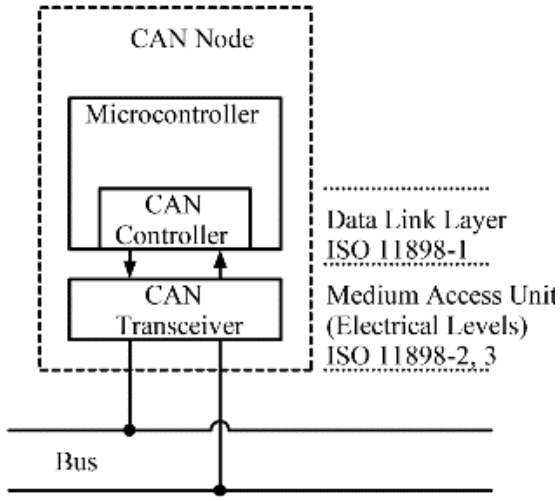

Figure 17. CAN Data Link Layer and Medium Access Unit [15]

While the CAN bus standards cover different solutions and realizations of the communications bus, the focus in this thesis is given to the communications methods relevant to this work. CAN bus discussed in this work focuses ISO 11898-2 high-speed CAN, with CAN 2.0A standard 11 bit identifier implementation, as the solution discussed use this for communications.

In practice, CAN high speed bus is based on two wires providing differential communication channel. The wires are typically named, CANL and CANL. The bus is per definition a linear bus, but in practice, a typical realization has stubs and the network can represent more star than linear bus. The bus is terminated by 120 Ω resistors in both ends of the bus. High speed CAN bus is illustrated in Figure 18.

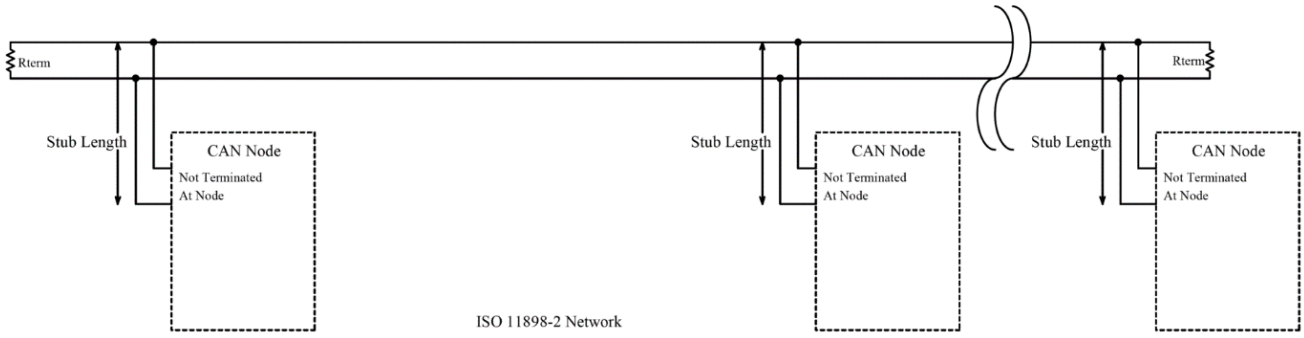

Figure 18. High speed CAN network bus topology [15]

The CAN bus is multi-master serial bus, that connects the the nodes on the communication bus. Two or more nodes are required to operate the bus. On CAN bus, each node can send and receive, but only one node can send message at time. In case more than one node are trying to send at same time, the arbitration process happens during the transmission as defined by the protocol.

2.7.1 CAN bus standard frame with 11 bit identifier

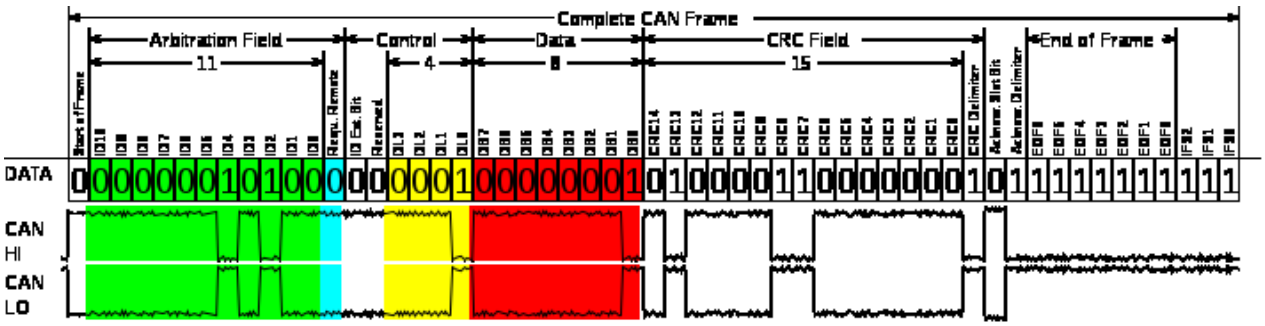

Figure 19. CAN base frame format [15]

For CAN bus communications, messages are sent to bus by nodes. The communications protocol uses message frame to encapsulate the information. The standard frame consists of start of frame bit, arbitration field, control, data, CRC Field, Acknowledge slot, Acknowledge delimiter and End of Frame as seen in Figure 19. The figure shows message of 1 byte length, the actual data length can vary from 0 to 8 bytes.

The CAN bus arbitration field contains the message identifier and remote transmission request. After the arbitration field, control field follows. The remote frames are not used in this work, and due not discussed. For standard message, the identifier extension bit is logical 0. This is used for extended frame format, which is another frame type out of the scope of this thesis. Next in the frame is data length code (DLC) that indicates 0-8 of data bytes to be transmitted. For the data fields, the actual data signals can be sent packed in the available 0-64 data bits (padded to 0-8 bytes). The CRC field uses cyclic redundant check algorithm to provide checksum to provide means to validate the integrity of transmission. CRC delimiter must be recessive bit (1) by CAN specification. The acknowledge slot (ACK) is used by receiver nodes to indicate successfully received message. The sender sends recessive bit and any node receiving valid frame will send dominant bit. If sender detects no dominant bit, the message must be resent. After acknowledge bit, acknowledge delimiter follows, this is always recessive bit (1). After this is sent end of frame signaling, which indicates the transmission is complete, and the CAN media is free for next transmission.

For the data transmission, all CAN nodes involved to communication in progress must be able to operate in same nominal bit rate or rates. Due to hardware implantations are non-ideal and conditions may vary, the actual bit rate may deviate some. CAN nodes synchronize the transceivers during the arbitration. Thus, CAN bus has built-in mechanism to enable the nodes to maintain synchronization.

The fields in CAN message also serve different purposes. The arbitration field is used for synchronization and arbitration on the shared media. During the arbitration part, dominant sender is selected. The dominant bus sender is the node able to send it's message through the shared media. Selection of dominant sender happens during the arbitration, as only one message can be sent at a time. The CAN nodes trying to send a message take actively part on the arbitration process to select dominant sender.

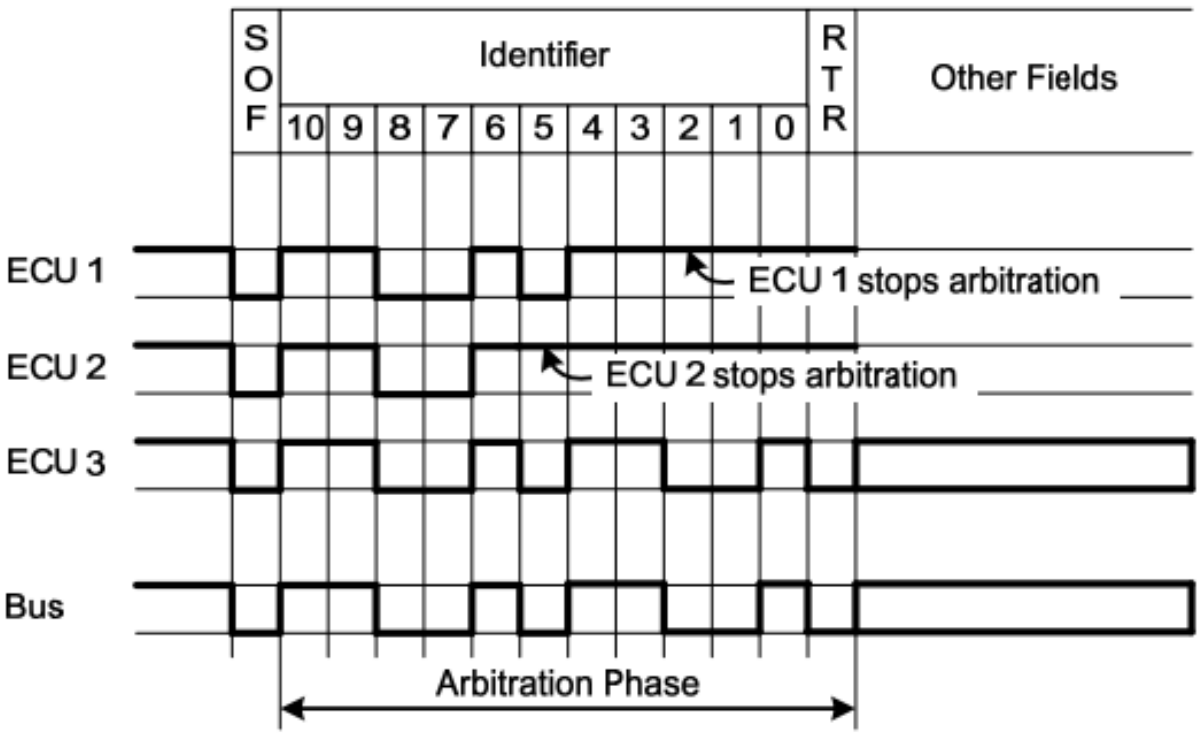

Figure 20. CAN arbitration process [16]

For the arbitration process, this is illustrated in Figure 20. Nodes with message in send queue start sending the message and the dominant sender continues sending it's whole message. In the figure, ECU 3 continues to send as it has dominant bit over ECU 1 in identifier bit 2. ECU2 loses the arbitration with collision on bit 5. For the CAN terminology, the logical 0 bit is considered dominant bit, logical 1 is considered recessive bit. If another node is sending dominant bit over node having recessive bit, collision happens for the recessive sender and dominant sender continues sending. The node sending message with dominant identifier has thus higher priority on the shared media and the recessive sender must attempt to re-transmit after the bus is free again. The message identifier defines a message type and must be an unique identifier on each CAN bus. If this is not met, the arbitration could happen after arbitration field during rest of the message, and this would violate the CAN specification.

2.8 Vehicle Control Unit

The systems of eMule platform presented in this thesis are controlled by a vehicle control unit, VCU. The VCU in eMule runs VTT in-house vehicle control code, that controls the in vehicle systems. For example the throttle is controlled by wire, the actual electrical motor is driven by inverter. Tho, the vehicle is not fully drive-by-wire, for example steering in the eMule at time of writing is implemented by mechanical linkage, however augmented with power steering.

The control algorithms for VCU are designed on Matlab/Simulink environment and the model is code generated and made to run on real time embedded computer. The model running on computer thus implements the control functionality on the eMule. The VCU implements control for the systems over two high-speed CAN busses and via additional digital input and output channels. The CAN busses in eMule run at different speeds, one at 500kbps, other at 250kbps. This is due not all equipment implement the CAN with same speed.

The actual eMule VCU is Electrobit EB 6120 vehicle control unit. The Electrobit EB61x0 series technical data are shown in Figure 21. The EB6120 has additional 4 GB Flash memory and additional connector for debugger and more input/output functionality. [17]

Technical Data

- ▶ High-performance Freescale Microcontroller MPC5200B with 400MHz
- ▶ 2 x 10 Mbit/s FlexRay (TJA1080 or RS485)
- ▶ 2 x high-speed CAN (ISO 11898-2)
- ▶ 1 x fault-tolerant CAN (ISO 1189-3)
- ▶ 1 x LIN
- ▶ 4 x analog input channels: 10 kHz sample rate, 12 Bit resolution, 0 to 20 V
- ▶ 16 configurable digital input or output channels
- ▶ PC connections via Ethernet, USB 2.0 or RS232
- ▶ Altera FPGA Cyclone EP2C70 with 256KB SRAM
- ▶ Supply voltage: 6,5 V to 30 V
- ▶ Robust automotive housing
  - • Measurements 150 x 100 x 25 mm
  - • Protection category IP65
  - • Guaranteed ambient temperature range: -30° C to +70° C
- ▶ Reliable high-quality ODU connectors
- ▶ Low power consumption (~5 W)

Figure 21. eMule VCU, EB 61x0 series technical data [17]

3 The experiment - PEM FCPM integration

This experimental part will describe the work committed towards eMule fuel cell range extender mechanical and electrical integration work made during summer 2017, as part of the authors contract with VTT as master thesis worker.

The project initial condition was such that the Prima Ecotech DCI 12A2 DCDC converter was available, previous generation Hydrogenics HyPM 16kW FCPM module that was mounted to bus, but not operational. The DCDC converter and previous generation Hydrogenics FCPM had been previously used in research. For the VTT project this thesis is based on, a next generation Hydrogenics HyPM HD16 module had been ordered from vendor, and was later available for this experiment when arrived.

The FCPM related power requirements were determined before the author started, based on the average consumption of the eMule on bus route 11. The range extender component power ratings follow the average consumption. The components, DCDC converter and FCPM to be used components were outlined by the project description for the author.

The project plan was to integrate the FCPM and DC/DC converter as modular range extender instrument subsystem for the eMule. The mechanical solution needed a reasonable transportable frame. For the total integrated solution, the mechanical and electrical functionality had to be tested and verified. Cooling and hydrogen fuel supply systems had to be arranged with a way or another to support the testing.

The work towards hybridization of the VTT eMule bus platform was divided into and executed in several smaller increments as milestones. Each milestone is to establish and verify a step forward but with small step introducing only a small number of new variables per test. The project major test milestones are highlighted in Table 3, the following sections will describe the experiment setup, and later work covers results section analyzing the outcomes of relevant experiments.

Main components to integrate within the scope of this work were PEM technology based Hydrogics second generation HyPM HD16 fuel cell module and electrical Prisma Ecotech DCI 12A2 DC/DC boost converter. The fuel cell module provides the energy conversion from hydrogen gas form into electric. While the DC/DC converter boosts the 40-80Vdc voltage level from fuel cell module to up to 700Vdc voltage level used by in HV BUS BAR, and thus the eMule powertrain.

Project Test Milestone
DC/DC converter recommissioning test
PEM FCPM CAN electrical interface test
PEM FCPM commissioning test
PEM FCPM integration test with DC/DC converter
Range extender integration test in bus

Table 3. Project major test milestones

3.1 Hydrogenics HyPM HD16 fuel cell power module

Hydrogenics HyPM HD16 FCPM used in this thesis is a 16kW PEM fuel cell power module from commercial fuel cell vendor, Hydrogenics. The fuel cell used in this work presents 2nd generation module of the HyPM HD16 series.

Previous generation device was also tested and evaluated previously at VTT and the device was available for the author to as an reference implementation. The previous generation platform was previously evaluated in past together between VTT and Aalto Topdrive project. The previous generation system was not operational during the work related to this thesis.

As comparison, the 2nd generation HyPM HD16 module upgrades are such as, more integrated control logic and more clear separation between logic and power distribution. Figure 22 shows the FCPM subsystem controlled devices. The HyPM HD16 fuel cell power module concept includes the components within HyPM boundary, while the inputs and outputs shown outside the boundary need to managed externally. The fuel cell module components are shown Figure 23, and main integrated components of the fuel cell module can be seen, such as recirculation pump, integrated pressure vessel, control valves and regulators. The additional system components required are forced air blower assembly including air filter and air flow meter, as well as coolant circulation with water pump. On top of this, there is load contactors. The integrated components structure is further explained in Figure 24.

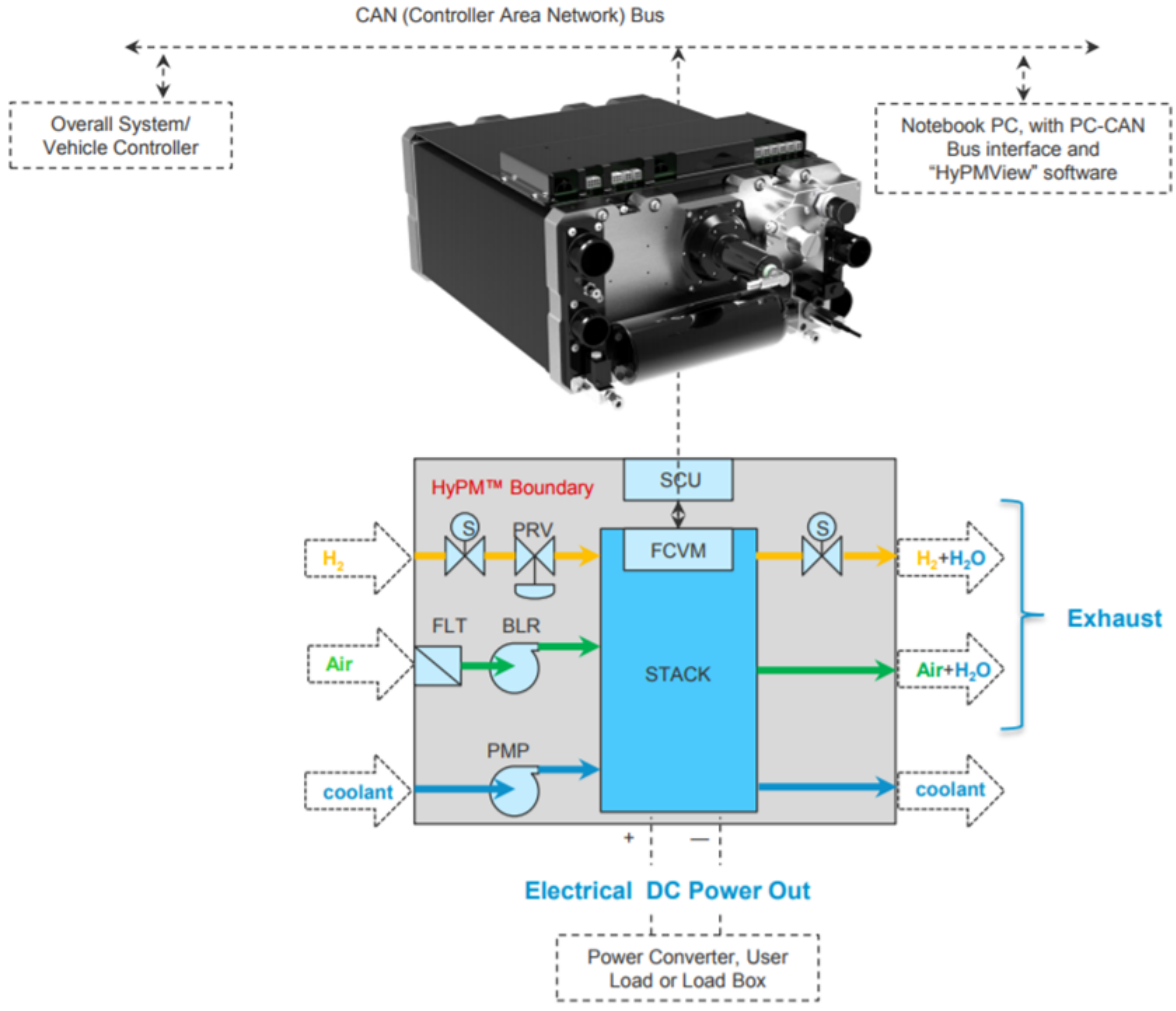

Figure 22. HyPM FCPM as subsystem [18]

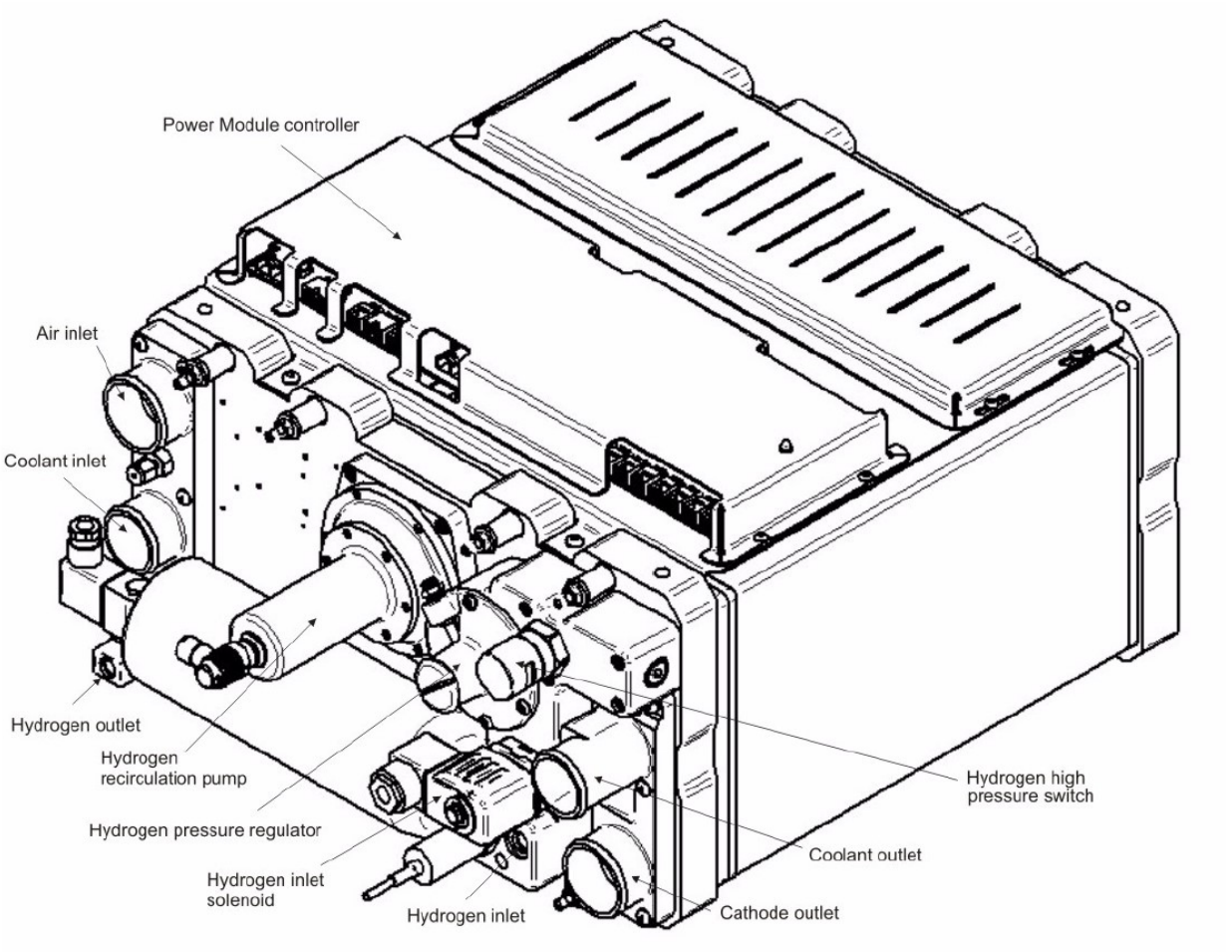

Figure 23. Hydrogenics HyPM HD16 fuell cell module components and connections [13]

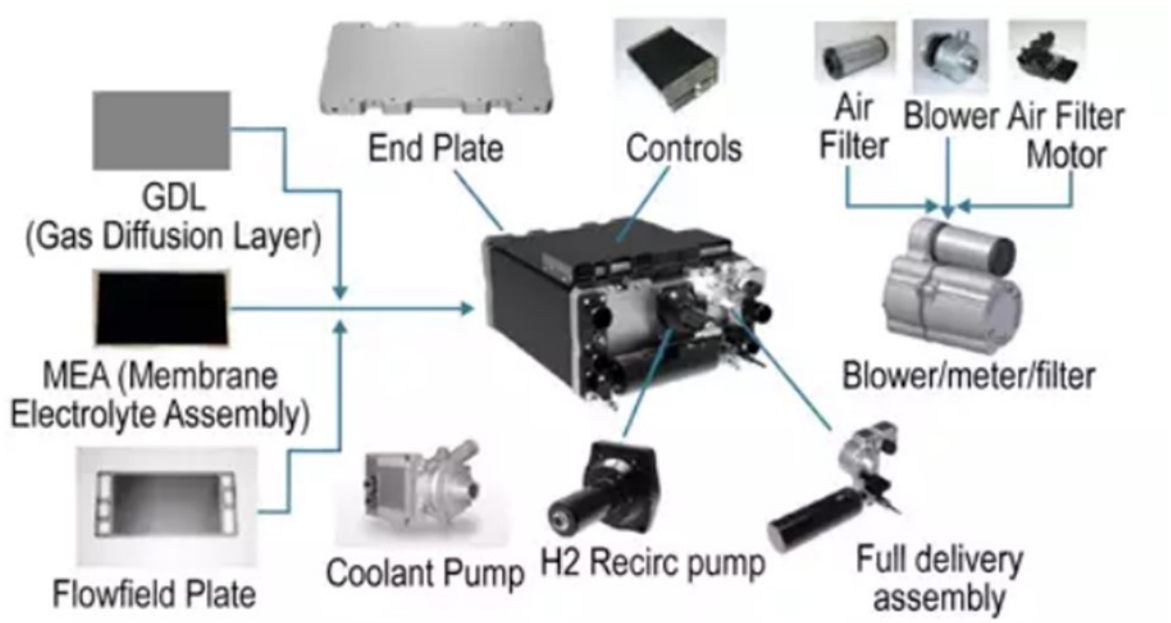

Figure 24. Subcomponents of Hydrogenics HyPM FCPM [19]

3.1.1 Instrumenting FCPM

Hydrogenics HyPM HD16 mechanical interface, seen in Figure 25, defines the gaseous and liquid inputs and outputs for the FC module. Inputs are for hydrogen and air gas and coolant fluid. The figure also introduces the related characteristics these. Outputs are cathode and anode exhausts from the module as well as the coolant fluid. Meeting the characteristics defined is considered as an requirement for the integration.

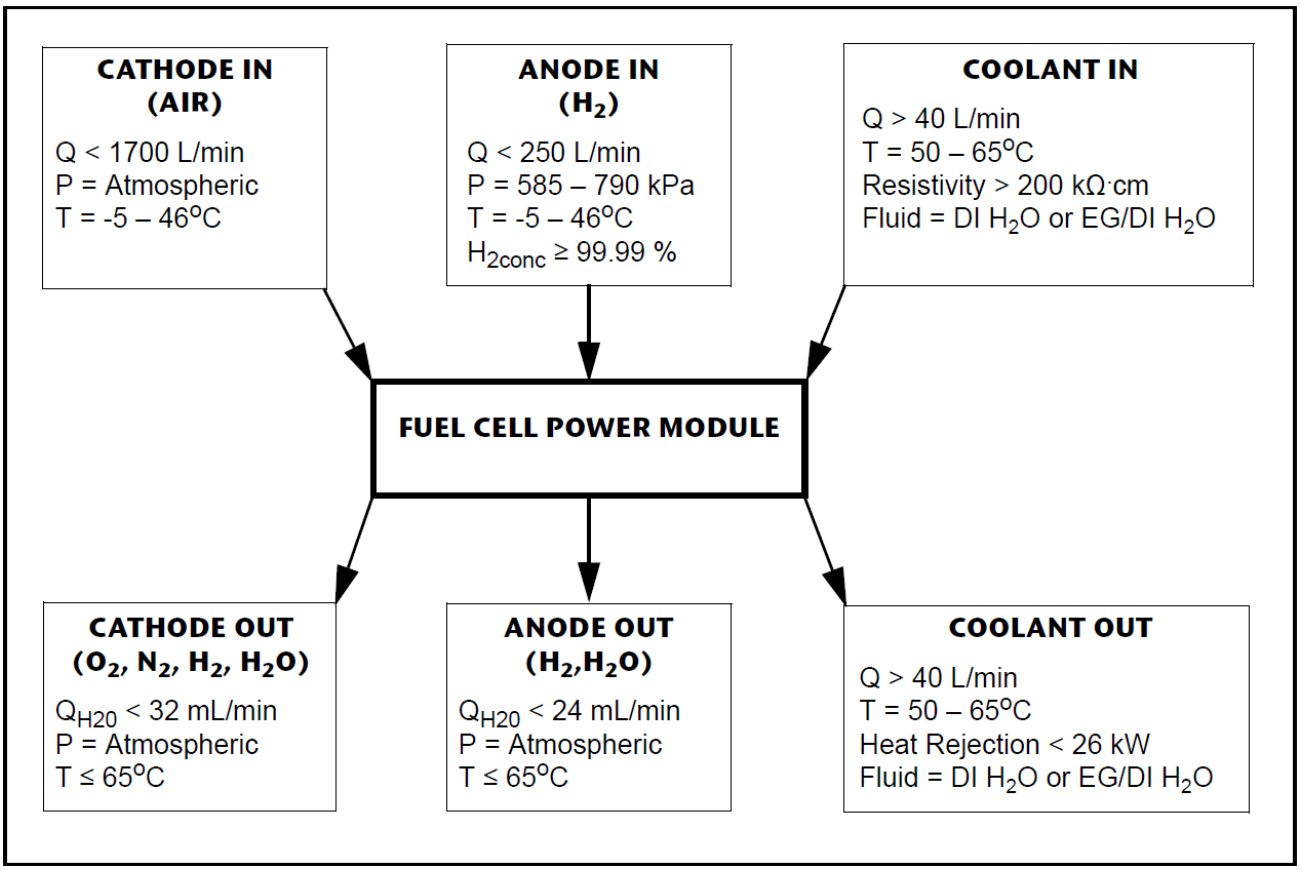

Figure 25. Hydrogenics HyPM HD16 mechanical interface [13]

In addition to mechanical interface, the electrical requirements for the module are defined in Figure 26. The fuel cell power module implements control logic board that controls the process devices related to the fuel cell operations. The fuel cell power module does not implement user interface beyond the CAN control bus interface that is used to control and observe the operations of the fuel cell module. The fuel cell manufacturer provides additional HyPMview software as reference control implementation, this software can be used to manually control and monitor the operations. The module logic board interfaces implement control over the process through devices controlled with low current signals. The power output of the second generation FCPM is completely separated from the 24V auxiliary power input used to run the logic board.

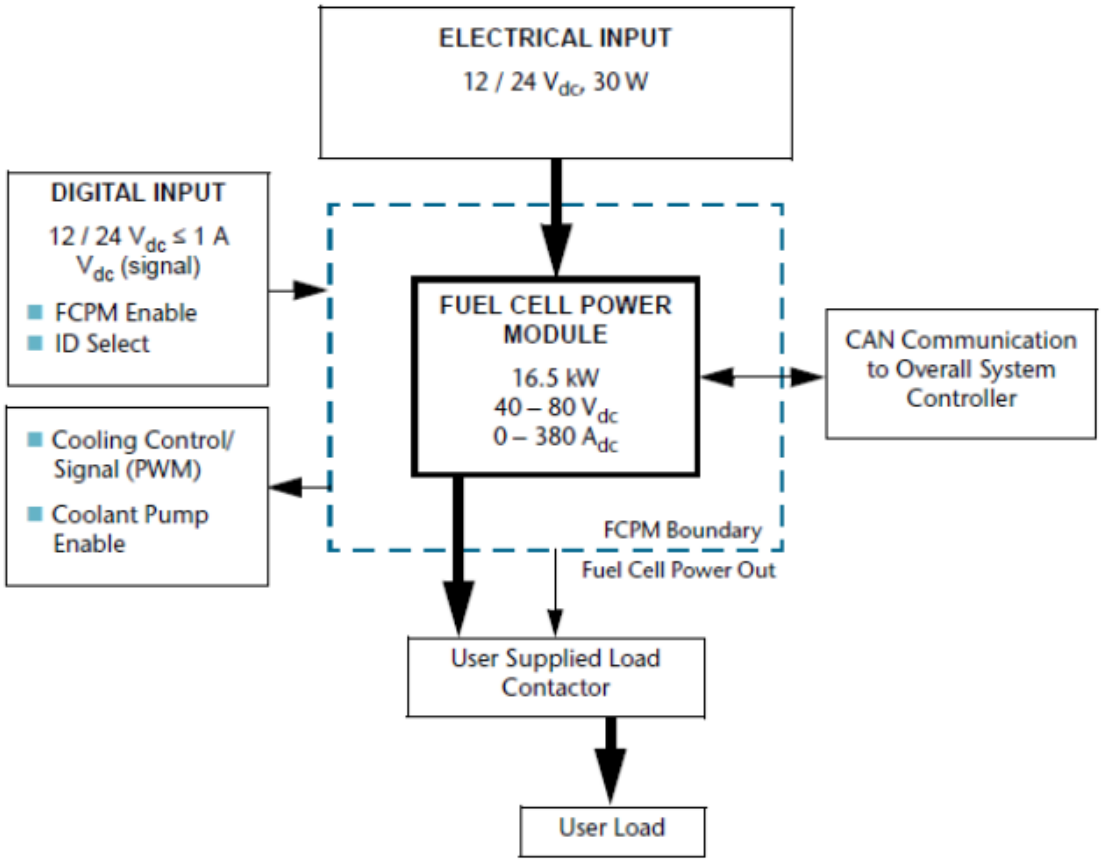

Figure 26. Hydrogenics HyPM HD16 electrical system signals and power interface diagram [13]

The Hydrogenics HyPM HD16 module can accept control power input with voltage of 12V or 24V. Also FCPM accessory device, coolant pump, needs external power input. The air blower for FCPM is connected to the fuel cell primary 40-80V power output rail. The application devices should also match the voltage level chosen for the Hydrogenics operating voltage.

In the eMule bus, there is an auxiliary battery with nominal bus voltage level of 24Vdc, typical to heavy duty vehicles. As the components delivered accept this voltage level, the accessory devices and voltage level used for integration is 24Vdc. The eMule auxiliary battery is connected to many peripherals within bus and is not to be considered stabilized. The integration uses additional 24Vdc to 24Vdc DC/DC converters to provide stabilized power train for the logic boards. The high current device like coolant pump draw power directly from the battery 24Vdc bus, due to the different current requirements.

3.1.2 FCPM control

Hydrogenics HyPM HD16 fuel cell power module has no direct user interface, rather the fuel cell is controlled via the CAN interface. The FCPM operating manuals have instructions including a state diagram chart for operating modes and state transitions. The state diagram is shown in Figure 27. The fuel cell operations are initiated and controlled by sending the FC module FCPM command, and fuel cell module sends FCPM state describing the current operational state of the fuel cell, both of these are sent as with 200ms intervals (5Hz).

The fuel cell vendor, Hydrogenics Inc, also provide reference software that incorporates functionality necessary to control and monitor the fuel cell power module operations as standalone hardware. Example views from the software, HyPMview user interface, are later shown in results part of this work.

For the actual power generation, the FCPM Command is Run. For the power generation, the fuel cell module implements two different modes, Current Ramp Mode (CRM) and Current Draw Request (CDR) mode. In both operation modes, the fuel cell will send out Current Draw Allowed (CDA) signal stating how much current is allowed to be drawn from the fuel cell. In current ramp mode, the FCPM operations monitors the current output and tries maintain CDA above the actual current drawn. The application can then ramp up the power consumption up to the CDA level given by FCPM. In Current Draw Request (CDR) mode, the FCPM can be used in closed loop mode on current demand and match the current request given through CAN command.

The other states apart from the Run, have specific functions like verifying the fuel cell integrity (Leak Check), purging the fuel cell gases with non-reacting gas (Anode Purge), preparing the fuel cell for sub zero storage (Freeze), priming the coolant circuit to remove air bubbles (Prime).

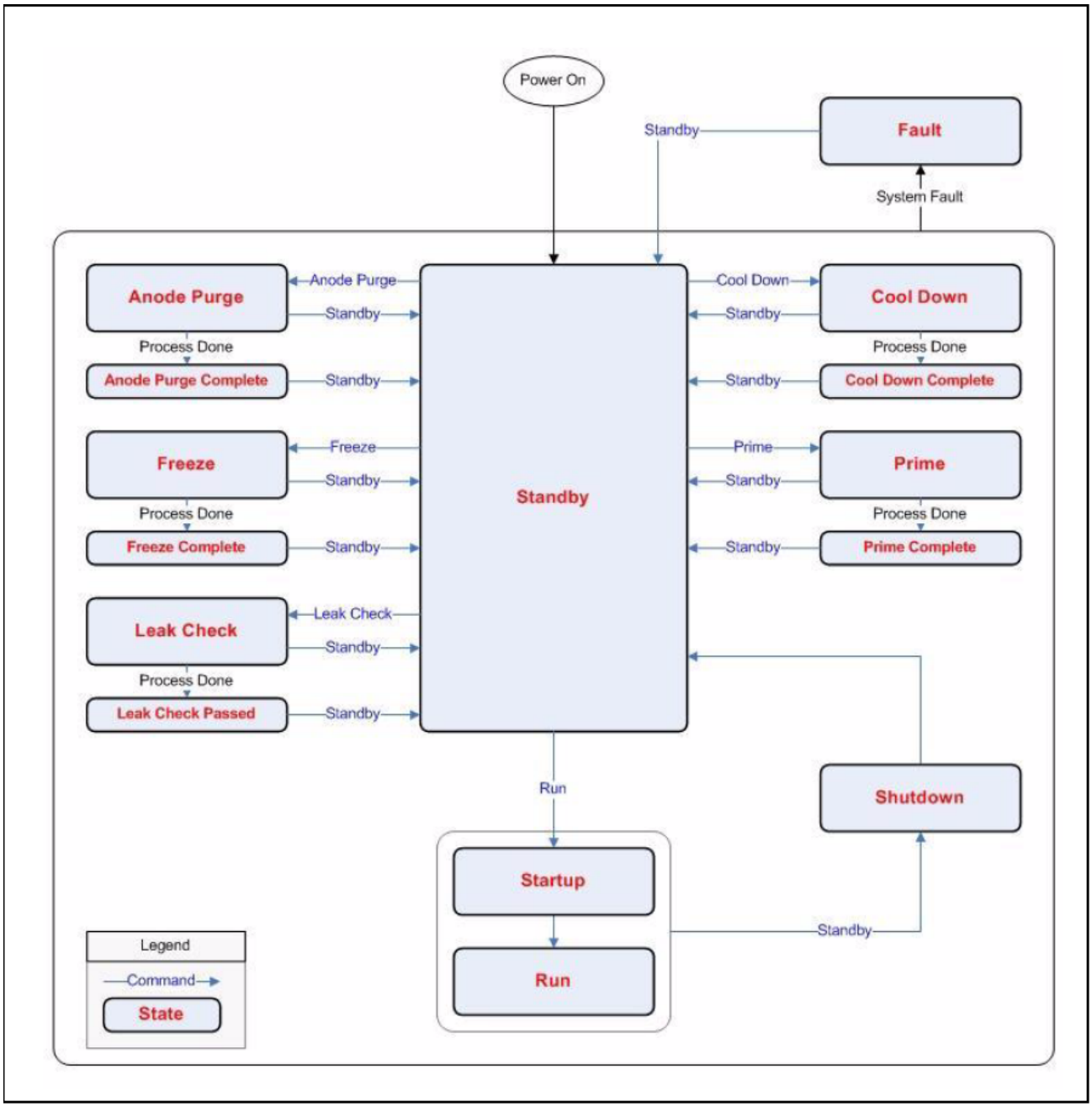

Figure 27. Fuel cell power module state transition diagram [13]

3.1.3 FCPM CAN interface test

As for the FCPM first commisioning test, the electrical interface wiring was prepared so the CAN control connection towards FCPM could be verified. For this, the FCPM was setup standing in VTT laboratory, and necessary electrical setup was built.

Enabling the software interface requires the wiring to be set up for FCPM CUSTOMER INTERFACE connectors J1 and J2. To control the device, the control wiring and power interface was constructed into a control box. The control box wiring is described in Appendix 3. For the testing, relevant signals are FCPM enable, 24V power for the control logic and CAN interface. The control box shown in Figure 28 consists of Phoenix contact connectors to breakout the wiring hardness from

FCPM connectors J1 and J2, banana type power terminals for 24Vdc power from lab power supply to the FCPM control logic and DB9 connector towards the PEAK CAN adapter.

The FCPM was shipped with hardware and software necessary to access the CAN control bus. The software is HyPMView and for CAN bus, and the shipment included USB-CAN adapter from Peak. These allow laptop to be used to operate the FCPM as standalone.

The planned purpose of this test was to verify the electrical interface functionality as milestone step towards the integration, as well to get some experience how the overall control interface works.

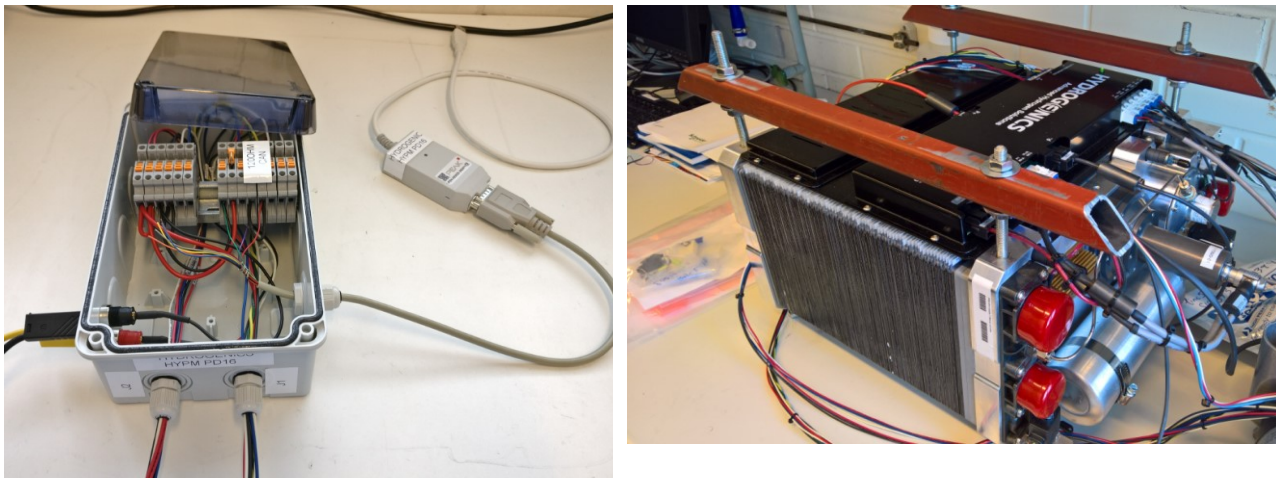

Figure 28. FCPM control box and PEAK CAN USB adapter. (on left) FCPM on table on right, control board with connections is on top, custom red metal bars were used as handles so the FCPM could be moved (photo by Antti Pohjoranta)

3.1.4 Commissioning test with FCPM on hydrogen

As the FCPM CAN control test was completed and aluminum structure parts had arrived, the structure was built and components integration started. During the build, all the gas and coolant circuits needed to be implemented and integrated to the system. In the rack structure, the coolant circuit is in lower deck, and the FCPM and DCDC converter are integrated in the middle. The rack has some space left below for the structure to resemble a shipping pallet, so the structure could be lifted with fork lift on demand. The test setup complete for commissioning test, together with the DC electrical load tester can be seen in Figure 29.

Commissioning testing proceeded with steps toward actual hydrogen testing. Prior to connecting the primary coolant circuit piping to actual FCPM, the coolant circuit was flushed first using DI water and the primary coolant pump. The pump was be operated with 24Vdc power and enable signal. The coolant pump current draw was noted to be high, up to 15A. Due to this, for the actual commissioning test setup, the coolant pump was powered by separate DC power supply, and the 24Vdc used by the instruments for control was from another DC power supply.

After the coolant pump was operated manually, for flushing the coolant circuit, the coolant circuit was emptied. Next step was priming the coolant circuit per the FCPM instructions. The coolant circuit was connected to FCPM and refilled with DI-water. Purpose for priming the coolant circuit was

to removing air bubbles from flow, and this was done again after refill. The FCPM has Prime-command for engaging the pump via controls. The command was sent via HyPMview, and it was also used to verify the actuator was operational.

As the coolant circuit was verified, next step was to verify the hydrogen circuit. For this operation, the hydrogen tank was installed and FCPM command Leak check was used. Leak check pressurized the FCPM with hydrogen.

The air blower circuit did not have separate test circuit, this was also to be powered from the FCPM DC output directly, and the FCPM DC output was engaged only when the fuel cell was operating.

For testing and operating the fuel cell, a load was necessary. The fuel cell should not be engaged without load for too long per instruction manual. Chroma DC Electric Load was used to provide load for the fuel cell in the commissioning test. The setup connections are shown in Figure 30.

Figure 29. Chroma DC Electric Load and FCPM assembled. Orange cables are from FCPM power output, and the DC electronic load is connected via black REMA MRC 320 connectors

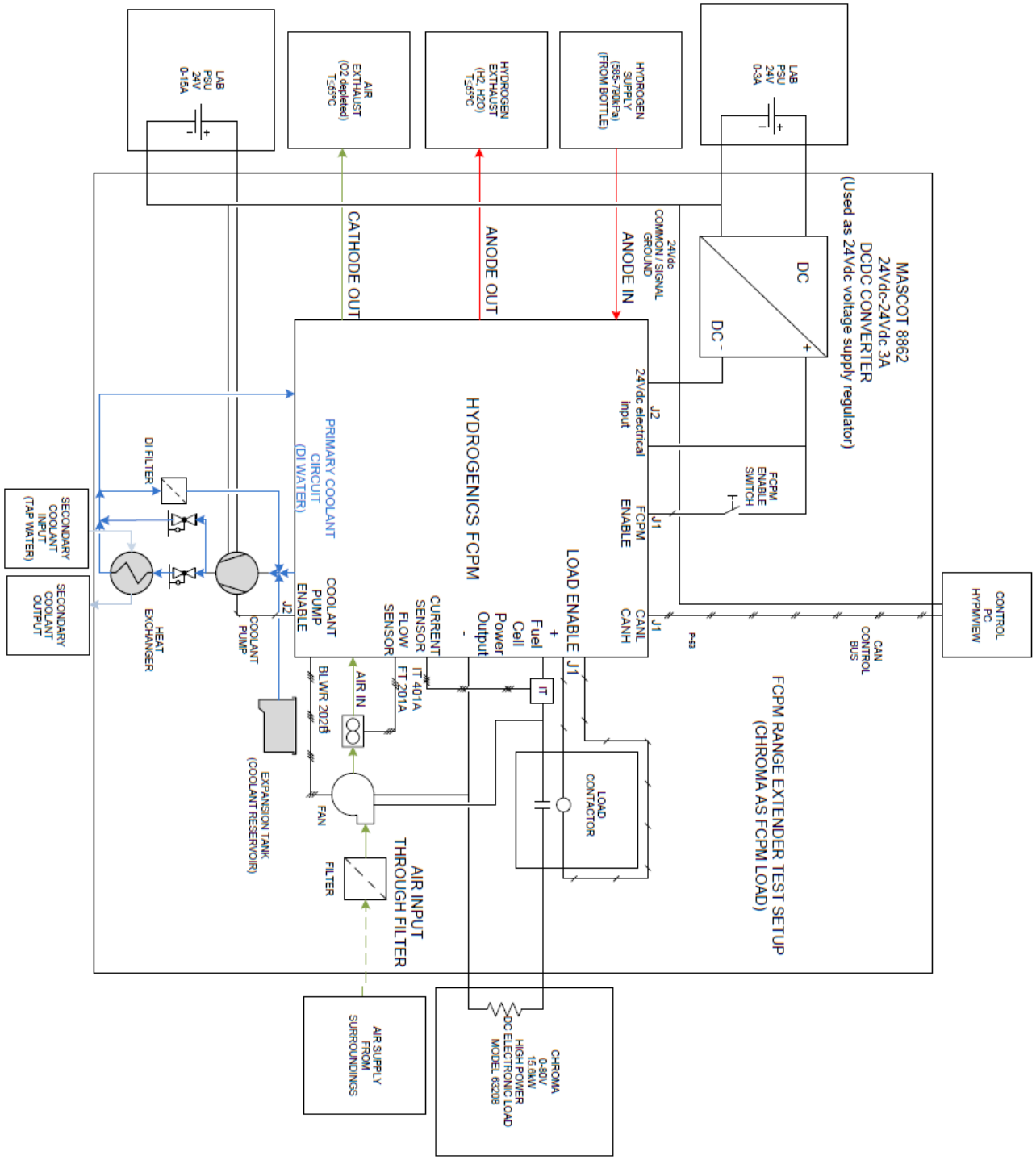

Figure 30. FCPM Range Extender module hydrogen commissioning test setup

3.1.5 FCPM efficiency and heat management

The FCPM efficiency is shown in Figure 31, and per this, the FCPM efficiency to electricity output is around 50%, while rest of the power is either consumed by the auxiliary devices such as air blower and coolant pump, or it is exhaust as heat. The FCPM operation manual instructions indicate, that as part of the integration, the cooling should be implemented so that the coolant temperature follows set point given by the fuel cell logic.

As seen in Figure 32, the fuel cell has gaseous exhausts as well as cooling defined in mechanical interface. However, the operations manual does not indicate the heat dissipation towards the coolant. As the fuel cell exhaust gas is heated oxygen depleted moisturized air, part of the heat dissipation is transferred together with the airflow.

As the primary coolant for FCPM is defined as DI water or glycol mixture, the FCPM coolant primary circuit was chosen to be connected through heat exchanger (HEX) within the eMule bus. As reference, also the previous generation installation from Topdrive was reviewed.

The heat coolant management was found non-trivial due to very limited power and pressure drop parameters given and wide possible operating environment. The FCPM module provides PID control process with PWM modulated output for a control valve, but the coolant pipe and flow configuration should be such that the valve is able to operate the system within the given parameters.

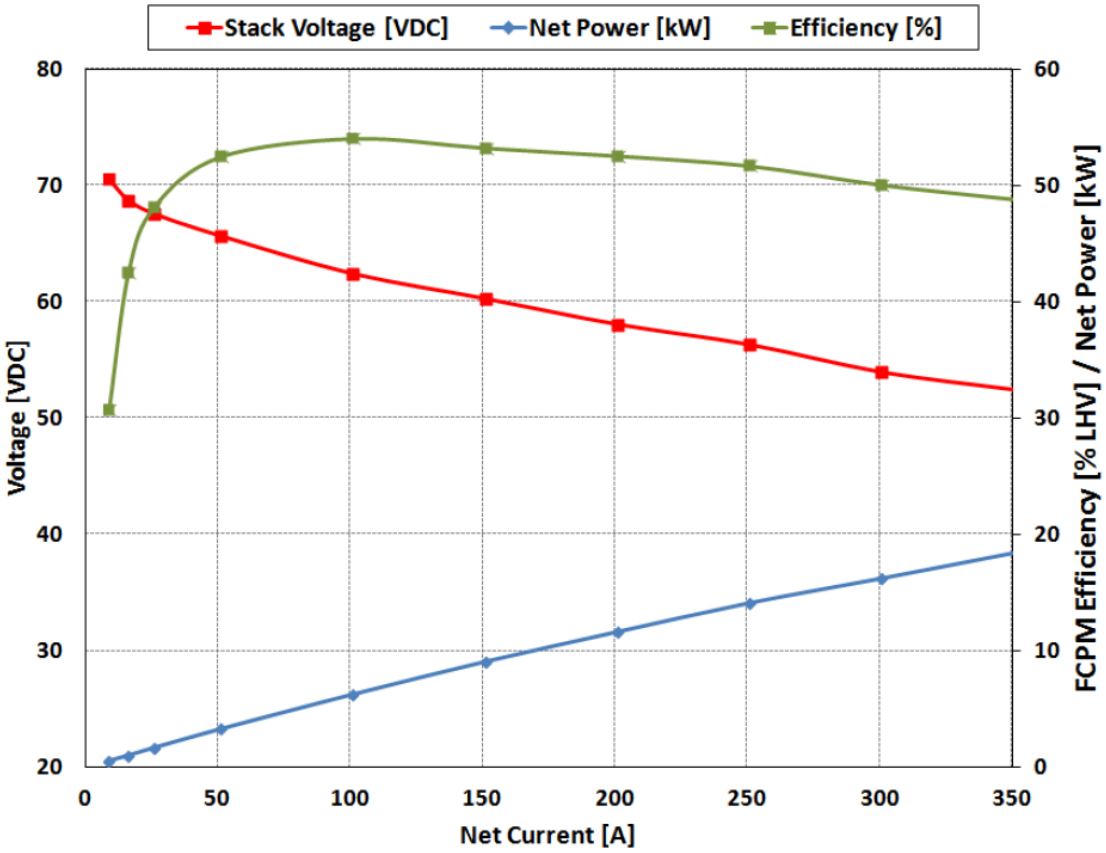

Figure 31. Fuel cell I-V chart, together with net power and efficiency (as given by the vendor in op-erations manual)

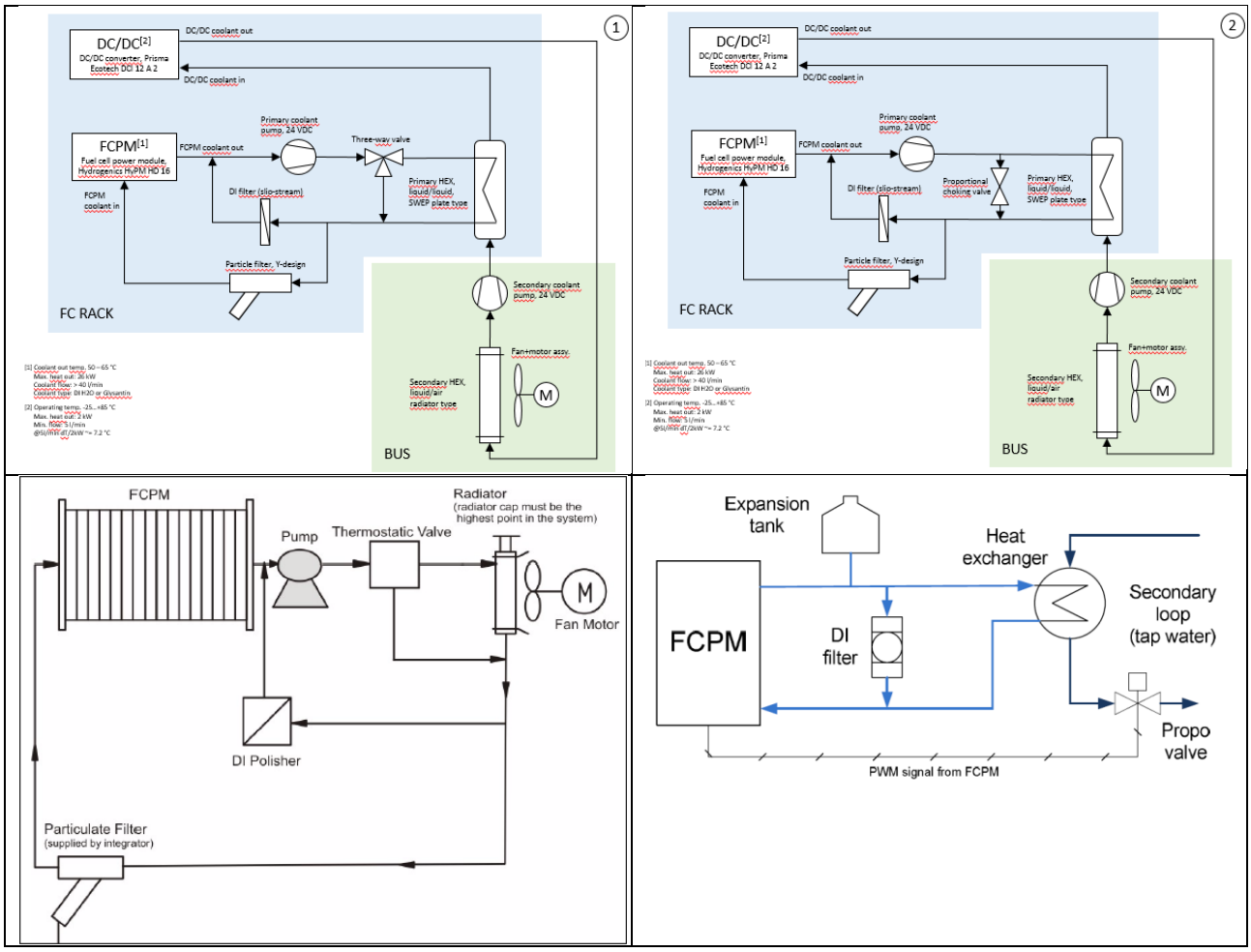

Figure 32. Different approaches considered for cooling. On top, solution proposals for this project from instructor, below are reference solution from FCPM instruction manual (right) and solution from previous generation FCPM commissioning manual

3.2 Prisma Ecotech DCI 12A2 DC/DC converter

Prisma Ecotech 12A2 DC/DC converter is a galvanically isolating16kW DC/DC converter used as boost configuration in the hybridization of eMule platform. The DC/DC converter can handle input voltage between 20-80Vdc and output side voltage between 250-700Vdc. Input current maximum is 370A and output current maximal is 40A. Datasheet lists efficiency to be more than 91% when the power transfer is more than 2kW.
Figure 33 shows DC/DC converter block diagram.

The specific DC/DC converter used in this work was previously commissioned in Aalto TopDrive project. Within the TopDrive project, the DC/DC electrical characteristics were charted and thus, the device was found to have prominent electrical characteristic features, such as low generated harmonics, to be used together with the fuel cell as well as the eMule bus DC power train.

Some of the DC/DC cabling and contactors used in this project are inherited from previous project. However, for example the control cable was found missing, and not all the software and instructions of the DC/DC converter were present. A cautious approach was taken to re-evaluate the re-commissioning of the device.

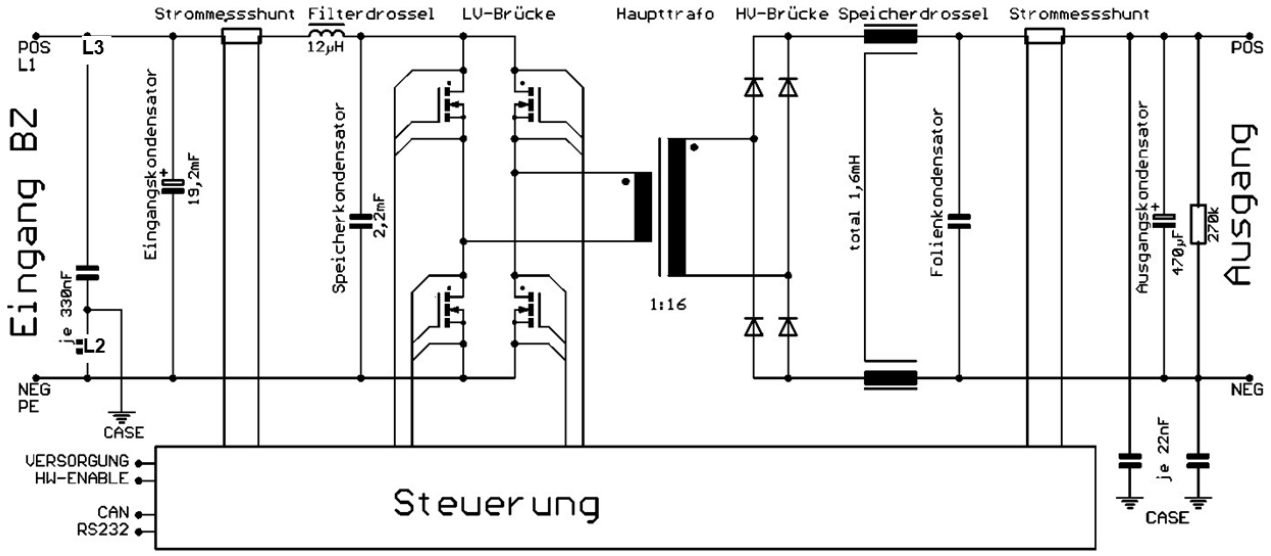

Figure 33. Prisma Ecotech DCI 12A2 power side block diagram and front panel connections [20]

3.2.1 Instrumenting DC/DC converter

The DC/DC converter has connections for both low and high voltage side using Pfisterer made connectors, two 1 pole connectors for low side + and - poles and 6 pole connector for high voltage side. The control plug is 18pin connector manufactured by Lemo, and provides the device control voltage, control signals such as enable and run signal, CAN bus and RS232 bus.

The DC/DC converter uses water for cooling, but the specifics of the coolant and operating environment are less strict than for the fuel cell. DC/DC operating temperature is specified between -25 to 80ºC.

When operating, the DC/DC converter is controlled through CAN bus. The DC/DC controller is controlled with five settings, defining the maximum duty cycle, maximum input current, run status,

minimum input voltage and maximum output voltage. The DC/DC converter will then operate in mode based on the limiting setting.

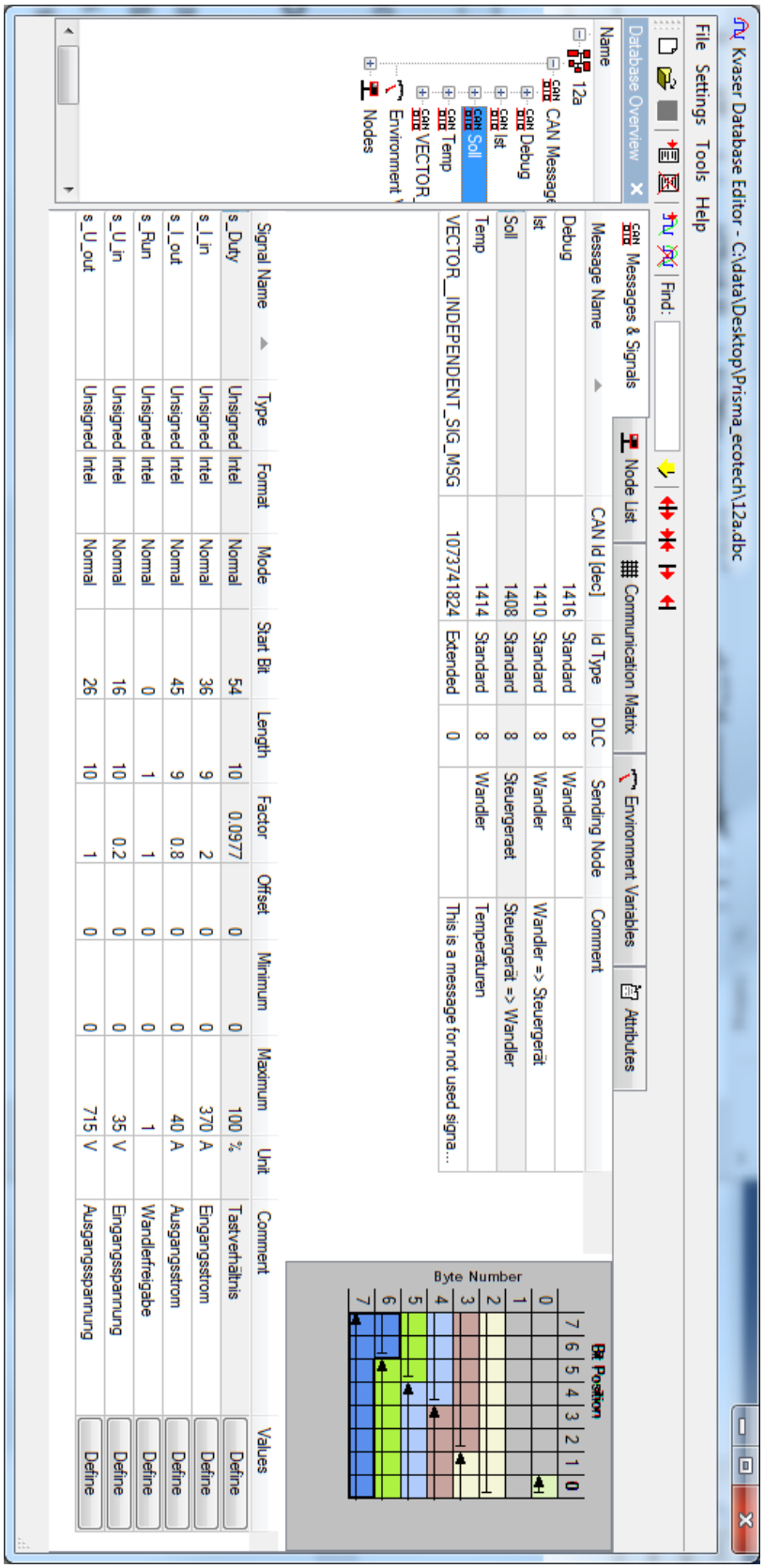

Figure 34. CAN message definition for Prisma Ecotech DCI 12A2 control message, as seen in Kvaser Database Editor

3.2.2 Re-commissioning testing the DC/DC converter

The initial condition of the DC/DC converter was somewhat unknown, as the DC/DC converter was previously used in other project but the final condition was not documented. The new Hydrogenics FCPM module was not yet available. It was chosen as first tasks on this project was to verify the DC/DC converter operations and configuration. As the converter is rated for high voltage and is able to drive high current as well, a test scenario with low risks was constructed as recommissioning test environment. The test scenario was constructed to verify the operations and configuration of the DC/DC converter, but also to demonstrate electrical safety and good engineering practice as high voltage levels were to involved. The test setup principal diagram is shown in Figure 35.

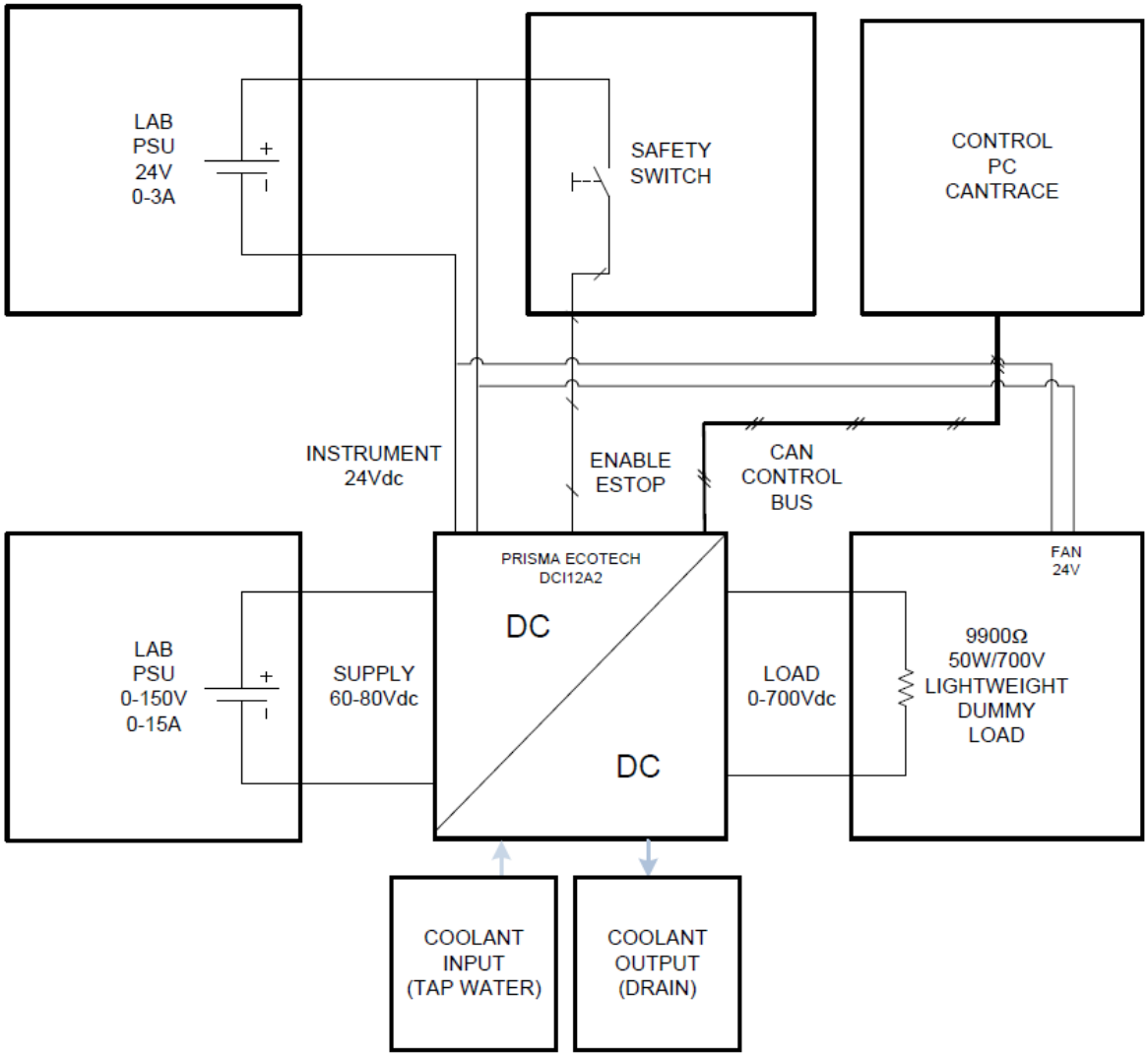

Figure 35. Prisma Ecotech DCI 12A2 DCDC converter re-commissioning test setup

A control cable with Lemo connector was not available to use from previous project. Due to missing control cable for DCDC converter a connector was needed. A new connector was provided by the vendor as result on inquiry on connector type. During the preparation to recommission testing the DCDC converter, a new interface cable and control box was prepared for the testing. The Lemo connector was installed into an instrumentation cable, and other end was mounted to a test control distribution box. Safety stop button was used to control the DC/DC converter operations. Details of

the control box connection towards DCDC converter are described in Appendix 2. Picture of the control box used is shown in Figure 36.

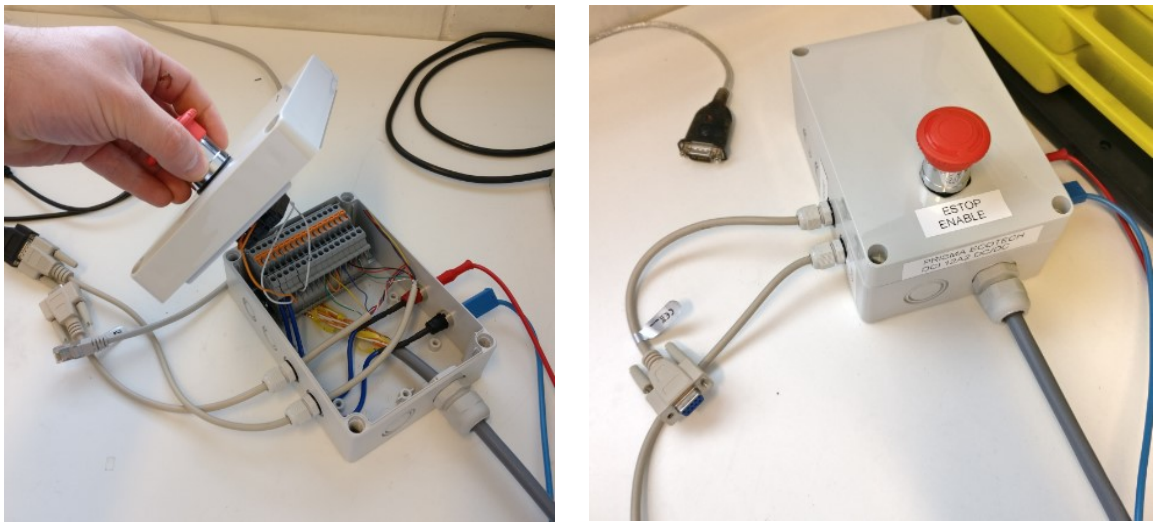

Figure 36. Control box for DC/DC converter, breakout for RS232, CAN and 24Vdc. Safety circuit with ESTOP safety button.

For the test setup, two DC power laboratory supplies were used. One DC laboratory power supply was used to provide 24Vdc operating voltage to the DC/DC controller control logic. Another DC laboratory power supply was used to provide input voltage for the DCDC conversion, the laboratory power supply chosen was able to cover the 60-80Vdc range with 15A maximum current output.

As the configuration of the DCDC converter was unknown, it was not known for certain that the DC/DC converter CAN interface was as in the original manufacturer documentation. The documentation indicated the configuration was configuration was customizable. In order to evaluate the DC/DC conversion control, a lightweight load to draw 50W was constructed. The equations 5 and 6 below are for determining suitable resistance value matching the voltage and power rating of 50W at 700V. For practical resistor availability, 3x3300ohm = 9900ohm resistor set was selected. This was considered as cautious dummy load, that would allow the DC/DC converter to sink small currents with low probability of causing any damage to the test setup.

The lightweight 50W dummy load for the test was made using standard power resistors. The lightweight load was constructed in to a box to comply with electrical safety. A cooling fan was included to setup to make sure the heat generated in resistors is vented out properly. In the setup, power resistors are mounted on a heat sink, the heat sink has a custom 3D printed adapter towards the mounting holes in case. The spacer doubles as riser to leave small air allowance between power and bottom of the case and heat sink. The chassis has mounting hole, threads were made to these holes and later machine screws were used to secure components together.

$$P = UI \ , 50W = 700V * I, I = \frac{50W}{700W}, I = \ 0.071A \quad (5)$$

$$P = RI^2, 50W = R * (0.071A)^2, R = \frac{50W}{(0.071A)^2} = 9800\Omega \quad (6)$$

Equations 5 and 6. Coupling 50W power with resistive load, determining proper value range

Figure 37. Lightweight load setup for testing, 3x3300ohm

Together with the load, a electrically safe control environment was constructed to test the DC/DC converter. The test setup is shown in Figure 38. The test setup includes following items,

- A computer with CANtrace software from TKE with Kvaser CAN adapter (1)
- Control box for DC/DC converter (24Vdc input, safety button, CAN, serial) (2)
- Lab PSU 0-30V / 3A (3)
- 1 x 12x2.5mm^2 cable and breakout box (700Vdc output) (4)
- Dummy load 9900Ohm / 700V with 24Vdc fan (5)
- Ecotech DCI 12A2 DC/DC converter (6)
- 2 x 75mm^2 cable with heavy duty connector (80Vdc input) (7)
- 2 x safety cover box for 50mm2 / banana connectors, for electrical safety (8)
- Lab PSU 0-350V / 15A (9)

Also following items were used but not highlighted in the picture,

- 2 x Safety banana cables 0.5m rated 1000V (black and red)
- Fluke multimeter (1000V rated)
- 2 x Safety banana connector cables 0.75mm^2 (80Vdc)
- 4 x Banana connector cables (24Vdc)
- 2 x black 10mm water pipe (cooling)

Figure 38. DC/DC converter re-commissioning test setup

As the Prisma Ecotech vendor provided Kvaser CAN database for the CAN messages. Due to this Kvaser CAN with TKE Cantrace software was chosen with adapter to control the DC/DC converter. The TKE Cantrace supports Kvaser CAN database directly. The setup together can convert the encoded signals from CAN bus into SI units when operating the device.

3.3 PEM FCPM Range extender

The target of the work at VTT was to construct reasonably movable modular fuel cell power module based range extender. To facilitate the project requirements, the integration required structure that could facilitate installation of the devices with auxiliary components. Previous work used industrial table on wheels as base for construction. For this work, aluminum profile based custom design was selected as target solution. The requirements for the structure were refined based on available space within eMule and worked towards constructing range extender construct. The selected also left some margin to during assembly modifications. The initial design was considered high level, enough to support material sourcing for the structure.

The range extender structure was designed and ordered while the FCPM was still pending for delivery. The range extender structure allowed the components to be tested in laboratory conditions prior to moving into eMule for integration testing.

This section covers the experimental work from range extender design and into integration testing into eMule. The section highlights, requirements, solutions, functional design decisions as well as safety aspects during the work.

3.3.1 Structure design

For the FCPM and DC/DC converter mounting, a Maytech 60x60 light profile structure was chosen as platform solution. The solution was considered to have good customized mounting of all necessary equipment, yet the configuration is flexible and allows fine tuning the details when assembled. The size of the structure was based on the space used by previous deployment, with some additional constraints, such as structure fitting below windows of the bus. Additional driving requirement was so that the structure could be lifted by below as pallet or rised from hooks above, to support for example lifting with forklift. Pictures of the structure shown in Figure 39, CAD model, profile quotation and assembled parts.

The structure was drawn with PTC Creo in 3D, using the 3D model of fuel cell and rough estimation of DCDC converter. After which, 2D drawing was made. The 2D drawing was used to drive the order of the custom parts from SKS Mekaniikka. Additional accessory parts were also used, such as mounting hooks, joints, fastening T-nuts for M6 and M8, as well as dampeners to be mounted below the fuel cell and adjustable machine feet. Joints and fasteners are shown in Figure 40, these come in different configurations, some can be inserted to T-slot only prior to assembly and others can be plugged to assembled structure. 2D drawing of the model is in appendix 1.

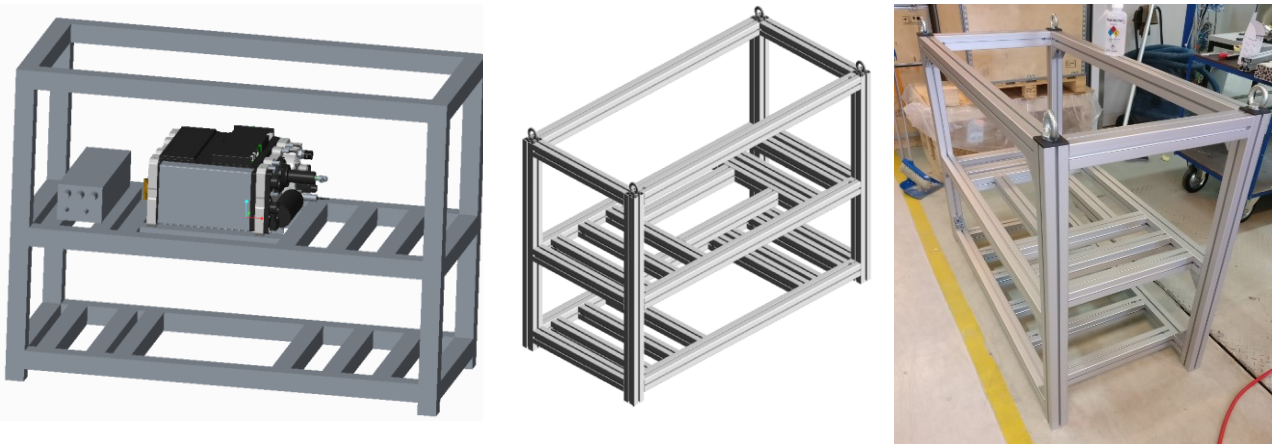

Figure 39. CAD model of structure (left), Maytech profile quotation (middle), assembled profile structure (right)

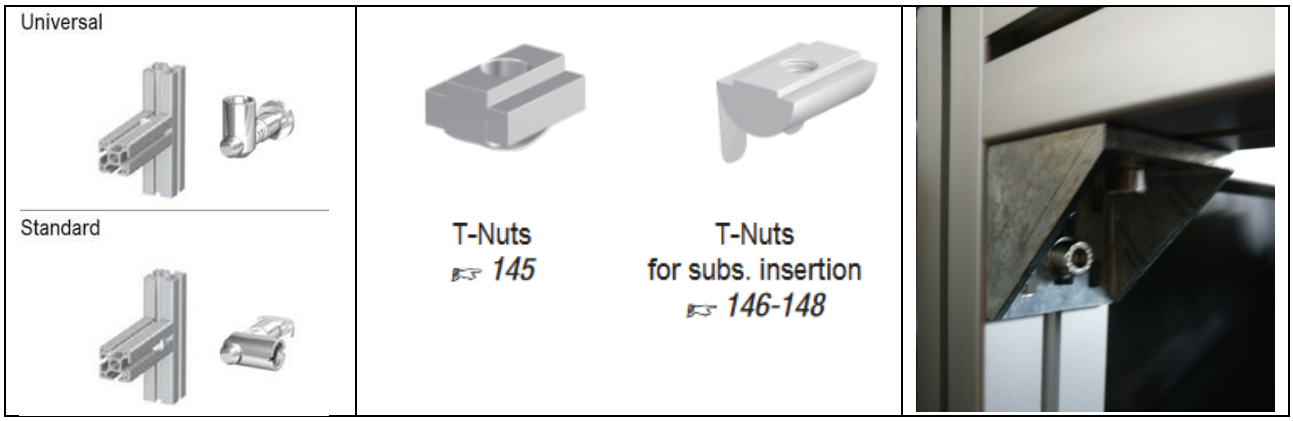

Figure 40. Accessories for the structure, joints (left), fastening elements (middle) and support L-fastener (right)

3.3.2 Components placings

Integration of the FCPM and DCDC included several components, the structure was made to fit into the bus, and to house all the components. Some of the components have additional requirements for locations and this section explains some. Other sections will give more specific details on some components, this section is to give overview on components placement within structure as well as functional requirements. The pictures seen in this section are taken during integration, not from final assembly, as the components can be seen more clear.

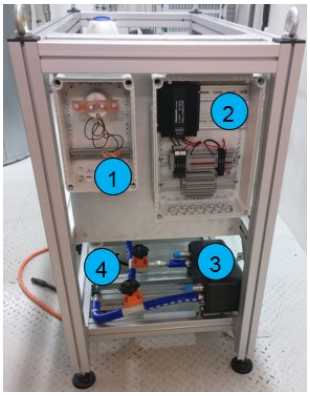

Figure 41. 1. Contactor between FCPM and DCDC bus 2. 24V voltage instrumentation and interconnect 3. Heat exchanger with cover 4. Manual control valves for coolant

In Figure 41 is shown locations of electrical boxes fitted on side of the structure, so the electrical boxes are easily accessible, for the installation, these would remain accessible also when the range extender rack is deployed into eMule. The heat exchanger and main water piping are assembled below the main system components so in case of water leakage, the leakage does not cause the instruments to flood.

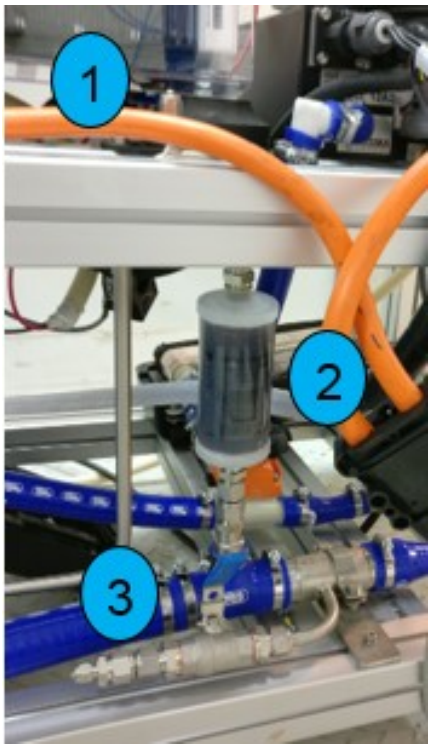

Figure 42. 1. Small air valve 2. DI-filter 3. Fill/drain valve and connector for coolant

In Figure 42, DI-filter installed to primary coolant circuit is shown. The flow direction in filter on the installation orientation is upwards, installing the DI-filter on other orientation, the water flow route could become more channeled within the filter and the lifecycle predictions would not apply. On top of this circuit, small valve can be seen that is used to purge air out of the pipeline. Also the pipeline includes fill/purge valve for the primary coolant circuit. Per the FCPM instructions, care should be taken not to exceed 200kPa pressure towards the FCPM, so for example no forced air exceeding the limit should be used when removing the coolant.

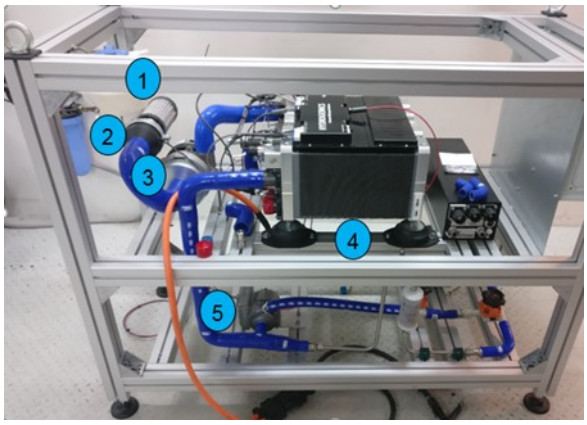

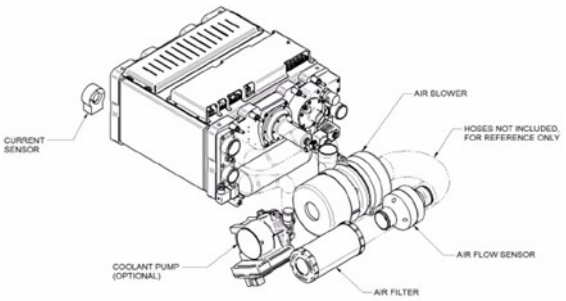

Figure 43. Component positions seen during assembly. Air pump (3) flow sensor (2) and filter (1) follow the reference picture (on right) Left is the reference picture from manual [13]. Also are shown in picture 4. Shock absorbers below FCPM 5. Coolant pump.

Figure 43 illustrates both confirming to manufacturer reference picture from manual for air blower and coolant pump installation, as well shows black shock absorbers installed below FCPM. Figure 44 illustrate coolant circuit expansion tank location above rest of the coolant circulation. Expansion tank is a car coolant circuit spare part component.

Figure 44. Expansion tank is installed as highest point of the primary coolant circuit

3.3.3 CAN identifiers in system

The PEM FCPM range extender is designed to be used in eMule as on the demand range extender and the design idea is the range extender could also be controlled by the vehicle control unit (VCU). The devices are to be integrated into eMule VCU CAN bus communicating on 250kbps as they are set up for this communication speed. For this, it was necessary to verify the CAN identifiers not conflicting between the range extender devices and other eMule CAN devices. The Table 4 shows CAN identifiers from Prisma Ecotech 12A2 Kvaser database and Hydrogenics HyPM HD16 combined into single list.

Only on identifiers was found between Hydrogenics HyPM HD16 and Prisma Ecotech 12A2 CAN database definitions and HyPM reserved identifiers definitions. As the CAN identifiers need to be unique as described in part 2, the conflict situation needed to be resolved. The identifier 0x580 is command message used to control the DCDC controller, while FCPM documentation lists this as reserved. The message identifier was not observed during CAN commissioning of the FCPM. In fact, the documentation defines the FCPM related identifiers to be base identifier + FCPM ID, the FCPM ID is a identifier that can be configured via the FCPM connector J2. The identifier is used to identify individual fuel cell power modules, in case the system consists of more than one fuel cell power module. All the message identifiers seen on the system had least significant number of the identifier as 1.

The CAN bus tools do not provide tools to identify if the identifier was actually used by the FCPM, so the FCPM manufacturer was contacted and requested for advice. The Hydrogenics Inc representative response was that the specific identifier was not used for the FCPM configuration to be integrated. The conflict was thus resolved by response of manufacturers representative

The eMule VCU has also other devices on the 250kbps bus, but per the CAN message identifiers documentation, no other devices had conflicting CAN identifiers. Due, the fuel cell range extender could be integrated also into the eMule VCU 250kbps CAN bus.

ID	Offset	Length	Type	Device	Description (+var name)
0x1C0-0x200				HyPM16	Reserved per Documentation C.2
0x1C0+fcpmid	0	8	uint8		Command / Heartbeat
0x1D0+fcpmid	0	16	uint16		Current Draw Request (0.1A/bit)
0x1E0+fcpmid	0	8	unint8		Undocumented (Presumed: request cell voltages)
0x240-0x280				HyPM16	Reserved per Documentation C.2
0x240+fcpmid	0	8	uint8		FCPM state
	8	8	uint8		Reserved
	16	16	uint16		Current Draw Allowed (0.1A/bit)
	32	16	uint16		Fuel Cell Current
	48	16	uint16		Fuel Cell Stack Voltage (0.1V/bit)
0x2C0-0x300				HyPM16	Reserved per Documentation C.2
0x240+fcpmid	0	64	bitmask		Faults & Alarms: See manual for bit definition
0x340-0x380				HyPM16	Reserved per Documentation C.2
0x340+fcpmid	0	16	uint16		Coolant Temp (0.1C/bit)
	16	16	uint16		Coolent Temp Setpoint (0.1C/bit)
	32	32	uint32		Reserved
0x3C0-0x400				HyPM16	Reserved per Documentation C.2
0x440-0x480				HyPM16	Reserved per Documentation C.2
0x4C0-0x500				HyPM16	Reserved per Documentation C.2
0x540-0x580				HyPM16	Reserved per Documentation C.2
0x580	0	1	boolean	DCI12A2	Soll / s_Run
	16	10	uint10		Soll / s_U_in (minimum input voltage, 0.2V/bit)
	26	10	uint10		Soll / s_U_out (maximum output voltage, 1V/bit)
	36	9	uint9		Soll / s_I_in (maximum output voltage, 1A/bit)
	45	9	uint9		Soll / s_I_out (maximum output voltage, 0.8A/bit)
	54	10	uint10		Soll / s_Duty (maximum output voltage, 0.0977%/bit)
0x582	0	1	boolean	DCI12A2	Ist / i_Runs (Mode Signal)
	1	1	boolean		Ist / i_Fault
	2	6	uint6		Ist / i_Code Mode:0 Fehlercode
	4	4	uint4		Ist / i_Moduos Mode:1 (Regelmodus)
	8	11	uint11		Ist / i_U_In (0.1V/bit)
	19	11	uint11		Ist / i_U_out (0.5V/bit)
	30	11	unit11		Ist / i_I_in (0.5A/bit)
	41	11	unit11		Ist / i_I_out (0.2A/bit)
	52	12	unit12		Ist / i_Duty (0.024414%/bit)
0x586	0	8	uint8	DCI12A2	Temp / Temp_Au (1C/bit Kühler untere Schalter vorne)
	8	8	uint8		Temp / Temp_Ao (1C/bit Kühler obere Schalter vorne)
	16	8	uint8		Temp / Temp_Bu (1C/bit Kühler untere Schalter hinten)
	24	8	uint8		Temp / Temp_Bo (1C/bit Kühler obere Schalter hinten)
	32	8	uint8		Temp / Temp_Trafo (1C/bit Temperatur Trafo)
	40	8	uint8		Temp / Temp_Folien_C (1C/bit Temp Folien-C)
	48	8	uint8		Temp / Temp_Filter_L (1C/bit Temperatur Filterdrossel)
	56	8	uint8		Temp / Temp_Int (1C/bit Temperatur Innenraum)

Table 4. Range extender device CAN identifiers and signals. Conflicting ID range highlighted.

3.3.4 Integration testing the DC/DC converter together with FCPM

To verify the range extender operations, a integration test was conducted with target power approximatedly 7kW with target output voltage 700Vdc. The devices used in test set up are seen in Figure 46, the fuel cell is powered from hydrogen tank. The system was operated from the laptop and the stove was used as load for the setup.

3pcs of stove heat elements were set up as load for the DC/DC converter, with approximately 26.3 Ω resistive load on each heat element, the elements were as series configuration so the voltage over each element was one third of the total voltage applied. The voltage division was also considered as electrical safety issue as the electrical stoves are rated for 400Vac. The calculus with estimated 79.5 Ω resistive load is shown in Table 5. Test plan power calculation for 700V, assuming using 3pcs of 26.3Ω stove heat elements as approximately 79.5 ohm load. Expected voltage-current calculated. below, and shows estimated load of 6.2kW.

The test setup followed the FCPM ramp mode configuration, the load was gradually increased as the FCPM indicated increasing allowed current signal. The first test was interrupted for further observation due to observed odor within laboratory air. It was not possible to pinpoint the exact source, but the stoves that had been in storage was main suspect, and no part of the experiment device was showing symptoms of issues preventing further testing. After this, the experiment was restarted and the configuration was tested up to 700Vdc on stove configuration, this being the planned target of the experiment. The test was driven using the DC/DC converter input current the main limiting factor while the rest of the operating parameters were considered as constants.

For the actual test, all CAN communication with DC/DC converter and FCPM was to be logged on the control software for further analysis.

P	7000	W	6163,522	U*I
U	700	V	700	
I	10	A	8,805031	U/R
R	70	Ohm	79,5	26,3*3

Voltage	Current	Power
300	3,773585	1132,075
350	4,402516	1540,881
400	5,031447	2012,579
500	6,289308	3144,654
600	7,54717	4528,302
700	8,805031	6163,522

Table 5. Test plan power calculation for 700V, assuming using 3pcs of 26.3Ω stove heat elements as approximately 79.5 ohm load. Expected voltage-current calculated.

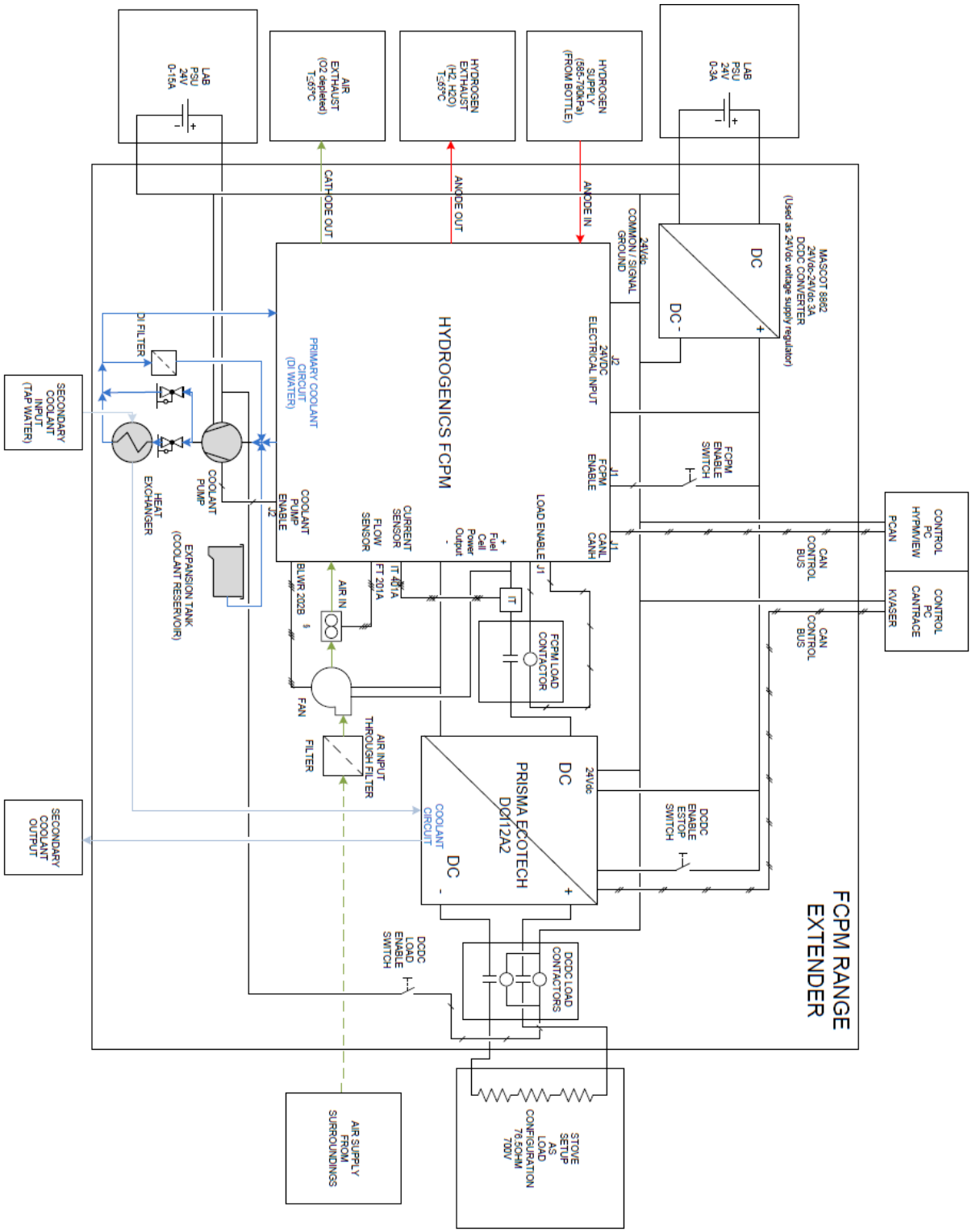

Figure 45. Integration test setup for FCPM with DCDC converter and stoves

Figure 46. Integration test setup, range extender assembly, hydrogen tank and electrical stoves con-figured as dummy loads for 700V setup

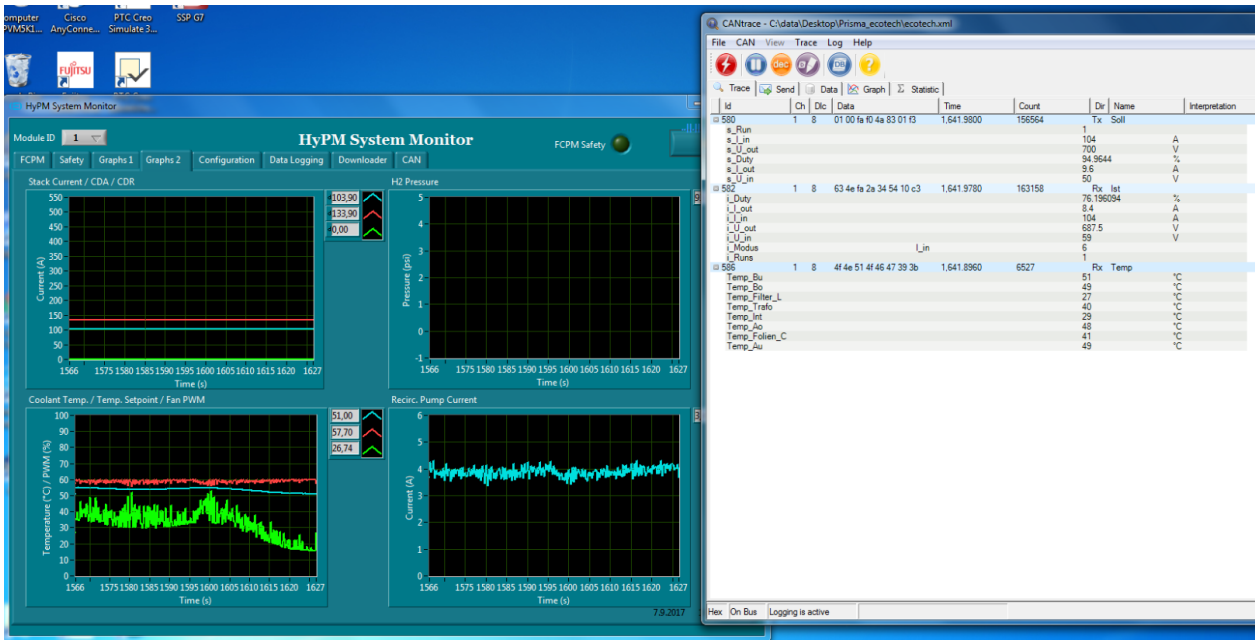

Figure 47. HyPMview for FCPM operations on left and CANtrace for DC/DC operations on right. CANtrace shows power output of 700V * 9,6A = 6.7kW

3.3.5 Range extender safety in eMule

As additional control layer for hydrogen safety, eMule had hydrogen safety systems installed as additional independent electrical circuit that has a function of bringing the system down in case safety circuit is triggered. The circuit can consists of different safety devices, such as sensors that monitor the operation conditions, in this case for example hydrogen sensor that measures the presence of hydrogen within the bus, as well as human triggered safety buttons. Hydrogen gas detector is shown in Figure 48. The safety control circuit was given as prior work to this thesis, and considered mainly as input for the range extender device. Thus, an short overall of safety considerations is given in this thesis.

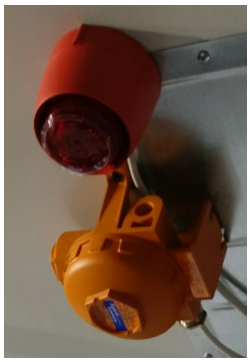

Figure 48. Hydrogen gas detector, the detector is certified to operate in environment with hydrogen

Triggering the fuel cell range extender safety circuit in the demonstrated eMULE platform will cause safety relay to release. The relay release will then cause signal E-STOP to the DC/DC converter and PEM FCPM module, as well as it will close solenoid valve, closing the hydrogen gas circuit from the primary hydrogen container. Also, the security relays will cause contactors between DC/DC converter and eMULE power bus to release and thus isolate the DC/DC converter from eMULE power bus. The E-STOP signal on DC/DC converter and PEM FCPM will trigger safety shutdown.

Before operating the range extender in bus, the environment and safety equipment were evaluated and tested for safe operations. A review using VTT standard safety form was evaluated, to verif the safety issues were considered and highlighted before testing. All safety equipment, including switches and gas detectors were primed and tested to verify safety circuits working as required. The gas detectors were first tested using hydrogen calibration gas, hydrogen calibration gas container can be seen in Figure 49. The calibration gas allows verifying the gas detector thresholds. For the hydrogen pipelines, the testing was conducted also using gauge to show the pressure within hydrogen fuel line. The hydrogen fuel line was primed with pressurized hydrogen, and it was observed the gauge value remains stable after the inlet is closed.

Figure 49. Hydrogen detector calibration gas container (left) and visual hydrogen line pressure gauge (right)

3.3.6 Integration testing in bus

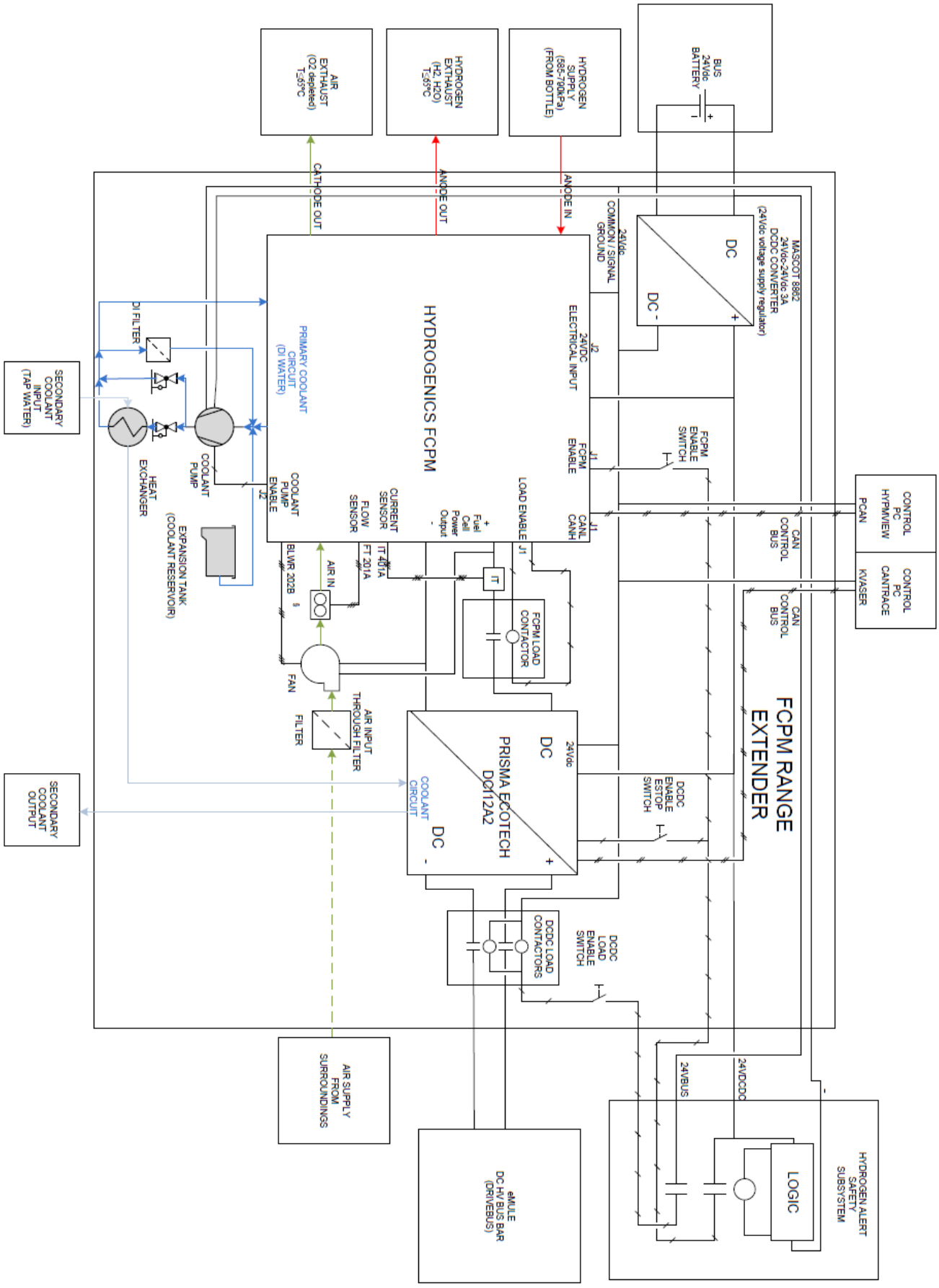

Figure 50. FCPM range extender configuration in eMULE

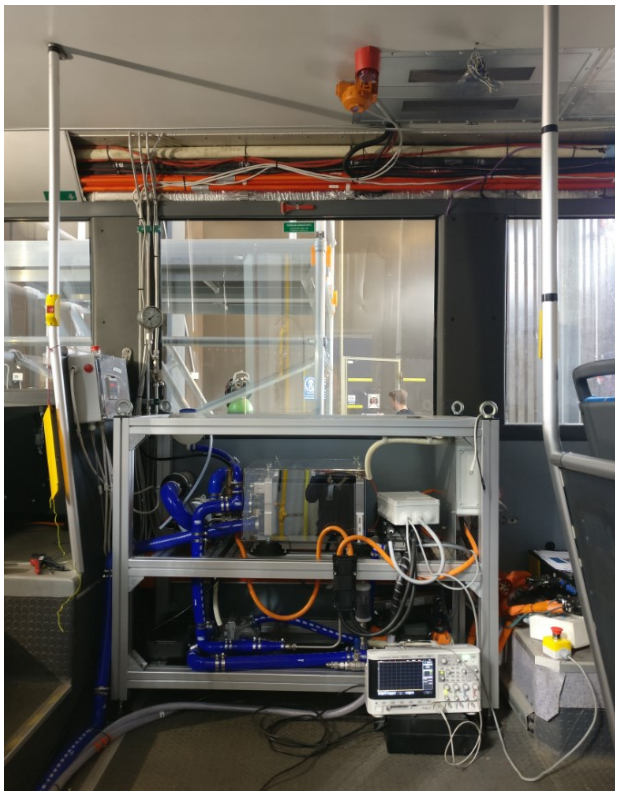

Figure 51. Left: FCPM range extender rack is located bus pram area, Right: Hydrogen tank on roof (front of the tank is intercooler and pantogram)

The previous experiment over dummy loads verified stable operation of the base design of the FCPM range extender apparatus. The control over the apparatus was understood and considered stable. The next step towards the integration was to interconnect the power output to the eMULE power train and to verify power transfer towards to in-vehicle power train.

The DC/DC converter power output was connected to eMULE power train via contactors and fuse. Then before commencing the power transfer, the interconnection set up required controlled power up to prevent power surge between eMULE power train and output capacitors. With small resistor, and 600+ V voltage difference between the capacitor provided conditions for rush current that would exceed the rating of the fast 50A fuse in between. For controlled interconnect, output of DC/DC converter output was precharged into voltage level close to voltage level observed on the power bus. After the precharge sequence, the interconnection was established by closing the contactors. In this configuration, the interconnect contactors were manually operated.

Also for this setup, the safety circuit with hydrogen detectors and safety shutdown buttons was incorporated into the setup. The safety circuit controlled hydrogen valve, estop enable signals for fuel cell and DC/DC converter, as well as the interconnect contactors towards the eMULE power train. Prior to running the actual test, operation of both hydrogen detectors and safety stop buttons was verified. One detector was located inside of the bus and one on roof of the bus. The test setup for FCPM range extender module is visible in 56.

3.4 Data processing and visualization

For the data logging and processing the results of testing, the FCPM and DC/DC converter CAN communications including telemetry data was collected into log files during the FCPM tests. Both of the two softwares used for CAN communication, CANTrace and HyPMview supported writing the CAN data into log file. CANTrace also supported writing out the signals in CAN data per Kvaser CAN database definition. HyPMview also supported logging of the FCPM state with custom intervals in comma separated values (CSV) format, each line presenting the FCPM state at given moment. In listing 1, the CANTrace log file format can be seen. The format of actual CAN message is shown in Table 6.

```
  1545.074000  1  582  Rx  d  8 63 4a e2 6a 35 56 90 c3
// Id: 1408 Msg Name: Soll
Signal list:
s_Run Value: 1
s_I_in Value: 104 A
s_U_out Value: 700 V
s_Duty Value: 94.9644 %
s_I_out Value: 9.6 A
s_U_in Value: 50 V

  1545.074000  1  580  Tx  d  8 01 00 fa f0 4a 83 01 f3
// Id: 1410 Msg Name: Ist
Signal list:
i_Duty Value: 76.342578 %
i_I_out Value: 8.4 A
i_I_in Value: 104.5 A
i_U_out Value: 686 V
i_U_in Value: 58.7 V
i_Modus Value: 6
i_Runs Value: 1
```

Listing 1. Snapshot of CANTrace log file with signals written out.

Timestamp	Channel	CAN ID	Direction	Dlc	Length	Data byte 1	Data byte 2	Data byte 3	Data byte 4	Data byte 5	Data byte 6	Data byte 7	Data byte 8
1545.074000	1	582	Rx	d	8	63	4a	e2	6a	35	56	90	c3

Table 6. CAN message log entry contents

Matlab was used for further data processing, the data was read from log files, processed and visualized using Matlab software. Matlab was selected as tool for processing for being widely known scientific data processing tool, and well understood. The approach taken was generic enough to work on both CAN log files, generated by CANTrace and HyPMView. The signals were recovered from CAN messages per the CAN definitions as part of the data processing in Matlab code.

The Matlab written pipeline to visualize the CAN data has been split into functional blocks, first block reads the CAN from file into Matlab as matrix, each row containing single CAN message. The first phase also takes care of parsing the hexadecimal values from log files. As second processing phase, signals from different CAN message types identified by the CAN identifier are prossessed back to signals encapsulated in the CAN messages. As the signal values are bit packed into data bytes as scaled, the data is reconstructed by frist using bitwise operations to recover the scaled

value and then multiplying it with correct multiplier. As final phase, the data is visualized using Matlab plot commands. The Matlab code uses little optimization to speed the process, this is done by counting pre-allocating the relevant data structure. The speed up from initial tested method of concatenating data row by row to array is quite significant. The difference in pipelines of processing data written out by CANTrace and HyPMView is their timestamp starting point, this is normalized in visualization part so that the first timestamp is considered as zero. The functional Matlab code for parsing CAN data is presented in appendixes.

Another similar pipeline is written and used for analyzing the CSV file by parsing the data from comma separated file into Matlab array. This was a straightforward process, a little effort was required to convert state into value so Matlab can treat the whole matrix as single datatype. Another thing taken into account during the processing is, some FCPM logs lack the individual cell voltage measurements, but as the matrix is constant size. As the voltage measurements lay at end of the line if present, the row processing code leaves the end filled with zeroes if the voltage measurements are not available.

4 Results and discussion

The project original target was complete to the hybridization of the eMULE vehicle to point where the vehicle could be driven with fuel cell in operation, together with fuel cell operated over CAN bus. The actual realized result is the documented in this work. The work realized into FCPM based range extender apparatus in eMule, with electrical and mechanical integration towards the vehicle as described. With-in the limited time available, the capability for testing the fuel cell power module while driving eMule was not reached. The control over the range extender was manually driven from independent station and the dependencies integration towards vehicle control unit were charted. The cooling solution was realized so it enabled the integration testing and charting of the operating conditions, the solution was manually operated cooling circuit run from tap water. To realize the independent cooling circuit in vehicle, more work is needed to complete this.

The previous section covers overall description on experiments towards the integration. In this section the experiment results are covered and discussed.

4.1 Initial commissioning testing

As shown in the experimental part explanation, initial commissioning tests were commenced on the FCPM and DCDC converter to basic electrical operations and communications with the hardware. As result of the initial testing, the method of operating the devices in to be range extender was established. This initial testing also proved the independent devices were in working condition.

4.1.1 Prisma Ecotech re-commissioning results

As result of the in lab re-commissioning testing, the DC/DC controller control was established via CAN bus using 250kbps CAN settings. The DC/DC controller manual shows the CAN settings as 500kbps. It was assumed, due to the previous work on the equipment, the settings were not factory defaults. Figure 52 and Figure 53 show the controls and status signals for the DCDC controller. According to the test results, the message signals follow the Kvaser database given signal definitions.

700Vdc output voltage was verified with Fluke multimeter. The Fluke was rated for measuring up to 1000Vdc.

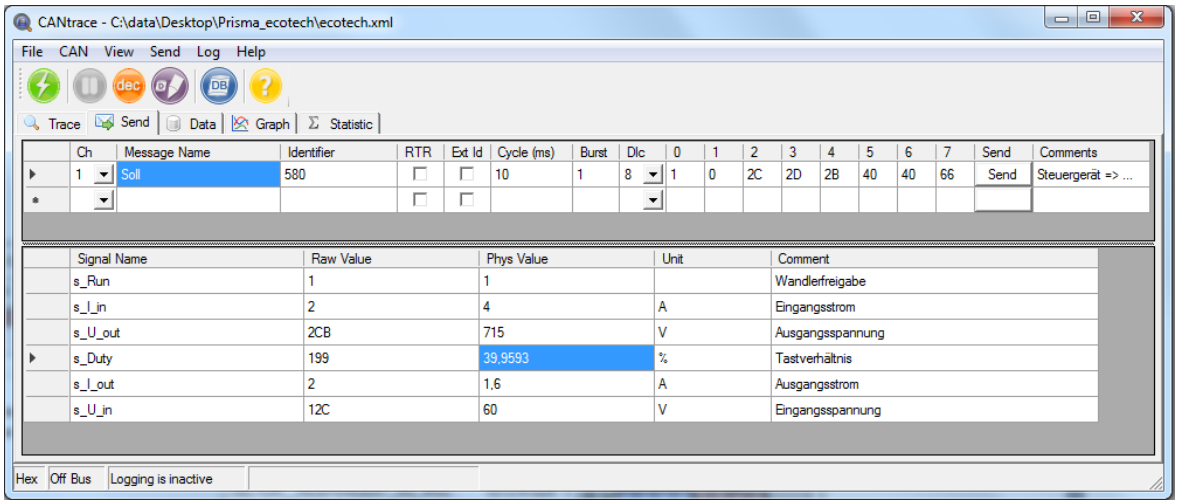

Figure 52. CANtrace Send-tab with physical values for DC/DC controller settings

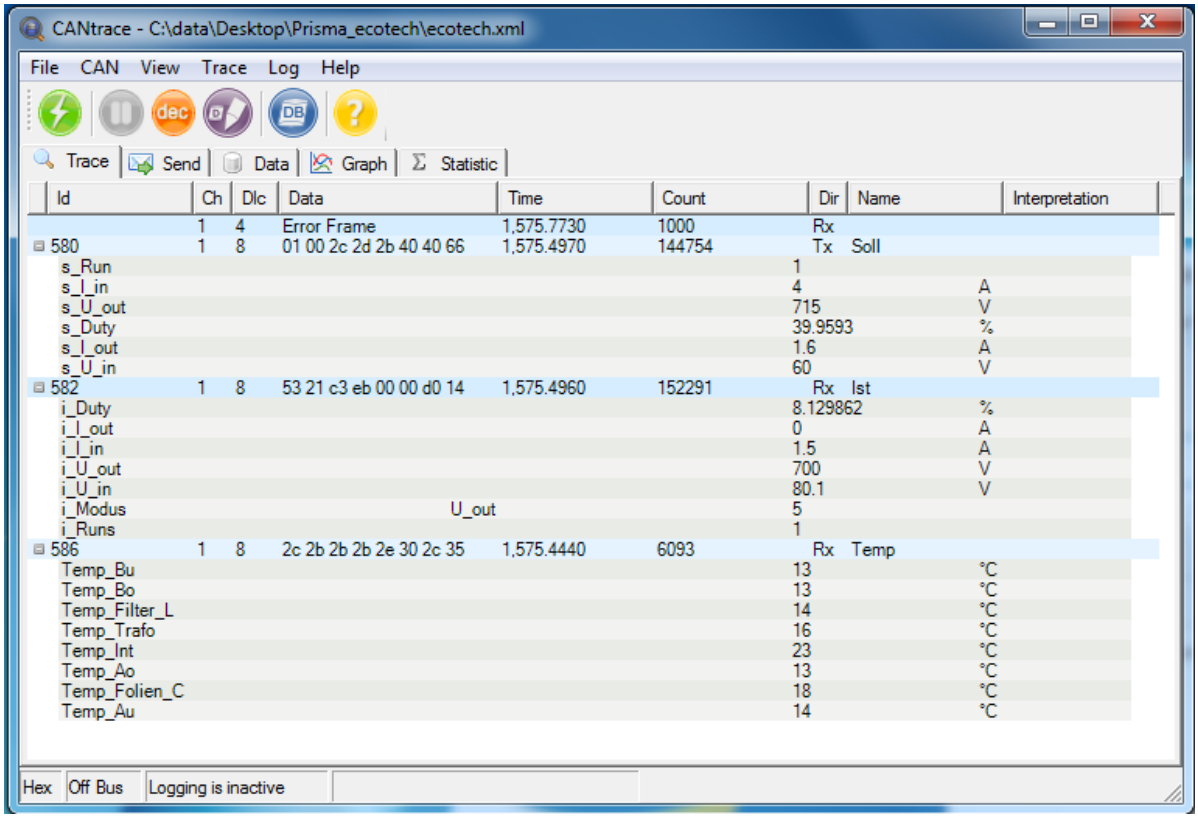

Figure 53. CANtrace Trace-tab with physical signal values for most recent CAN messages

4.1.2 Hydrogenics HyPM HD16 FCPM commissioning test results

The Hydrogenics FCPM commissioning from receiving crate towards integrated part of the range extender configuration involved testing several stages.

In first stage, the FCPM was powered and CAN communications from HyPMview software user interface was established. The test setup required manual CAN terminator on CAN bus, 120Ω resis-

tor was installed between CANL and CANH communications lines to get communications established. As part of the test, HyPMView allowed identify the FCPM module, and also provided list of received CAN IDs used for the initial communications, as seen in Figure 54.

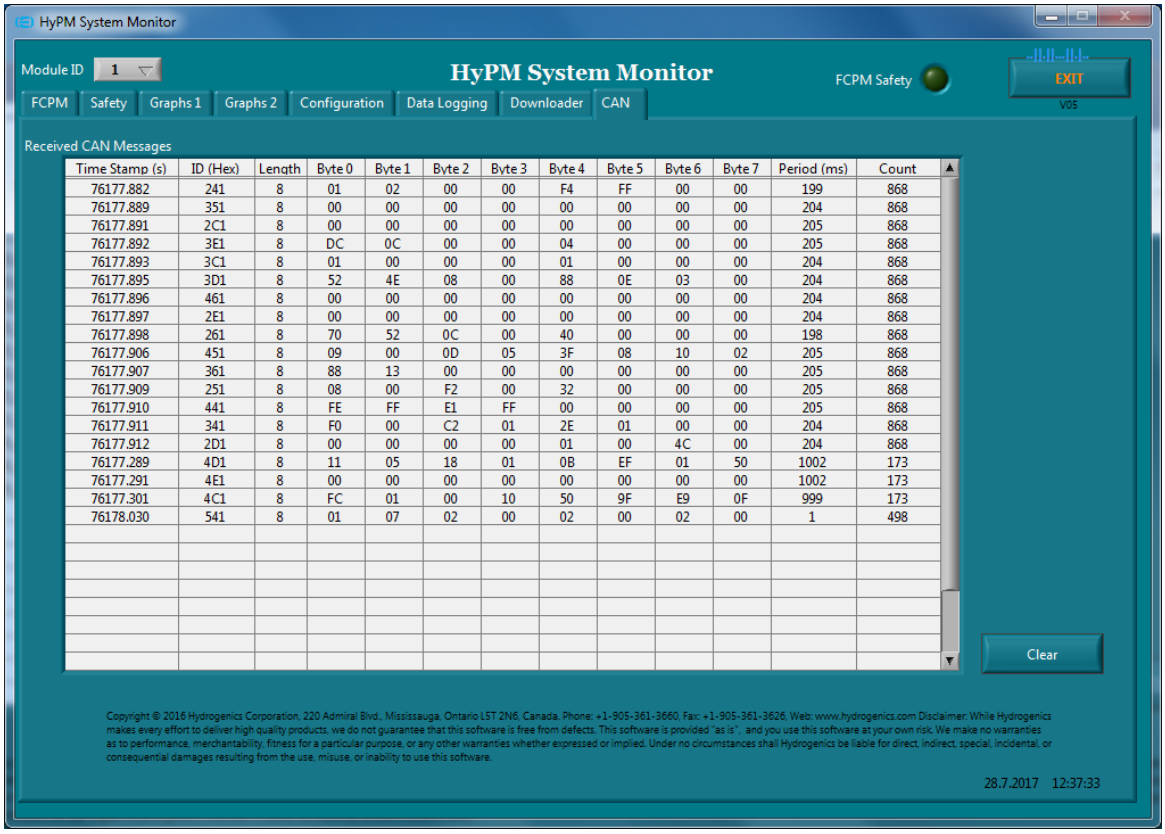

Figure 54. HyPMview software view, CAN message IDs (seen in second column)

Next functional test for FCPM was to prime the coolant circuit using the operation mode Prime. The purpose of thise mode is to commands the FCPM to operate the coolant pump. This step was also instructed as part of instructions in the manual. The purpose of Prime mode is to circulate the coolant and remove air from the circulation. The air moved towards designated air outlet valve near DI filter and towards the coolant reservoir, and air was purged during the process.

After priming the coolant subsystem, the instructions identified additional verification step for hydrogen subsystem integrity check. This mode was identified as Leak Check in command interface Operation Command as seen in Figure 55. The figure shows Leak Check Passed state, as after the FCPM completed pressurizing the hydrogen. The figure also shows the H2 pressure “97,5 ps” after completed test.

The user interface HyPMview at top shows the FCPM state, current power state, as well as the total runtime and energy generated by the module. Below the FCPM state are shown the current operating characteristics of the FCPM module. Below this is the I/O state for the valves and auxiliary devices. In the bottom, it is possible to enable the module to send each cell voltage and the user interface will show these as chart. The cell voltages give indications on fuel operations details, such as health and balance of each cell.

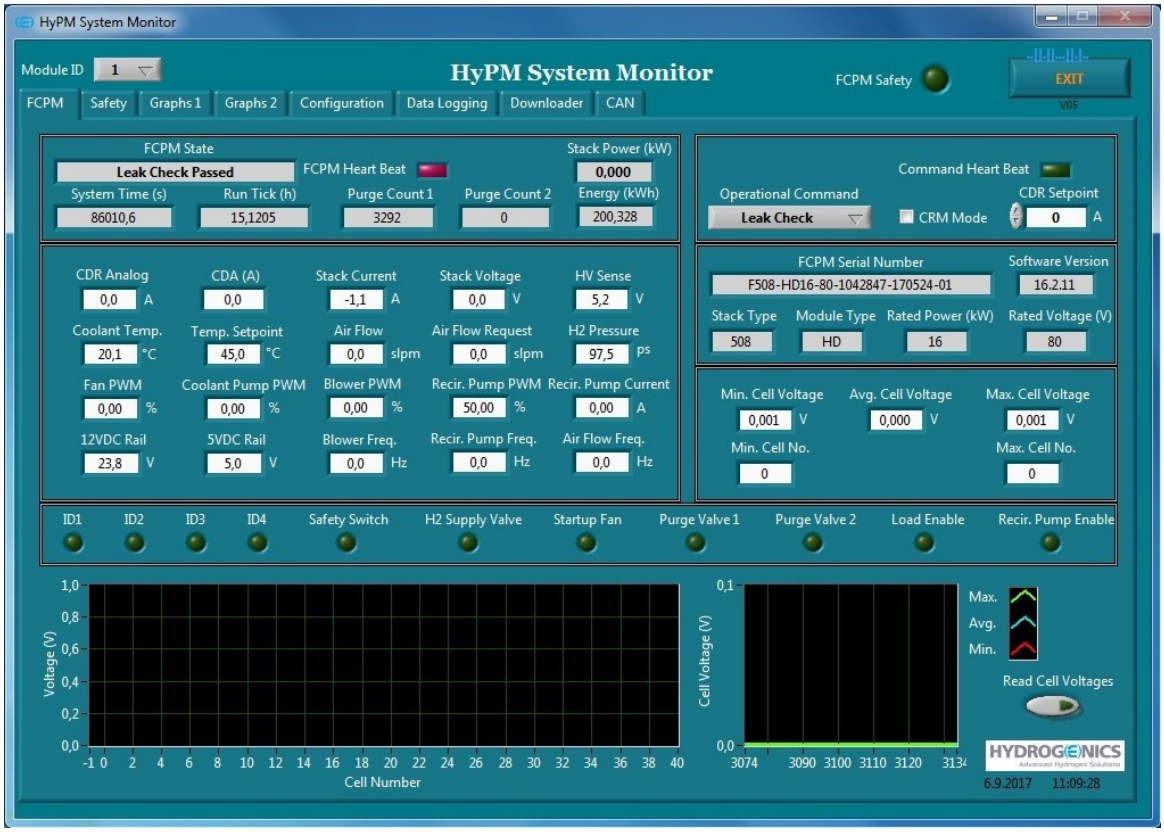

Figure 55. Hydrogenics HyPMview software user interface, Leak Check Passed

After priming the coolant and verifying the hydrogen subsystem, next step was to bring the FCPM into operations. The relevant FCPM Operation Command for this is Run, this moves the FCPM State to Run. When executing the command, FCPM initiates startup sequence, the air blower will work as initial load, this is most likely used also to stabilize the voltage. According to manual the module should not be operated with no load condition.

On FCPM startup sequence, the power module engaged the hydrogen fuel cell fo power generation, and the fan acted as initial load. After bootstrap, the FCPM enabled the power output contactors and started indicating load capabilities with CDA (Current Draw Allowed) signal.

During this test, Chroma Electronic DC Load was used to as current sink in constant current (CC) mode. The load was manually operated and load was gradually increased. The Chroma DC Electric Load user interface values could be also used to cross validate with the values seen in HyPMview, example in Figure 56. In Figure 57, a snapshot of HyPMview can be seen showing the signals in Run mode. Cell voltages are shown in bottom of the figure, the cell voltages seen in picture drop some as the load is increased in steps. In the HyPMview display, it can be alse seen the temperature setpoint for coolant is not yet reached, set point request from FCPM is at 60ºC while actual coolant temperature is 24.5ºC.

More complete breakout of FCPM signals is provided in Appendix 5. During the commissioning test, the FCPM load was increased up to 160A constant current load. The derived resistor graph shows the actual series resistor value of the 3 resistive stove elements being a bit higher for what was used in the planning calculus, the due to small variance in resistor values of the elements used.

Figure 56. Chroma DC Electric Load user interface could be used to verify the results (used in constant current mode). Load setpoint at 90A. Inputs indicate voltage at 59.8V, current 89.9A and power at 5.38kW. Picture by Antti Pohjaranta

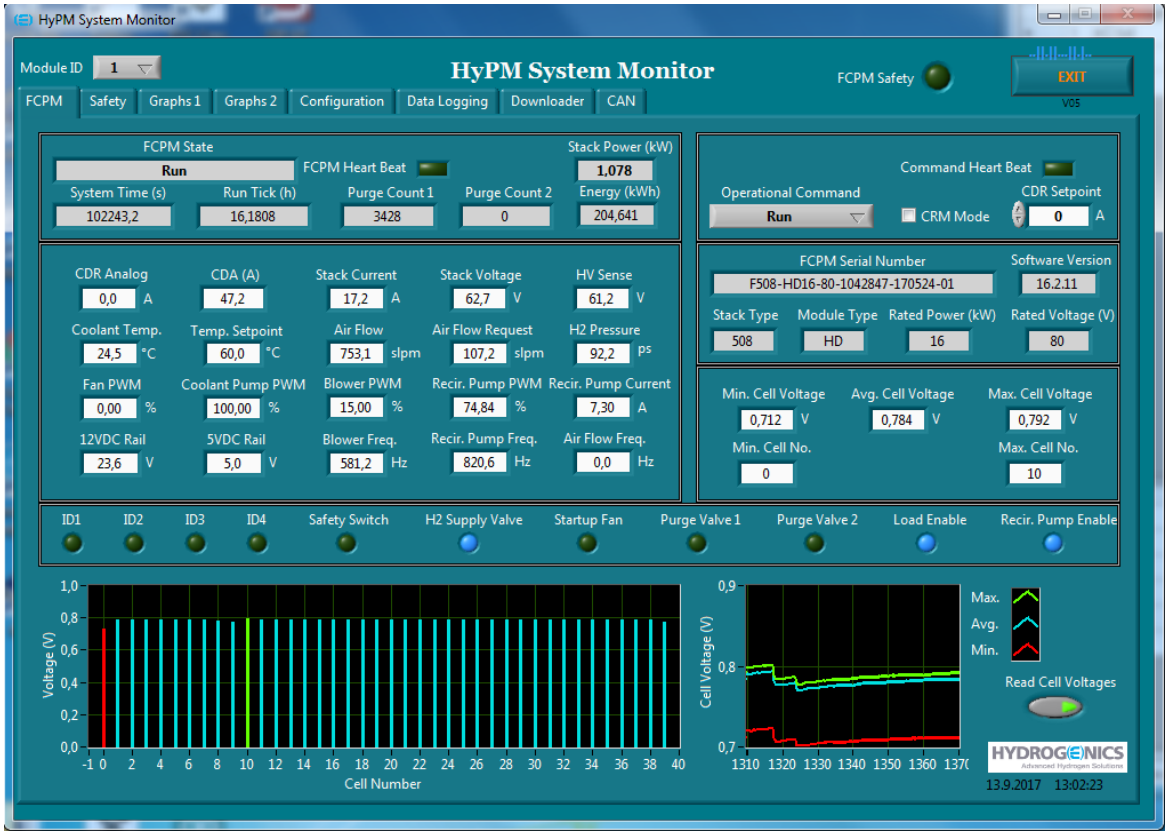

Figure 57. Hydrogenics HyPMview software user interface during FCPM ramp up. Power output shows output power of approximately 1kW

4.2 Integration

From the initial conditions, there was DCDC converter and documents available, as well as the FCPM order in pipeline to be delivered. The initial work was made towards supporting full integration of the next generation FCPM to eMULE vehicle. And when all components were received and first tested and commissioned in laboratory, to proceed into integration testing in eMule.

The integration progress was verified by incremental experiments explained in previous section. The experiments enabled both to verify the progress and to gain insight over the fuel cell power module operations. Also research was made to enable the complete the integration towards the vehicle control unit over CAN and to better understand the operating conditions and requirements needed to complete the in-vehicle coolant circuit. The data analysis completed on the test data gathered while running the experiments also provides good grounds for further analysis for the operations of the device.

For the electrical integration, work was made towards understanding the requirements on interconnecting the eMULE power systems together with the fuel cell power module range extender.

As well as the methods of controlling the power transfer with the DC/DC converter were explored. These includes steps of establishing controlled interconnect of the high voltage power connection between the eMULE power bus and DC/DC converter, ramping up the power output of the fuel cell power module, as well as possibility to drive the fuel cell by current and by voltage.

4.2.1 FCPM output voltage vs purge cycle analysis

As part of the experiments, it was a point of interest to analyze the data gathered to see how the output voltage of FCPM is affected by the actual functionality of the power generation process. The FCPM module manages the hydrogen intake and exhaust as part of the apparatus internal process. The exhaust valve purges part of the anode gases periodically to exhaust. This is due the hydrogen content of the anode gas is consumed by the power generation process. Figure 58 is generated from FCPM test data gathered with FCPM and stove test load. In the figure, the FCPM output voltage can be seen to have relationship towards the increase of current load. The periodical purges can be seen to affect the anode gas pressure within FCPM, but the output voltage does not show symptoms of being affected by the purge cycles.

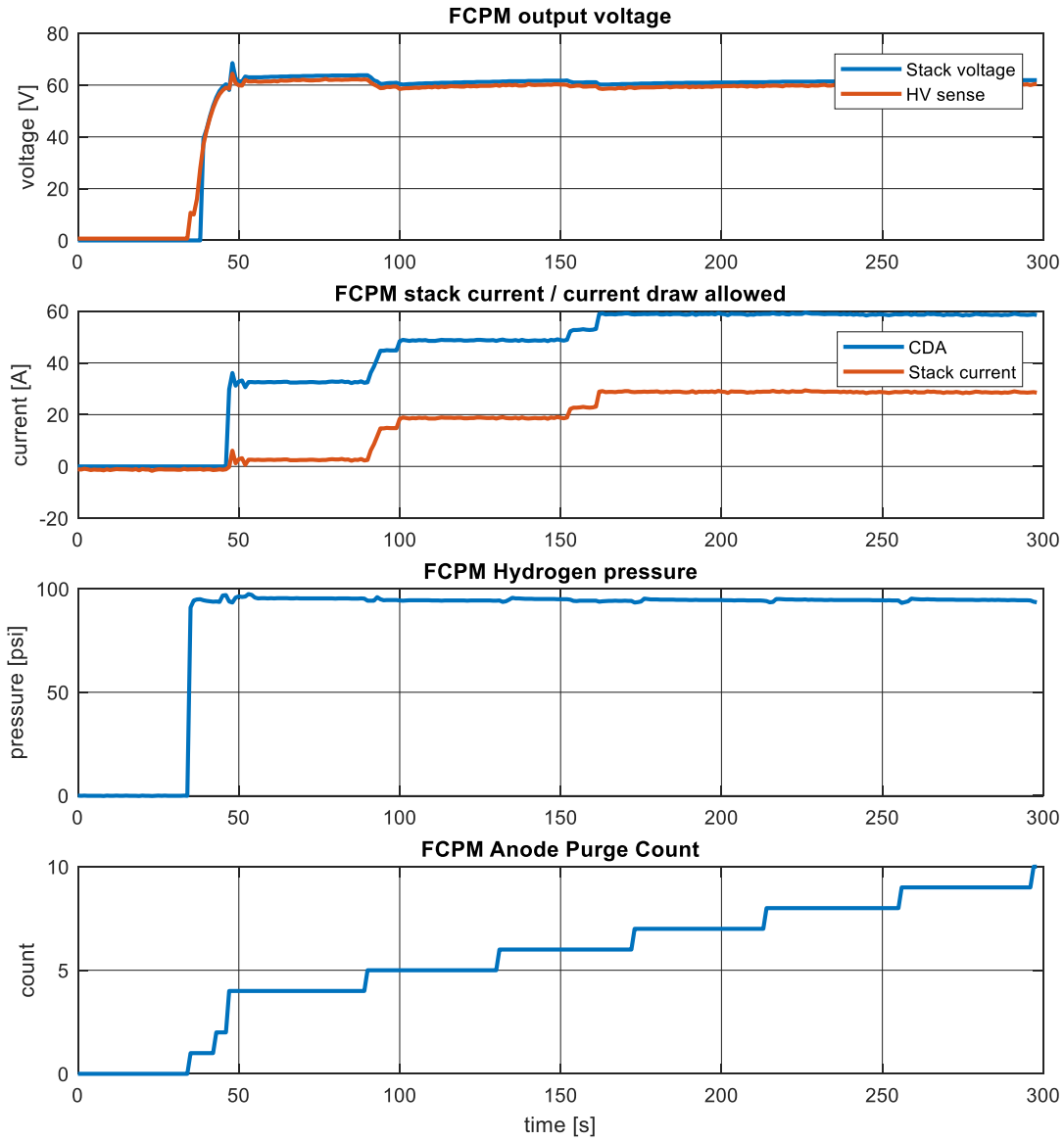

Figure 58. FCPM output voltage, current, hydrogen pressure and purge count

4.2.2 HV DC BUS interconnect precharge sequence

As in the experiment description noted, the power on sequence for FCPM range extender requires pre-charge sequence to equalize the DCDC converter output voltage to battery voltage. This happens before closing the contactors to interconnect the range extender to eMULE power train, the HV DC BUS. In the experiments, the process was driven manually via DCDC converter setpoints. These were controlled through DCDC Ist CAN message via CANTrace send interface. The results are now illustrated with-in Figure 59. DCDC converter plot for first 150s of eMULE integration test.

Results seen at graph explained,

- At 0 seconds, the CAN log file begins, the logging is enabled in software
- Around 40 second of the experiment, the DCDC converter input voltage rises to around 60 volts. At this point, the FCPM is engaged and FCPM has enabled the output enable signal that closes the contactor between FCPM and DCDC converter input.
- The DCDC regulation mode is 0 before around 70 seconds. This mode is described as Initial/Stop and means the DCDC converter is not running. After this time, other signals can also be seen. he lack of signals is because the Ist CAN messagedriving the DCDC converter is not sent before this.
- After around 70 seconds, when the setpoint signals show up, the setpoints for DCDC converter are Input voltage minimum 50V, input current max 2A, output voltage maximum around 630V, output current maximum 0.8A, and duty cycle maximum 97%.
- At this point, the input and output current ramp at the graphs and output capacitor is charged. DCDC regulation mode visit mode 7 during this event, denoting the output current limit when charging the capacitor.
- Around 110 seconds, the DCDC output voltage rises slightly above the setpoint and DCDC duty cycle drop down to 0. At this point, the contactors towards eMULE DC HV BUS are closed by manual switch, and the eMULE DC HV BUS voltage is slightly higher than DCDC output voltage. The converter regulation mode is at U_out state, denoting the output voltage is the driving constraint. As the DCDC converter output voltage is higher than setpoint, the converter does not convert more energy from input side.
- Around 140 seconds, the voltage setpoint is rised above the voltage from eMULE DC HV BUS, regulation mode 2 denotes the power conversion ramps and mode 6 denotes input current limit. Output current resolution is not enough to show the small power transfer of around 2A*65V=130W at output side.

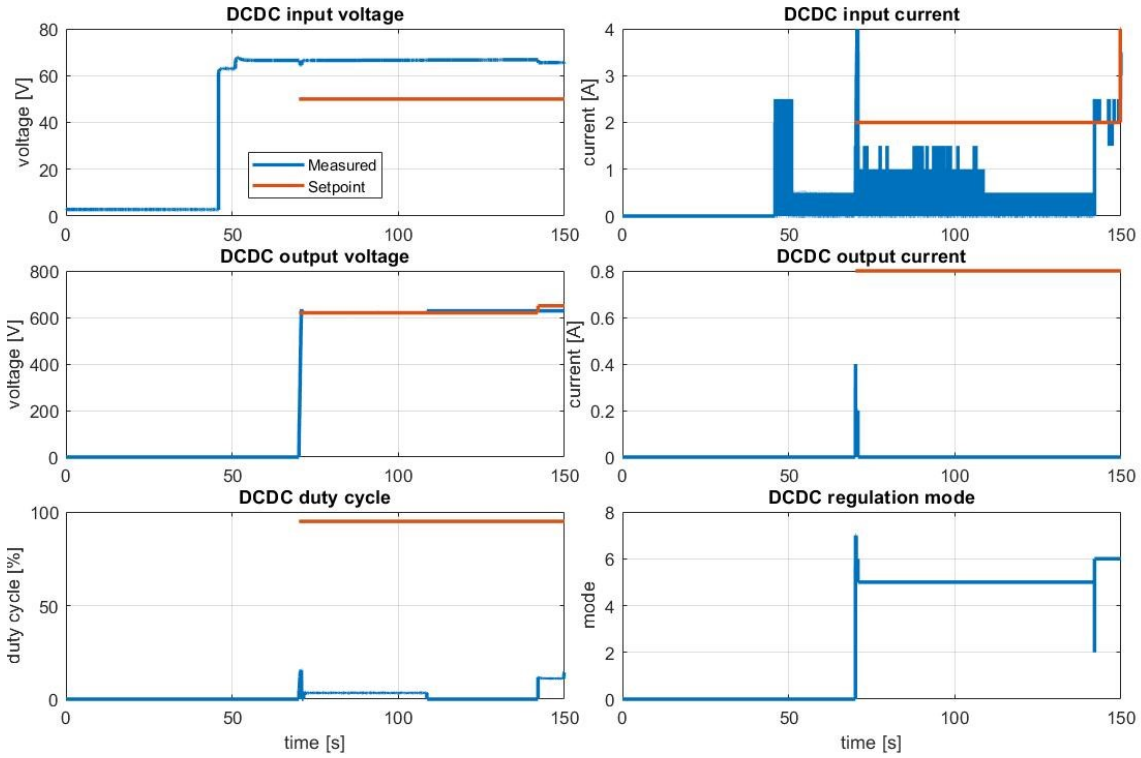

Figure 59. DCDC converter plot for first 150s of eMULE integration test

4.2.3 Integration testing in bus, measure noise in 700Vdc HV line

There was also a test run to attempt measure noise on 700Vdc HV line when charging batteries with FCPM. Target on this testing was to understand the base frequency of DCDC converter and harmonics seen on HV DC line.

This attempt resulted to some small anomalies and conclusion the test setup constructed was not fully adequate to establish the AC noise on DC HV line. Also there was hard deadline on the project due to the author personal reasons.

The first attempt failed due to failed fuse, this was most likely due to failed manually operated precharge sequence as explained in anomalies section below. Second attempt there was no hardware issues, but did not yield very detailed results, and the oscilloscope configuration used in attempt to capture the result was not configured in adequate manner to facilitate analysis on results.

Also it was noted, for some reason, hydrogen pressure is again lower than in initial tests, as well as that the fuel cell voltages oscillated. Figure 60 illustrates the fuel cell voltage oscillations, while also showing the stack power output 6.6kW and output current around 120A.

The noise measurement result was thus inconclusive. Due to hard deadline on project end was reached, and no further practical work part at VTT facility was conducted within the scope of this work. Further work possibilities are discussed in future research opportunities part of this thesis.

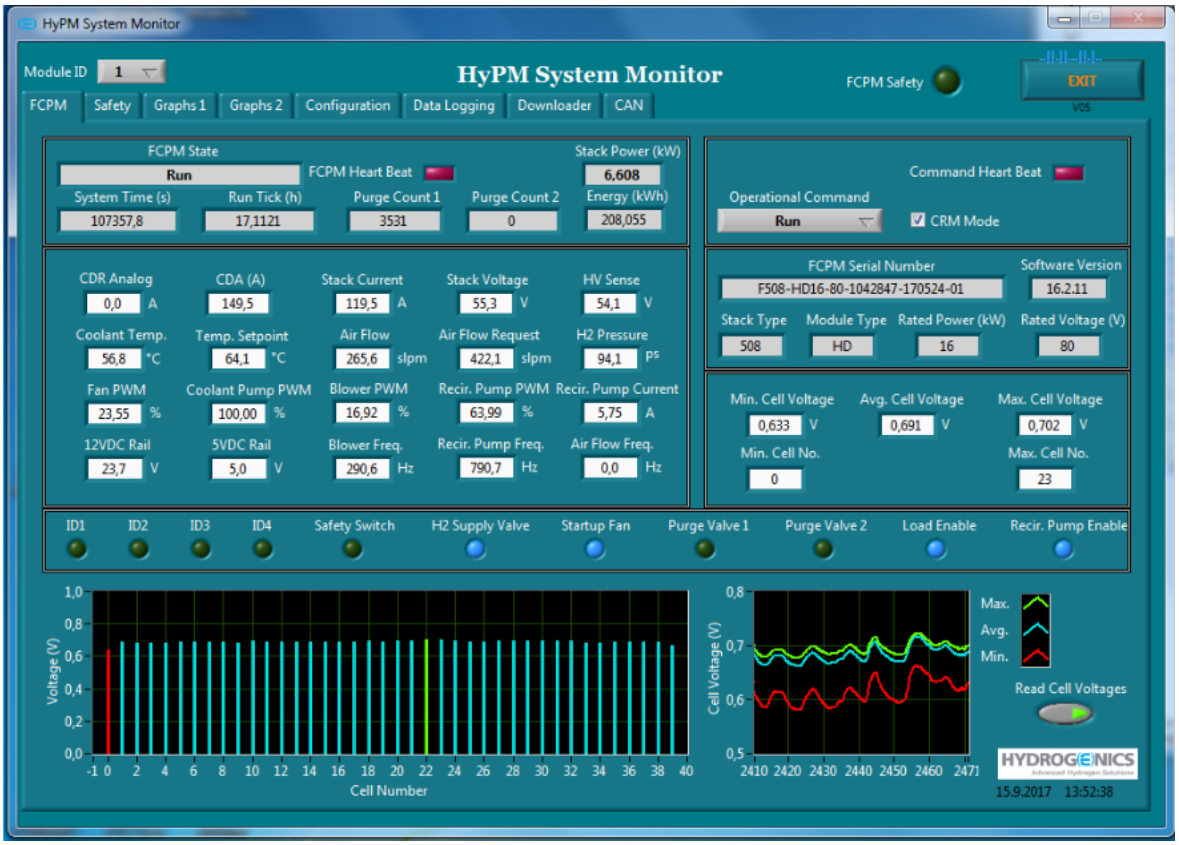

Figure 60. FCPMview while increasing power output

4.2.4 CV mode test

During the integration test, most tests were executed using DCDC converter in current loop mode by using the current as the limiting factor, this was previously referred as constant current mode (CC). In addition to constant current mode, it was also demonstrated the DCDC converter can be used in constant voltage (CV) mode, and use the minimum voltage request from FCPM as dominating limiting factor. The results can also be seen in Appendix 7, between time 1700-2000s, Range extender in bus. Figure 61 shows the DCDC converter setpoints and measurements during test. The test was executed with-in eMule test environment. The purpose of this test was also to see how the FCPM finds new operating point if the output voltage is floated above the measured constant current mode voltage. DCDC converter minimum input voltage setting resolution was 1 volt, so the control precision was of this setting was limited by this resolution.

Some of the reference articles indicate, maximum power point tracking (MPPT) algorithm could enable optimizing the operating point of fuel cell. The sources introduce additional layer of control for both current and voltage setpoints on the fuel cell and DCDC controller. This result was conducted in open loop mode, and only DCDC control signal was operated during test.

The test result does not yield into much conclusive result on weather MPPT algorithm is feasible or not, rather illustrates controlling DCDC input voltage setpoint alone yields the current to drop. This could be interpreted as moving along the I-V chart introduced before in Figure 31, as would be expected when operating in open loop mode. Research papers on the MPPT topic are available, but many of these are based on theoretical models in simulated environments.

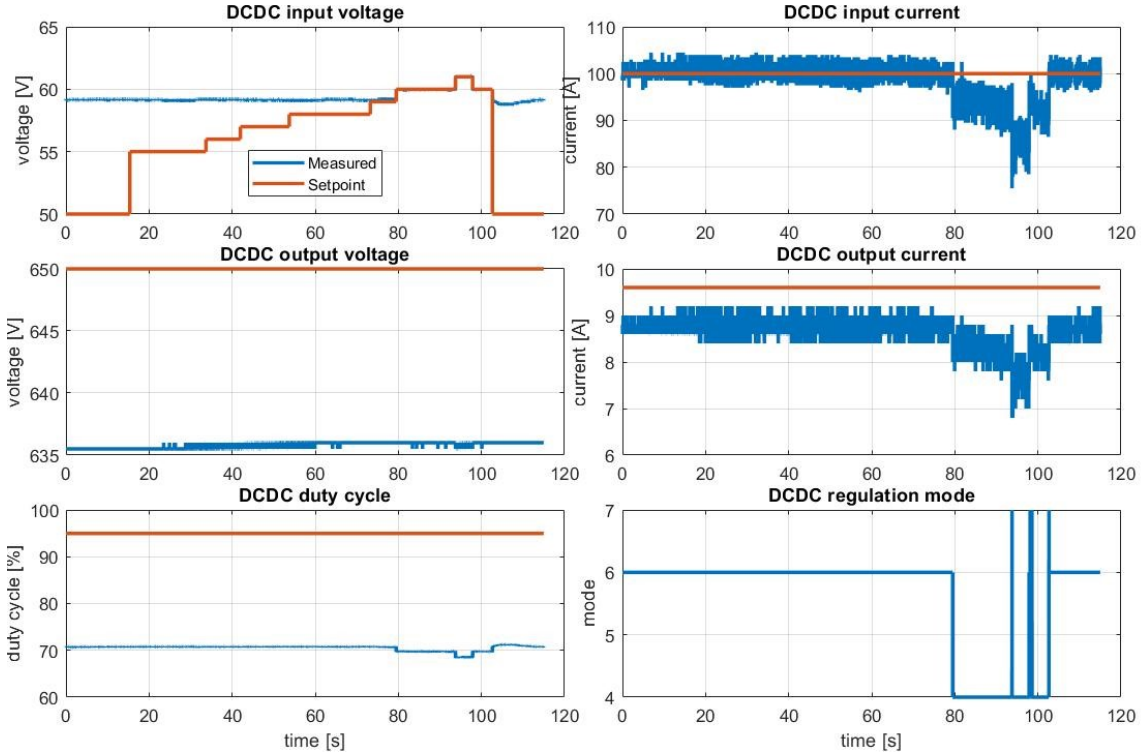

Figure 61. CV mode test experiment results, DCDC converter setpoints and measurements

4.3 Processing experiment results

The Matlab code to process the experiment results is part of this work as these provide ground for further integration and solution analysis on the FCPM range extender. The log data is not very effective tool without tools to visualize it properly. During making of this thesis, effort was put also to visualize the results for reader.

4.3.1 Matlab optimization

As for Matlab side of data processing, understanding of the underlying platform functionality can be beneficial when processing data. Matlab is software developed by Mathworks, and the name is short for matrix laboratory. Matlab functionality has been optimized for processing of matrix form data, and keeping this in mind, the solution optimization can be achieved.

As Matlab was chosen for the platform to process the data collected during experiments, implementing a method with reasonable run time enabled more easy access to the data. Table 7 gives example of same functionality implemented with for loop and with matrix operations. In Table 8, Matlab tic-toc functions are used to benchmark the methods, and this shows the execution time of roughly 0.2 seconds on matrix method compared to 10 minutes of execution time with loop method. It can be observed, optimizing the code to use operations matrixwise rather than as for-loop can yield significant improvement on execution time.

```
function [ istdata ] = parseist ( candata )

lines=size(candata,1)

ist=candata(:,4);
count=size(ist(ist==1410),1)
count=0;
istdata=zeros(count,8);

for i = 1:lines
    timestamp=candata(i,2);
    id=candata(i,4);
    if(id==1410)
..
        data1=candata(i,8);
..
        runs=bitand(data1,1);
..
        row=[timestamp,double(runs),dou-
ble(modus),uin,uout,iin,iout,duty];
        istdata(count,:)=row;
    end
end
```

```
function [ istdata ] = parseistoptimize( candata )

lines=size(candata,1)

% Select ID 1410
istcandata=candata(candata(:,4)==1410,:);

timestamp=istcandata(:,2);
data1=istcandata(:,8);
..
runs=bitand(data1,1); % bit1
..
istdata=[timestamp,double(runs),double(modus),uin,
uout,iin,iout,duty];
end
```

Table 7. Code (shortened), left one is loop, right one is unwind as matrix operations

```
>> tic;[istadata]=parseistoptimize(candata);toc
..
Elapsed time is 0.199920 seconds.
>> tic;[istadata]=parseist(candata);toc
..
Elapsed time is 581.444448 seconds.
```

Table 8. Comparison of execution time for two methods of parsing signals from CAN data

4.3.2 Matlab images

During the writing of thesis, feedback was given per graphs showing the DCDC and FCPM signals for bad use of space. Getting the graphs readable required some work and additional tools. Part of the solution for this was to use matlab extension, subplot_tight. This allows setting customized margin between graphs and better usage of space.

This was available from,
https://se.mathworks.com/matlabcentral/fileexchange/30884-controllable-tight-subplot

Another solutions included defining constraints for the figure plotting in matlab, for example line:
`figure('units','normalized','outerposition',[0 0 0.5 1])`

This defines the size of window matlab opens in normalized size on height and width. The figure aspect ratio is kept when the images were inserted to the actual thesis. It was also good advice from instructor, there is a difference weather the image was just copied, or exported in between Matlab and Microsoft Word.

4.4 Anomalies

This section documents the anomalies recorded during the integration and testing the range extender configuration. As anomalies, the author accounts unforeseen issues that arised during integration due to phenomena not predicted but required attention during the work.

4.4.1 DCDC output connector short circuit

The DCDC converter was tested during the integration into range extender configuration with stoves as load and laboratory power supply as power input. The DCDC converter did not report the output voltage to rise, rather stayed in 0V with currect limit mode. The fault was localized to the DCDC HV output connector, the connector assembly pins were assembled wrong.

The connector was repaired, the connector was inherited from previous project and the connector had some internal interlocks loosen. Most likely the connector had been opened during previous experiments. Analysis is that the connector might had been dropped when the components were moved from lab to another.

During the following tests, the connector was observed more carefully and the connector is planned to be replaced with new components. Appendix 4 has the assembly document for the connector. When carefully assembled according to the document, the connector is designed confirm environmental scope of the interconnect as required.

For the DCDC converter, the operations algorithm was considered quite robust in case of current limit, as it was not able to increase voltage, the setup did not experience any damage.

Figure 62. DCDC output connector

4.4.2 CO alarm in laboratory

Laboratory used for integration testing the FCPM experienced CO alarm when the FCPM module was powered down. During the shutdown, FCPM purged the gases from the fuel cell stack. The hydrogen purge/exhaust pipe had T-section in the pipe to allow water to flow downwards and the section up wise. The CO detector is also very sensitive to hydrogen. Figure 63 illustrates the exhaust water container and CO detector position relative to the hydrogen tank seen on both pictures.

Improved solution could be to have water in the container so the lowest pressure drop route would be through planned venting pipe leading upwards instead.

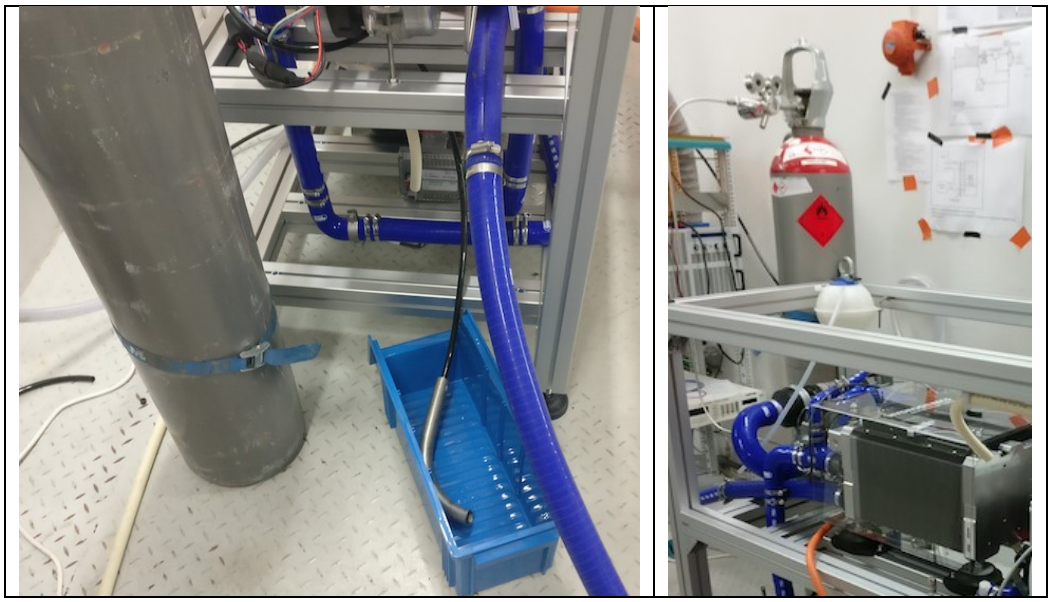

Figure 63. Left is hydrogen exhaust route for condensated water, right picture shows location of the CO alarm. CO detector is orange item mounted on wall.

4.4.3 FCPM air flow alarm

One alarm was accounted and recorded with FCPM during test run sequences. The module reported air flow when not running. No actions were necessary due to anomaly, but capture of HyPMview window of safety tab showing the event was recorded to be presented as example of FCPM Safety Message Log, this is shown in Figure 64.

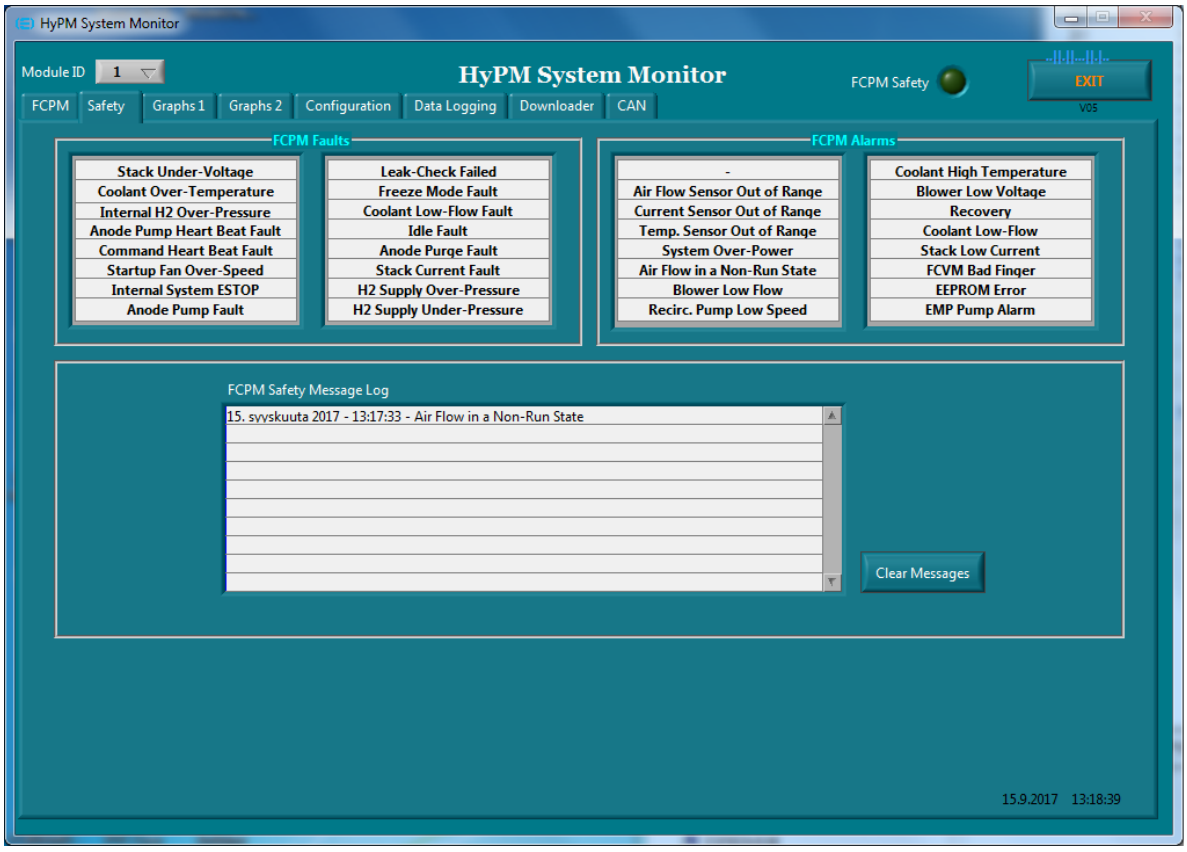

Figure 64. HyPMview alarms

4.4.4 HV fuse blown

During the experiments in eMule, the FCPM was engaged and the HV DC connection towards the eMule DC HV BUS did transfer power when test setup was being brought up. The experiment was shut down and fault was localized to blown 50A fuse. The root cause was estimated to be caused by incorrect pre-charge sequence when connecting the DCDC converter to DC HV BUS. Unless the voltage levels are manually equalized by setting the DCDC converter output to observed battery voltage level, the voltage difference in output capacitors of DCDC converter can cause surge enough to blow the fast 50A fuse. Picture of the fuse in Figure 66.

As the test data was recorded on CAN, the data can be illustrated. The Figure 65 shows the test data trimmed to events,

- At around 5 seconds the DCDC input rail voltage from FCPM is connected
- From around 50 seconds, the DCDC converter CAN setpoint message appears. The DCDC converter operations are engaged, but the DCDC input current setting is too low to properly charge the output capacitors.
- The most likely point of DC HV BUS contactor interconnect engage is around 65 seconds as no DCDC converter setpoint is seen to drive the, however the voltage ramps up. But the current needed to charge the capacitor exceeds the fuse rating.
- At 85 seconds, the next ramp is driven by input current setpoint.

After the anomaly, the fuse was replaced and test was re-executed afterwards successfully, with emphasis given on the pre-charge sequence execution.

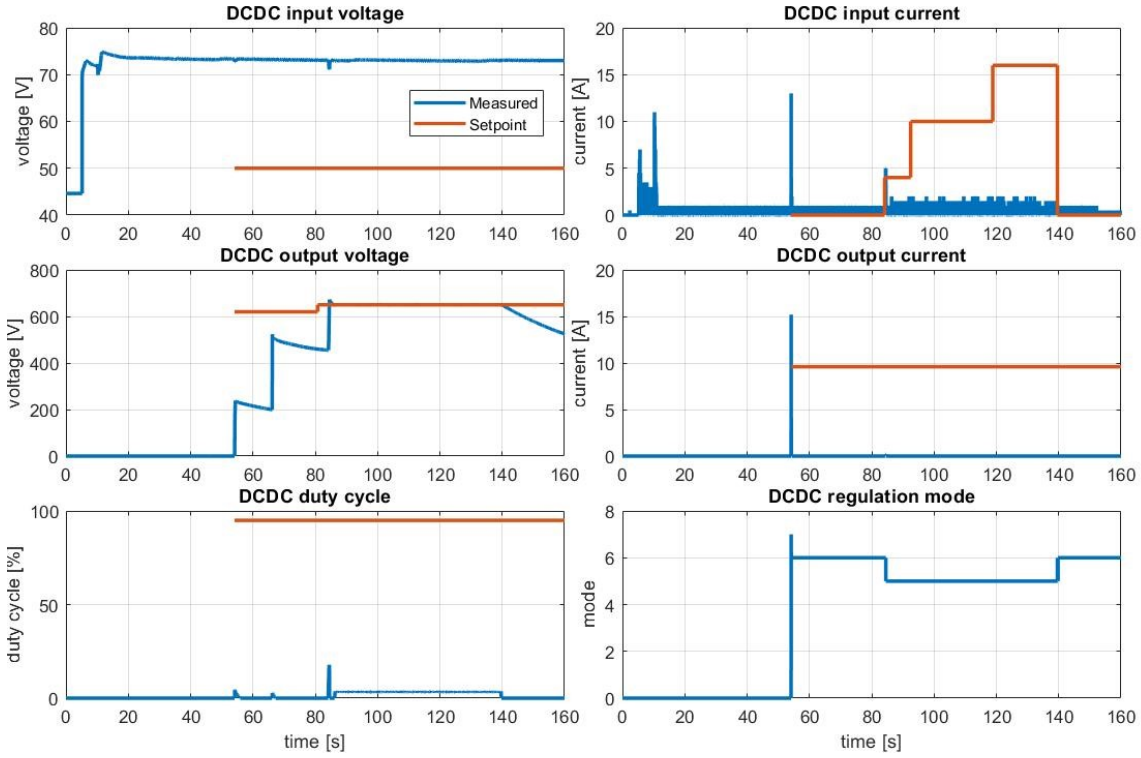

Figure 65. Test data plot out (trimmed to 110-270s from original data)

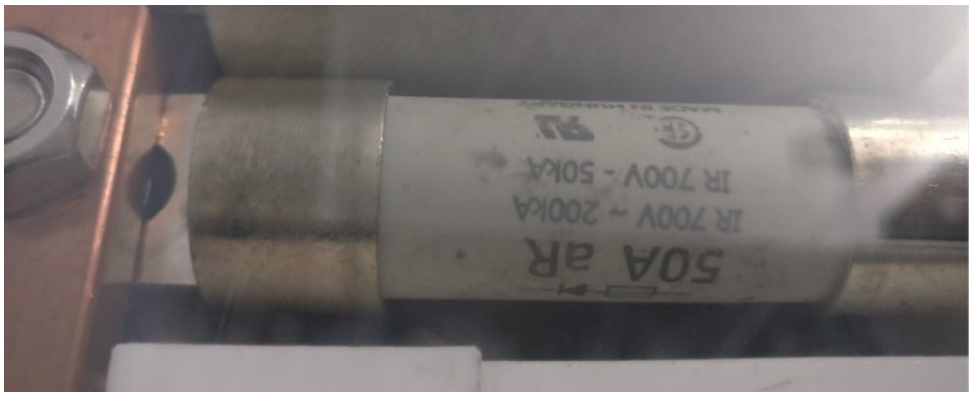

Figure 66. HV fuse in DC HV BUS rail, rated for 50A

4.4.5 CAN log timestamp anomaly

When processing the experiment data from CAN log, the processing pipeline gave out graphs with extended experiment duration, up to 44000 seconds. The cause was pinpointed to CANTrace log file. The workstation used for the system was HP EliteBook with two CAN adapters, one Kvaser and one PEAK adapter. Both CAN busses were interconnected in this test, and data was recovered from log file generated with HyPMview, as both software logged all data.

Root cause for the anomaly might be increased CAN message rate or issue on having two different CAN adapters on same system.

```
// Id: 961 Msg Name:
Signal list:

  1766.101000  1  3c1  Rx  d  8 9b 02 e3 02 f5 02 00 0a
// Id: 977 Msg Name:
Signal list:

  1766.102000  1  3d1  Rx  d  8 b2 1e 09 00 60 28 03 00
// Id: 705 Msg Name:
Signal list:

  1766.102000  1  2c1  Rx  d  8 00 00 00 00 00 00 00 00
// Id: 1121 Msg Name:
Signal list:

  44715.776000  1  461  Rx  d  8 00 00 00 00 06 09 48 00
// Id: 609 Msg Name:
Signal list:

  1766.103000  1  261  Rx  d  8 26 d5 0f 00 00 00 39 00
// Id: 1105 Msg Name:
Signal list:

  44715.777000  1  451  Rx  d  8 0b 00 11 05 43 08 10 02
// Id: 865 Msg Name:
Signal list:

  44715.777000  1  361  Rx  d  8 96 18 00 00 44 1f 3a fe
// Id: 849 Msg Name:
Signal list:
```

Listing 2. CANtrace log file LogFileFcpmDcdcBatteryFuse.txt part with time skew

4.5 Future research opportunities

As result of this work, the integration towards bus works on electrical and mechanical level give sufficient integration level for testing towards vehicle power electrical side. Due to the deadlines and selected goals during the work, the fuel cell range extender integration was not fully complete to allow mobile operations on the vehicle. Further work is required for example on the coolant system as the coolant temperature was operated by manually valves and secondary circuit used tap water.

Also, for example the given hydrogen tank supply solution used in the experimental part was considered to be temporary solution for duration of the integration test, not the actual solution for the vehicle. Even additional steps might be necessary to confirm regulations to operate the vehicle with FCPM range extender on public roads. The initial test was not planned as such.

Yet, the integration work committed together with this documentation lays path towards complete integration. Some steps regarding such integration steps were also partially researched simultaneously during the practical work. The integration level established already enables further practical research on multiple areas and fields regarding the solution.

In this subsection, possible points of future research interests are discussed.

4.5.1 Coolant subsystem

The mechanical integration in the experiment was implemented using manual valves. The FCPM implements functionality for the thermostatic control over the coolant and subsequent tuning of the PID control values that can be controlled within the fuel cell module logic. In Figure 67 the HyPMview configuration tab, the controls over the coolant control output signal are shown. This allows tuning the thermostatic controller in some extents.

The result section of this thesis also shows the control logic control signal towards the valve as supported feature, but the actual control during the experiment was by manual valves. The actual electrical signal from J2 connector was not monitored, just the HyPMview value logged over CAN. When implemented, the FCPM supports temperature control over more than single method, such methods are for example PID PWM signal from J2 or as temperature set point over CAN (ID 0x340+fcpmid).

As additional requirement, the coolant circuit flow is defined in the FCPM requirements for water. The requirement is 40l/minute. The documentation states that if coolant other than water is used, the temperature variation over the FCPM should remain similar.

Figure 67. HyPMview window capture, configuration tab

4.5.2 Full power 16.5kW output from range extender

This thesis covers testing the FCPM up to 160A, the limit was introduced by two factors in electrical side. One reason was due to use of the old inherited isolation connectors and 200A isolating contactor between FCPM and DCDC converter. The power loss on additional resistance in path between the FCPM and DCDC converter was considered a risk on high current in case the current path is verified for low impedance. New connectors and contactors were in order pipeline during this work, but the focus was finishing the integration.

On mechanical side, the manual valves used to operate the coolant circuit were of additional concern. Together with the fact the coolant flow was not observable, the flow rate requirement could not be verified during the test. The coolant flow can affect the internal equilibrium of the fuel cell stack temperature, and inadequate flow could potentially cause hot spots to form in the stack. The reasons of this requirement are not listed out in the instructions manuals. The coolant system should be improved for more robust setup.

For full power tests, the electrical and mechanical improvements described should be enough to allow the full 16.5kW power output from range extender.

4.5.3 Closed loop control of the FCPM current control

The tests concluded were manually driven tests and no attempt was put to use Current Draw Request (CDR) message towards the FCPM. In the experimental test seen in this work, the FCPM was driven in open loop mode and FCPM was only given Run command. The DCDC converter was

used to drive the power requirements towards the FCPM. For the FCPM control, there is also option to use the FCPM in closed loop and indicate the current request towards FCPM.

This could be used as alternative approach when ramping up the power output from FCPM. Also, closed loop control could potentially facilitate further MPPT topic related testing (discussed briefly in section 4.2.4).

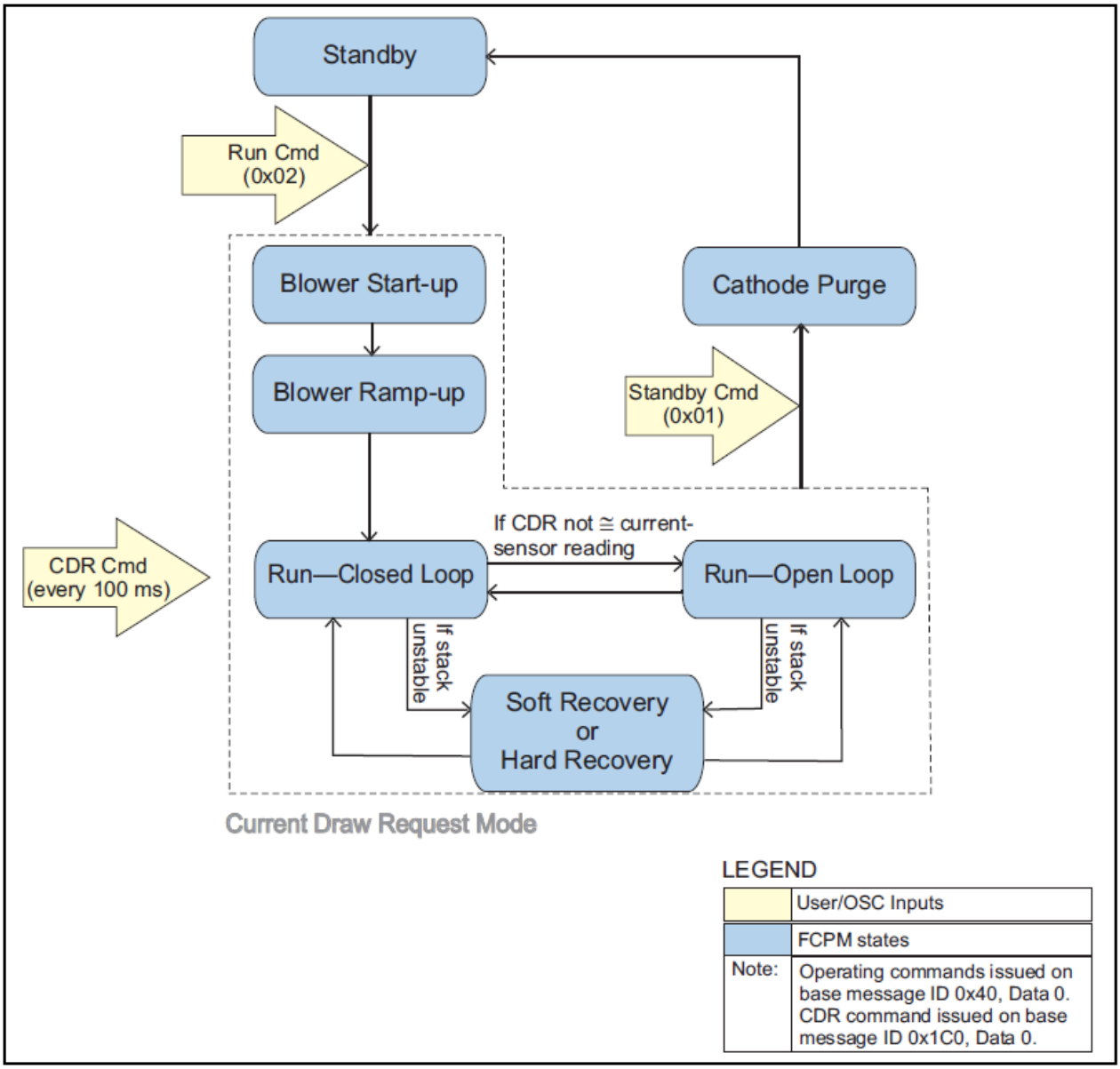

Figure 68. FCPM Run: Current Draw Request Mode, State Transition Diagram [21]

4.5.4 Cold environment, water and coolant circuits

One of the target research objectives on eMule fuel cell research is related to the cold northern climate. As the fuel cell process involves use of water, freezing temperatures are challenging. Overall the cold operating conditions affect needs to be further evaluated. As part of this work, the requirements were only lightly chartered.

The part that was researched partially was coolant process, it will also need to adjust properly to the environment and control needs to have enough dynamic operating range to allow the secondary coolant circuit operate both hot summer day as well as cold winter day environments.

The integration testing was completed with DI water as primary FCPM coolant and tap water as secondary circuit. Option for sourcing BASF Glysantin® FC G 20-00/50 for coolant was also explored as part of the work. The product is tested to be material compatible with typical FC applications, and gives some material compatibility data on the datasheet as can be seen in Figure 69.

Material compatibility	As the development of fuel cell systems is rather innovative, the compatibility of the coolant with construction materials has to be tested for the individual application. BASF offers respective lab tests. The following types of construction materials have been tested with Glysantin FC G products. Compatible: Stainless steel, titanium, aluminum, copper, brass, graphite, PTFE, PE Not compatible: Zinc, galvanized steel, cast iron, carbon steel Polymer materials and elastomers often contain considerable amounts of fillers and adjuvants, which might impact the electrical conductivity of the coolant. Examples are EPDM, PVC, PA 66, silicone rubber, Viton, etc..

Figure 69. BASF Glysantin FC G 20-00/50 coolant datasheet, material compatibility [22]

BASF gave the coolant availability in 120l (127,8kg) containers. The primary coolant circuit used in the experiments was measured to contain around 4 liters when emptied. For small scale integration, the container size was considered suboptimal as the liquid price was in price range of 10+ EUR per kg. But as required by research and being compatible with other automotive applications, the size is not likely to be an issue, rather inconvenience.

4.5.5 Using the excess heat for in vehicle heating

As the fuel cell electrical output efficiency is around 50%, rest of the energy is released as heat. As the bus is designed to have environmental control, energy is also used to drive the air conditioner as was shown in section 2.4.2. For example in arctic operating environment, the overall hydrogen powered efficiency could be improved if the excess heat could be used directly to heat the cabin during winter.

This would require additional heat exchangers, piping and control logic to manage the energy flows from coolant into cabin heating. For example, the coolant circuit still needs to maintain the setpoints requested by the FCPM control . Thus concept could be for example introduced by control algorithm distributing the excess heat between cabin heating and exterior radiator when excess heat is available.

4.5.6 Control algorithm and VCU control

Fuel cell hybridization of the eMULE platform enables interdisciplinary research between VTT fuel cell, alternative energy and automotive research groups. In house integration of commercial fuel

cell module allows understanding of the integration aspects for the fuel cell module, and testing for example different higher level control algorithms.

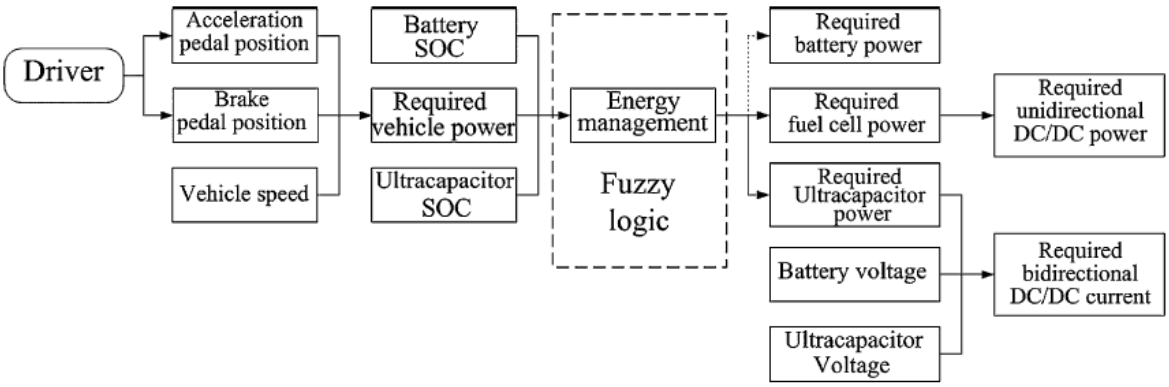

Figure 70. Powertrain energy management example [4]

Such algorithms can control energizing the fuel cell and energy management for powertrain components, including the range extender. The algorithm can include for example planner based on which electrical bus power sources are to be engaged while a bus is driving on route to optimize the availability, costs and range based on specific needs. At moment of writing, using energy from battery is most cost effective solution than powering from hydrogen. Example of powertrain energy magement can be seen in Figure 70, this literature reference also included ultracapacitors.

The higher level control logic towards the fuel cell and DC/DC converter was not finished during the work, but compatibility of the controls was evaluated. To complete the integration towards VCU, the high level control logic needs integration towards the eMule VCU CAN bus. The requirements and compatibility with the eMule systems were reviewed and the CAN identifiers were found not conflicting with the eMule 250kbps CAN bus, so the devices could be directly connected to this VCU 250kbps CAN bus.

First the VCU code needs to be made to communicate with the FCPM and DC/DC converter as well as the controls of DC HV BUS contactors. The VCU needs to implement CAN controls and power up sequences such as the power up precharge sequence as lower level control and later the higher level planners can be implemented as higher level controllers over the base functionality.

Also while the Prisma Ecotech DC/DC specified maximum output side voltage 700Vdc is enough to charge the eMule batteries, it still has some minor conflicting specifications specification in certain usage cases in eMule.

For example the fast battery charge will charge the batteries with voltage levels at 800Vdc. The Prisma Ecotech DC/DC converter must be disconnected from the voltage rail before the voltage is expected to rise above the maximum specified voltage for the converter. Due to this, another DC/DC converter option might need to be considered.

When implementing actual logic for the FC and DCDC hybrid control, it is also necessary to observe the power consumption is not a constant and the battery voltage level will be affected differently when the battery is being charged or discharged. As the DC/DC controller is controlled by voltage and current, the relationship of these is not constant on output side when the battery level changes. The current Prisma Ecotech DC/DC module can be also driven in current mode from the input side, and input side is less likely to be affected by the changes in output DC bus and thus could be able to deliver constant power mode.

5 Conclusions

As for the integration work, the work resulted as mechanical and electrical integration as modular range extender deployment on the eMule. The components were integrated together into rack chassis that allows the range extender assembly to be deployed to the bus. The fuel cell range extender needs further work on coolant system, control integration, integration testing, as well as the chassis needs to be securely mounted to the vehicle in order to enable mobile operations on eMule. During the work, the coolant circuit was arranged with temporary manner, as actual solution was not yet available.

As original goal, it also covered enabling the range extender module to be operated vehicle control unit control as well as operated while driving, during this the authors working period. The vehicle control unit control was not however tasked to the author. The working period was during mid-summer, and in Finland this season is main holiday season with typical 4 weeks of vacation.

The original initial plan was somewhat abstract. The plan was made towards integrating the range extender assembly on wheeled table. While the actual range extender realized with custom-built aluminum structure, this needed to be ordered from manufacturer. As for projects in general, changing requirements during project are recognized to affect the costs and project schedules, with least impact when prepared as early as possible. As given work assignment for the master thesis project was abstract, together with fixed deadline of the practical work, meeting the redefined requirements did not allow all original goals to be met. Original work description was also planned for 6 months period, while the practical work had time window of 3 months.

Figure 71. Forklift fits under the range extender rack, making the rack reasonably movable

For the technical approach, the solution quite much follows those documented in the technical material provided by the FCPM manufacturer. The technical complexity seen in the experiments overall did not give much surprises. Yet still, author had learned new aspects on high voltage coupling of circuits. For example, the pre-charge sequence when establishing the power rail connection from DCDC converter to eMule HV BUS was something new to author. Some of the project goals were

not fully taken into account when the frame was still on design table but realized well in the actual product. Figure 71 illustrates fork lift can fit under the rack. The height of the lower shelf was considered during design to enable fork lift, but the constraint used to design rack side was the trolley space in vehicle. But the forklift fit from the side, as well.

For authors personal interest, it would have been interesting to give more time and research a bit if the closed loop control allows moving on the IV chart and to evaluate feasibility of maximum power point algorithm (MPPT) with DCDC and fuel cell to see if there is local maximum for the efficiency, as some literature might suggest. In theory, would allow the ratio between current and voltage to vary some while power would be kept same. The fuel cell equations also include negative impact for the current. For this part, trying to explain this internally within my team, the author found it hard to explain the theory partly due to lack of common terminology on matter.

For technical side, this thesis contribution is on added value given by documenting the details of the implementation of the described FCPM based range extender solution. For the Hydrogenics FCPM part on findings, worth noting that for this thesis author, documentation for two generations of HyPM solutions were available. Author expected the latest generation documentation to be also more specific and maybe improved, but the case is, some of the CAN communications diagnostics documentation was dropped from the documentation for new generation. Thus, availability of documentation for two generations of FCPM was beneficial on understanding operation the FCPM.

For the eMule and fuel cells in busses in general, the target in big picture is to research on fuel cell feasibility on last mile electrical busses. For example, the battery technology does not yet provide energy to weight efficient solution to keep the bus driving for a day with single charge, similar to fossil fuel operated vehicles do. The fuel cell technology could enable full day operations when the vehicle tanks would be filled at depot overnight. Therefore, the bigger picture question is for example weather the operating costs of fuel cell hybridized solution fleet of busses can be competitive together, when comparing to for example costs on deploying electrical charging stations on bus route instead. Comparing the solution into charging electrical bus fleet is also yet more multi-dimensional as this might also have impact on the power grids. The typical transmission capacity by the suburban utility grid is not sized for energy requirements of rapid charging of multiple electrical busses.

Overall, working with fuel cell team at VTT was able to give author the overall picture on where the fuel cell technology of today stands.

6 References

[1] Z. O. Sharaf and F. M. Orhan, “An overview of fuel cell technology: Fundamentals and applications,” *Renewable and Sustainable Energy Reviews,* vol. 32, pp. 810-853, 2014.

[2] V. Ayfer and R. Macario, “Fuel cell vehicles: State of the art with economic and environmental concerns,” *International journal o f hydrogen energy,* vol. 36, pp. 25-43, 2011.

[3] Ballard, "Fuel Cell System Development for Freight Transport Applications," Ballard, August 2016. [Online]. Available: https://cdn2.hubspot.net/hubfs/2007428/LP%20and%20TY%20Pages/Fuel%20Cell%20System%20Development%20for%20Freight%20Transport%20Applications/ballard-fuel-cell-system-development-freight-transport-applications.pdf. [Accessed 4 1 2018].

[4] D. Gao, Z. Jin and Q. Lu, "Energy management strategy based on fuzzy logic for a fuel cell hybrid bus," *Journal of Power Sources,* vol. 185, pp. 311-317, 2008.

[5] M. Mahmoud, R. Garnett, R. Ferguson and P. Kanarouglou, "Electric buses: A review of alternative powertrains," *Renewable and Sustainable Energy,* vol. Reviews, no. 62, pp. 673-684, 2016.

[6] J. Halme, ”Sarjahybridijärjestelmän energiaväylän ohjaus,” Teknillinen Korkeakoulu, Espoo, 2008.

[7] J. Laurikko, M. Pihlatie, N.-O. Nylund, T. Halmeaho, S. Kukkonen, A. Lehtinen, V. Karvonen, R. Mäkinen and S. Ahtiainen, "Electric city bus and infrastructure demonstration environment in Espoo, Finland," Kintex, 2015.

[8] K. Erkkilä, N. Nils-Olof, A.-P. Pellikka, M. Kallio, S. Kallonen, S. Ojamo, S. Ruotsalainen, O. Pietikäinen and A. Lajunen, "eBUS - Electric bus test platform in Finland," Barcelona, 2013.

[9] H. U. o. Technology, “Polymer electrolyte membrane fuel cells,” [Online]. Available: http://tfy.tkk.fi/aes/AES/projects/renew/fuelcell/pem_index.html. [Accessed 28 October 2018].

[10] N. Karami, "Control of a Hybrid System Based PEMFC and Photovoltaic," Universite Aix-Marseille, Marseille, 2013.

[11] M. Kammerer, "International Hydrail Conference, HyPM Fuel Cell Power Modules & Systems," 18 June 2014. [Online]. Available: https://hydrail.appstate.edu/sites/hydrail.appstate.edu/files/9_Kammerer.pdf. [Accessed 31 January 2018].

[12] M. Kammerer, "Hydrogenics Maritime Workshop Presentation," 15 June 2017. [Online]. Available: http://www.fch.europa.eu/sites/default/files/5.%20Mark%20Kammerer%20-%20Hydrogenics_Maritime_Presentation.pdf. [Accessed 31 January 2018].

[13] Hydrogenics Corporation, "HyPM HD 16 Installation, Operation and Maintenance Manual, DOC. P/N: 1042947-01 rev 1 (generation 2 HyPM)," Hydrogenics Corporation, Ontario, 2014.

[14] M. Ragaju, J. van Rensburg, J. F. and H. C. Pienaar, "Full Bridge DC-DC converter as input stage for fuell cell based inverter system," in *Proceedings of SATNAC*, South Africa, 2012.

[15] Wikipedia, "CAN bus," Wikipedia, [Online]. Available: https://en.wikipedia.org/wiki/CAN_bus. [Accessed 31 January 2018].

[16] K. Park and K. Minkoo, “Advanced Bit Stuffing Mechanism for Reducing CAN Message Response Time,” in *Automation*, InTech, Dr. Florian Kongoli, 2012.

[17] Elektrobit Automotive GmbH, "Datasheet_EB61x0_en_screen.pdf," Elektrobit, Erlangen, 2010.

[18] B. Pitschak, "Hydrogenics Company Presentation," March 2016. [Online]. Available: https://www.now-gmbh.de/content/1-aktuelles/1-presse/20160310-wettbewerbsfaehige-zulieferindustrie/4_marktplatz-pitschak-hydrogenics.pdf. [Accessed 31 January 2018].

[19] M. Kammeree, Interviewee, *Email conversation between Sampsa Ranta and Mark Kammeree.* [Interview]. 17 December 2017.

[20] PRISMA ecotech GmbH, "DCI 12A2 DC-DC-Wandler 16kW Hardware-Dokumentation," PRISMA ecotech GmbH, Norsingen, 2017.

[21] Hydrogenics Corporation, "HyPM HD 16 16kW Hydrogen Fuel Cell Power Module Installation and Operation Manual, DOC. P/N: 1037316-01 (generation 1 HyPM)," Hydrogenics, Ontario, 2010.

[22] BASF, "Glysantin FC G 20-00/50 Technical Information," BASF, Ludwigshafen, 2016.

APPENDICES

Appendix 1. Mechanical structure 2D drawing

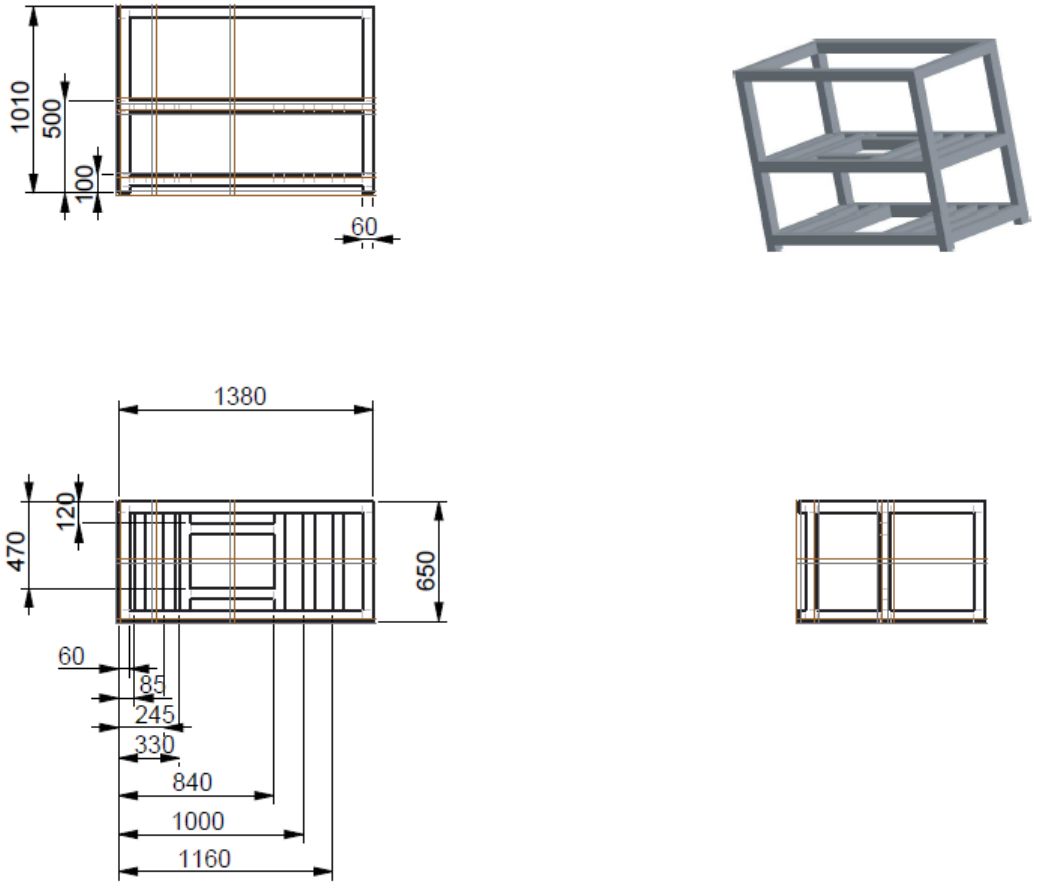

Figure 72. 2D drawing for FCREX structure

Appendix 2. Control cable for DC/DC converter

Cable	Connector pin	Name	Description	Connection to
1 orange	1	KL31	Supply ground	BANANA BLACK
1 white	4	KL30	Supply 18V..33V	BANANA RED
2 orange	2	KL15	Active / enable	BANANA RED via SAFETY STOP
2 white	5	Run	Run	BANANA RED via SAFETY STOP
3 orange	9	Bootstrap	Bootstrap	NC
3 white	-	NC	not connected	NC
4 orange	-	NC	not connected	NC
4 white	-	NC	not connected	NC
5 orange	13	RS232 GND	RS232 Ground	RS232 DE-9 pin 5
5 white	14	RS232 TX	RS232 Transmit	RS232 DE-9 pin 2
6 orange	13	RS232 GND	RS232 Ground	RS232 DE-9 pin 5
6 white	18	RS232 RX	RS232 Receive	RS232 DE-9 pin 3
7 orange	15	CAN H	CAN H	CAN DE-9 pin 7
7 white	16	CAN L	CAN L	CAN DE-9 pin 2
8 orange	17	CAN GND	CAN GND	CAN DE-9 pin 5
8 white	-	NC	not connected	NC
+ 0.5 wire	1	KL31	Supply ground	BANANA BLACK

Table 9. DCDC converter control signals in recommissioning test control box

Appendix 3. Control cable for FCPM

Connector J1

Connector pin	Name	Direction	Connection to	Notice
1	Do Not Use		NC	
2	ID Select 2	Input	NC	
3	ID Select 4	Input	NC	
4	CAN High	Bi-directional	CAN DE-9 pin 7	
5	CAN Low	Bi-directional	CAN DE-9 pin 2	
6	FCPM Enable	Input	BANANA RED	Phase 2 / Rewise connection
	E-stop		NC	6.6.7 Emergency Shutdown
7	Do Not Use		NC	
8	Signal Ground	Gnd	CAN DE-9 pin 5	
			BANANA BLACK	
9	Load Enable	Output		Phase 2 / To FCPM-DCDC contactors
10	ID Select 3	Input	NC	
11	ID Select 1	Input	NC	
12	Do Not Use		NC	
13	Do Not Use		NC	
14	Do Not Use		NC	
15	Do Not Use		NC	

Connector J2

Connector pin	Name	Direction	Connection to	Notice
1	Power	Power	BANANA RED	
2	Power	Power	BANANA RED	
3	Power ground	Gnd	BANANA BLACK	
4	Power ground	Gnd	BANANA BLACK	
5	Fan Control Signal	Output PWM 1kHz		Phase 3 / not implemented yet
6	Power	Power	BANANA RED	
7	Power	Power	BANANA RED	
8	Power ground	Gnd	BANANA BLACK	
9	Power ground	Gnd	BANANA BLACK	
10	Cooling Pump Enable	Output PWM 1kHz		Phase 2 / To cooling pump

Table 10. FCPM converter control signals in commissioning test control box

Appendix 4. Heat exchanger design calculation

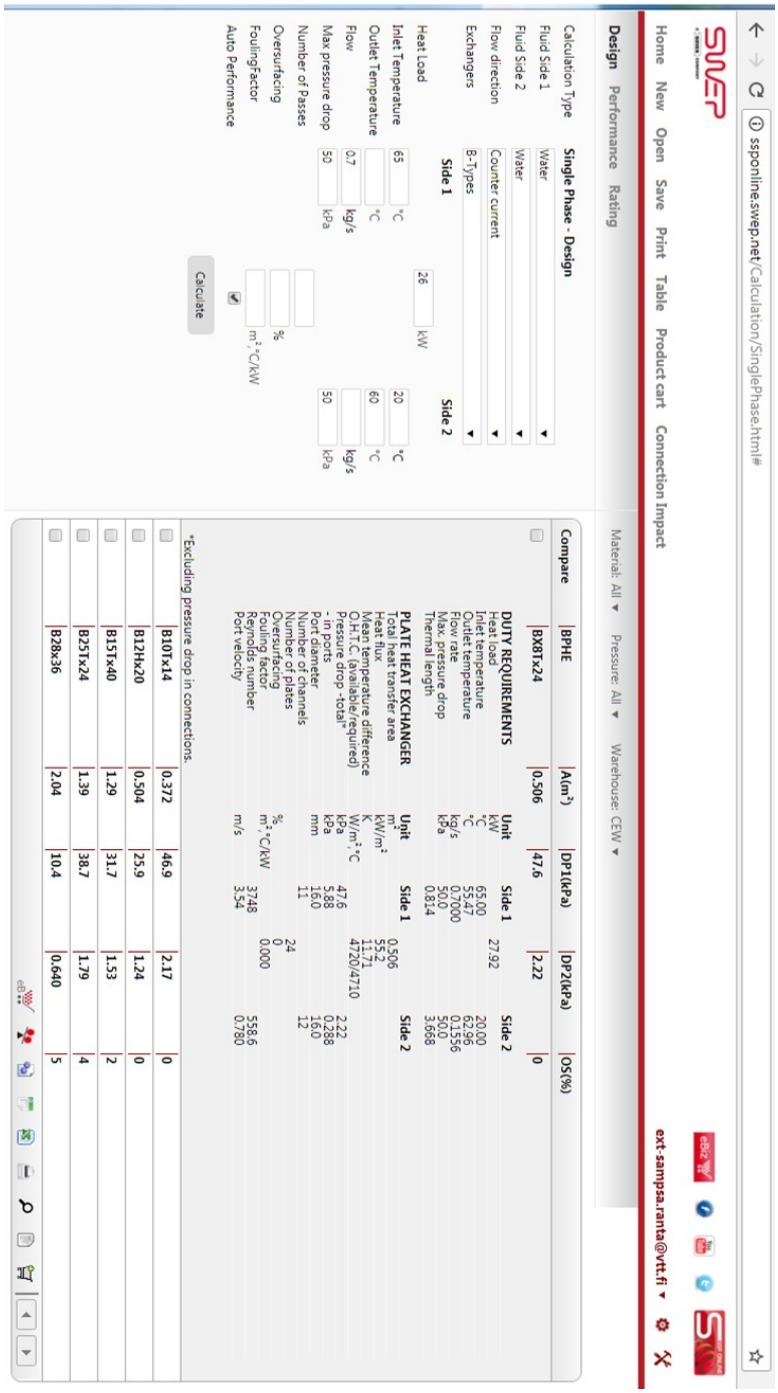

Figure 73. SWEP tool used for selecting heat exchanger

Appendix 5. PFISTERER 5-pole connector mounting instructions

Mounting introduction
PLUG P0 connector Nr. 350 208 -002 / -004 **PFISTERER**

To ensure a reliable function of the connector, the following assembly sequence should not be altered. Assembly alternatives: Instead of contact pins also contact sockets may be mounted. A mixed assembly is possible, too.
Caution! The sealing in the connector housing must match with the cable in order to achieve a protection grade of IP 67.

Step 1
Strip cable to 7mm

Step 2
Slide closing cap over all wires.

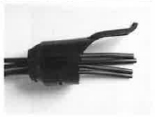

Step 3
Slide sealing over all wires.

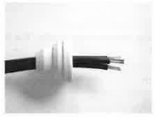

Step 4
Slide pressure disc over cables with small opening towards sealing. Large ring surface showing towards sealing side.

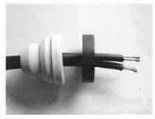

Step 5
Compress contacts.

Mounting introduction
PLUG P0 connector Nr. 350 208 -002 / -004 **PFISTERER**

Step 6
Push contact into the plastic insert until it locks. To insert the middle contact widen the plastic insert.

Step 7
Push plastic insert into the connector housing. The rib at the plastic insert has to go into the notch of the housing

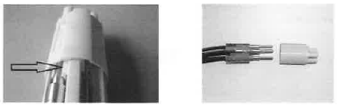

Step 8
Push contact housing into connector housing. The rib at the contact housing has to go into the notch of the connector housing.

Step 9
Slide pressure disc, sealing and closing cap onto the connector housing. The pin at the housing surface snaps into the hood. At last, attach the silicone sealing ring.

Mounting introduction
PLUG P0 connector Nr. 350 208 -002 / -004 **PFISTERER**

Technical Data – P0 Connectors

Mechanical Data

Flange housing	Thermoplastic Polyamid PA 46	Flammability UL 94 V-0
Connector housing	Thermoplastic Polyamid PBT fiber reinforced	Flammability UL 94 V-0
Contact housing	Thermoplastic Polyamid PA 46	Flammability UL 94 V-0
Contact material	Copper alloy	
Contact surface	Gold plated	
Mating cycles	> 500	
Sealing	NBR 70 Shore	
Temperature range	-40°C to +125°C	
Connecting method	Crimp	
IP protection	IP 67 acc. to DIN 40050 (locked)	
Cable diameter	5 – 12 mm (with sealing)	
Conductor cross section	Power 2mm contacts : 2,5 – 4,0mm²	

Electrical Data

Number of poles	5 + PE	
Number of contacts	6	
Pollution degree	2 (mated:3)	
Contact diameter (mm)	2	
Rated voltage	VDE: 250V/630V, AC	
	UL: 600V, AC	
	CSA 600 V, AC	
Test voltage	2,5 kV/6 kV, AC	
Rated current	VDE: 9/30A	
	UL: 30A	(2mm contacts 22A)
		(1mm contacts 10A)
	CSA 30A	(2mm contacts 22A)
		(1mm contacts 7.5A)
Through resistance (mOhm)	< 3	

PFISTERER Kontaktsysteme GmbH
Geschäftsbereich Komponenten / Business Unit Components
Industrial Product Management
Rosenstr. 44
D - 73650 Winterbach
Phone +49 7181 7005 301
Fax +49 7181 7005 333
dialog@pfisterer.de
www.pfisterer.de

Appendix 6. Results of PEM FCPM commissioning test

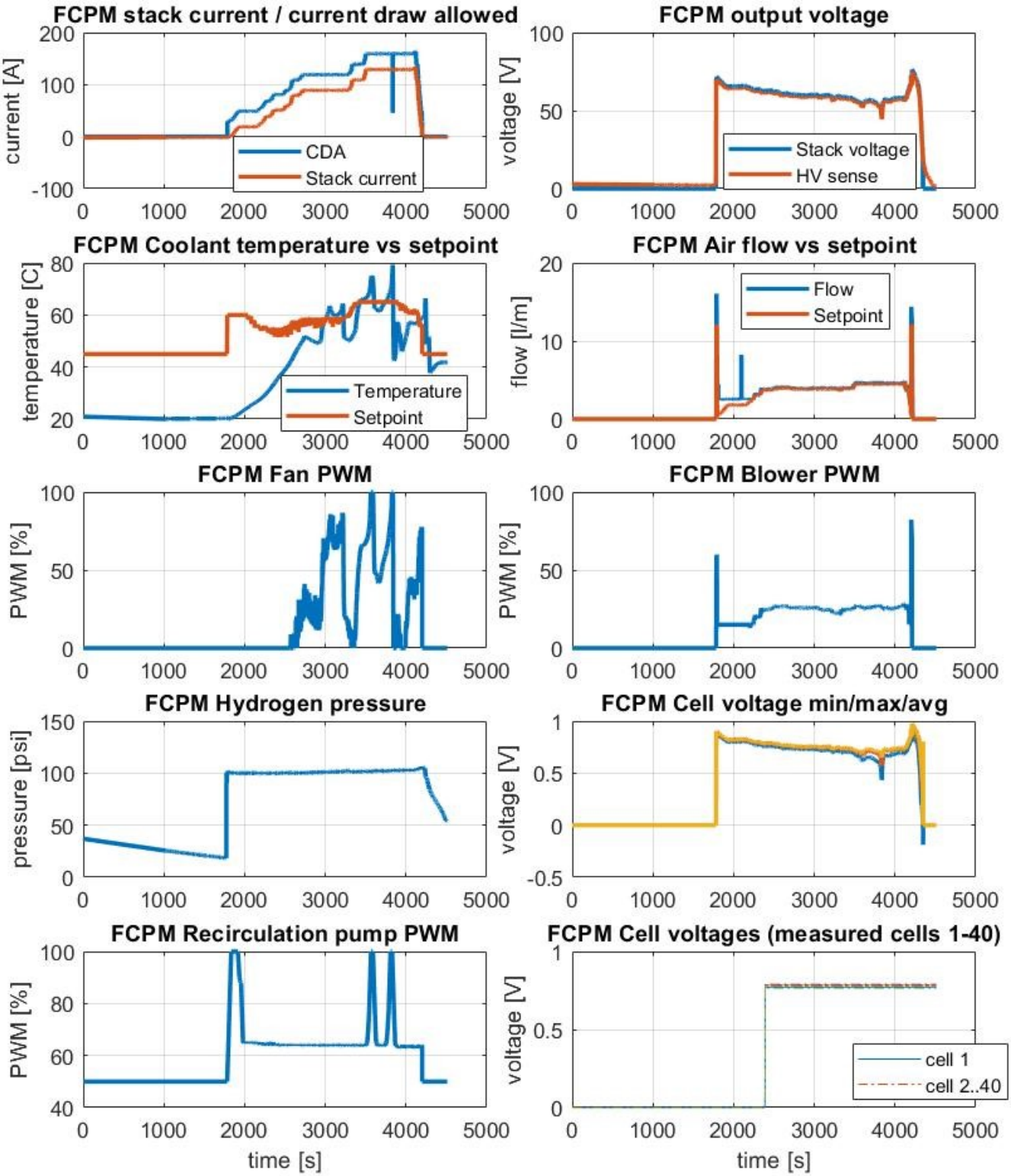

Figure 74. FCPM status data plotted, data gathered from HyPMview CSV log, 1 second logging interval

Appendix 7. PEM FCPM and DC/DC integration test results (Stove load)

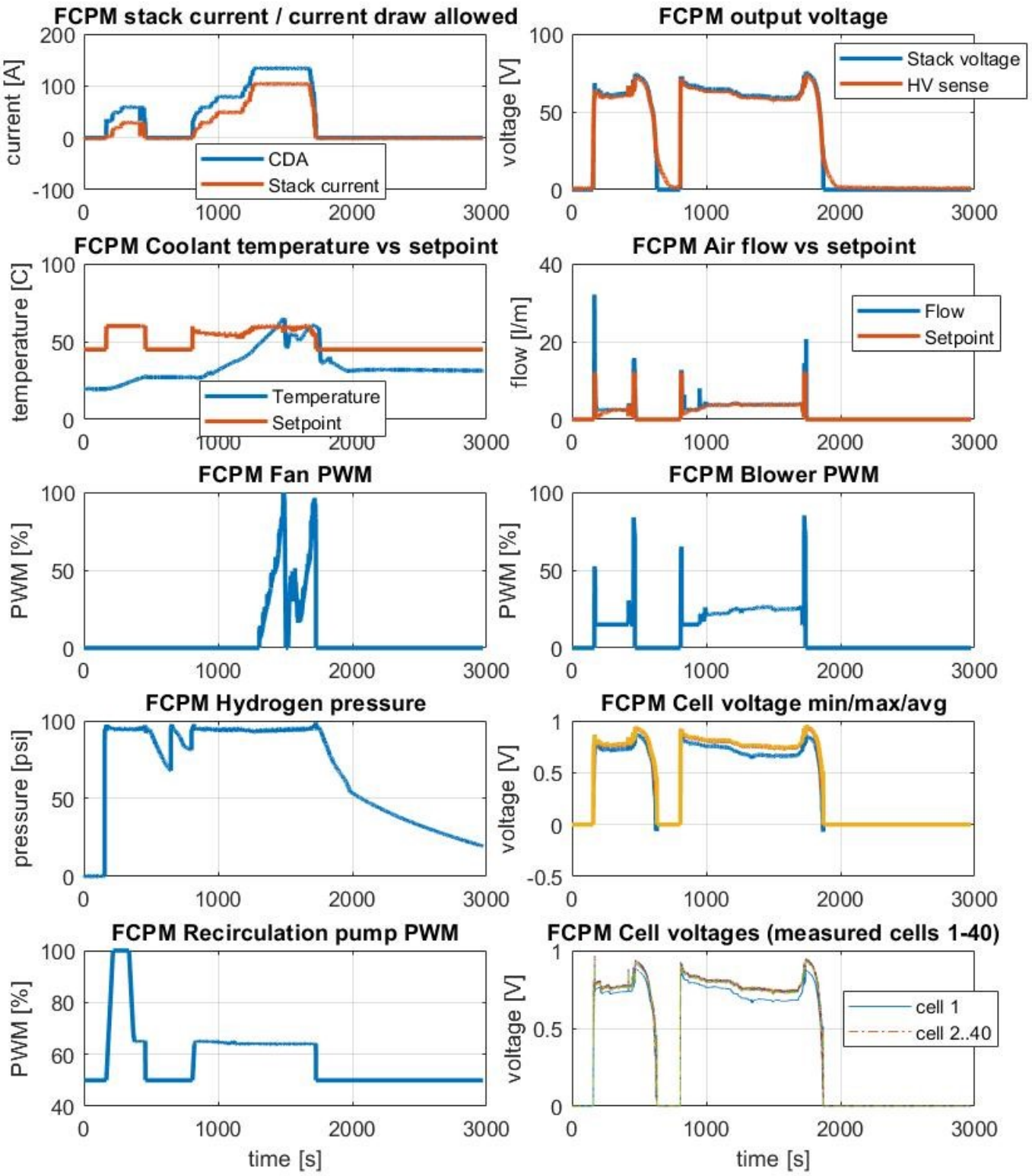

Figure 75. FCPM status data plotted, data gathered from HyPMview CSV log, 1 second logging interval

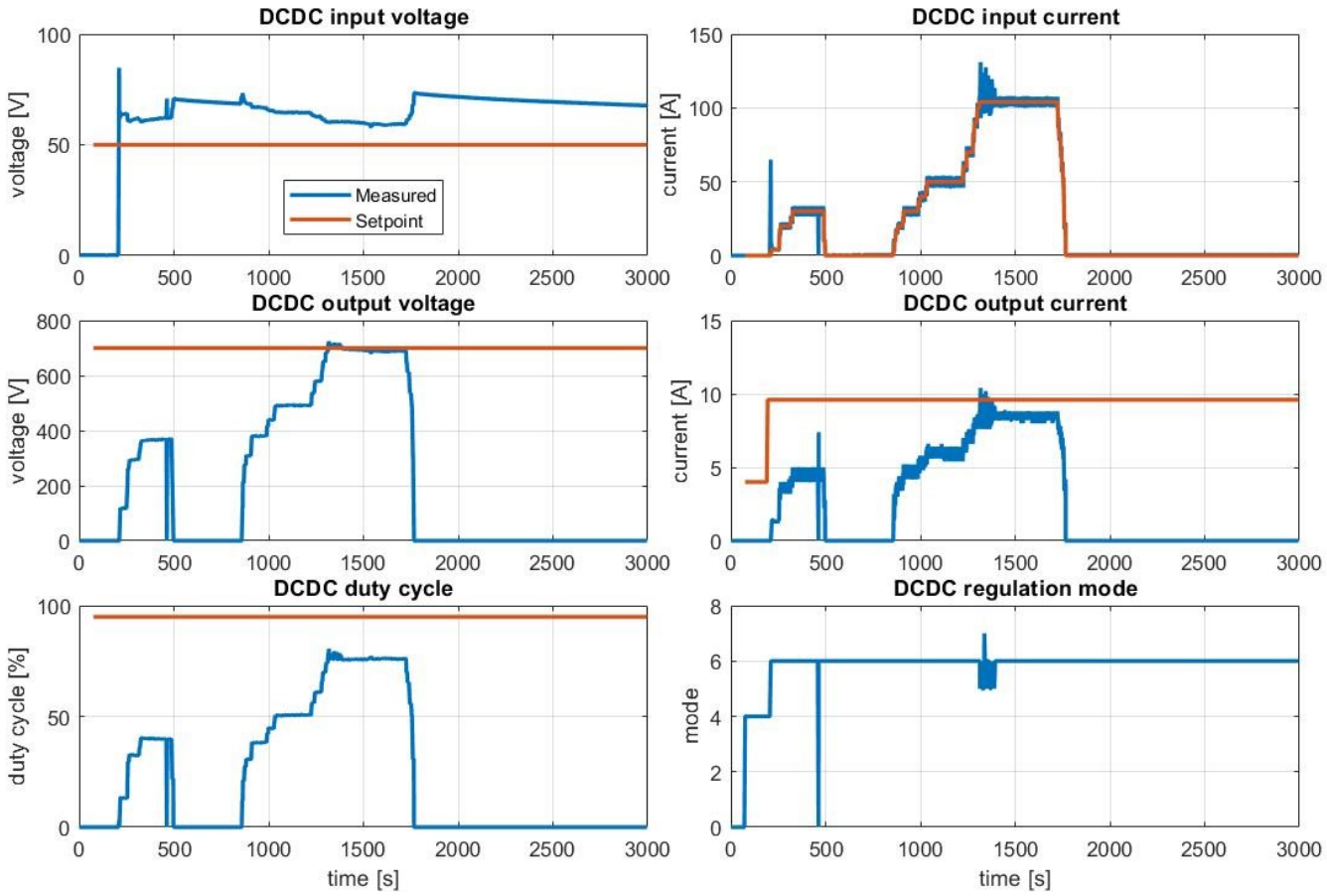

Figure 76. DCDC converter setpoints and measurements

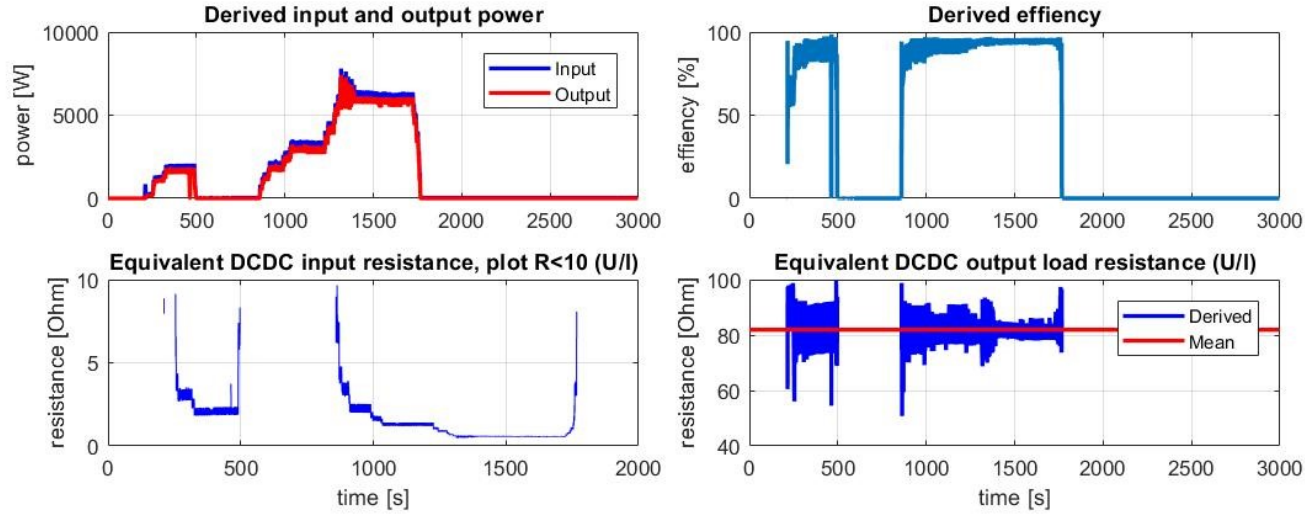

Figure 77. DCDC converter derived values: equivalent input and output load resistance, power and efficiency derived from measured values

Appendix 8. Range extender in bus, integration test results

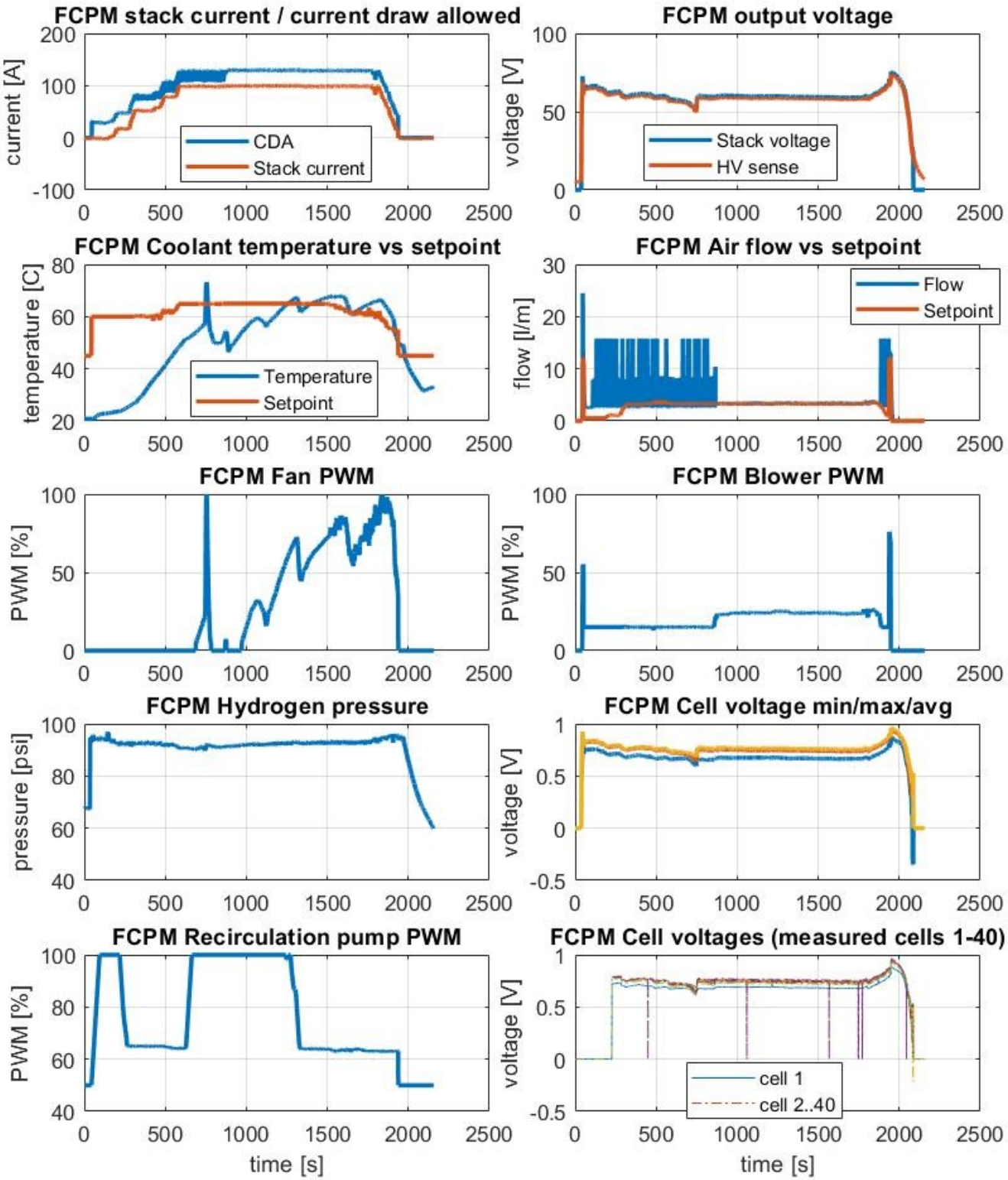

Figure 78. FCPM status data plotted, data gathered from HyPMview CSV log, 1 second logging interval

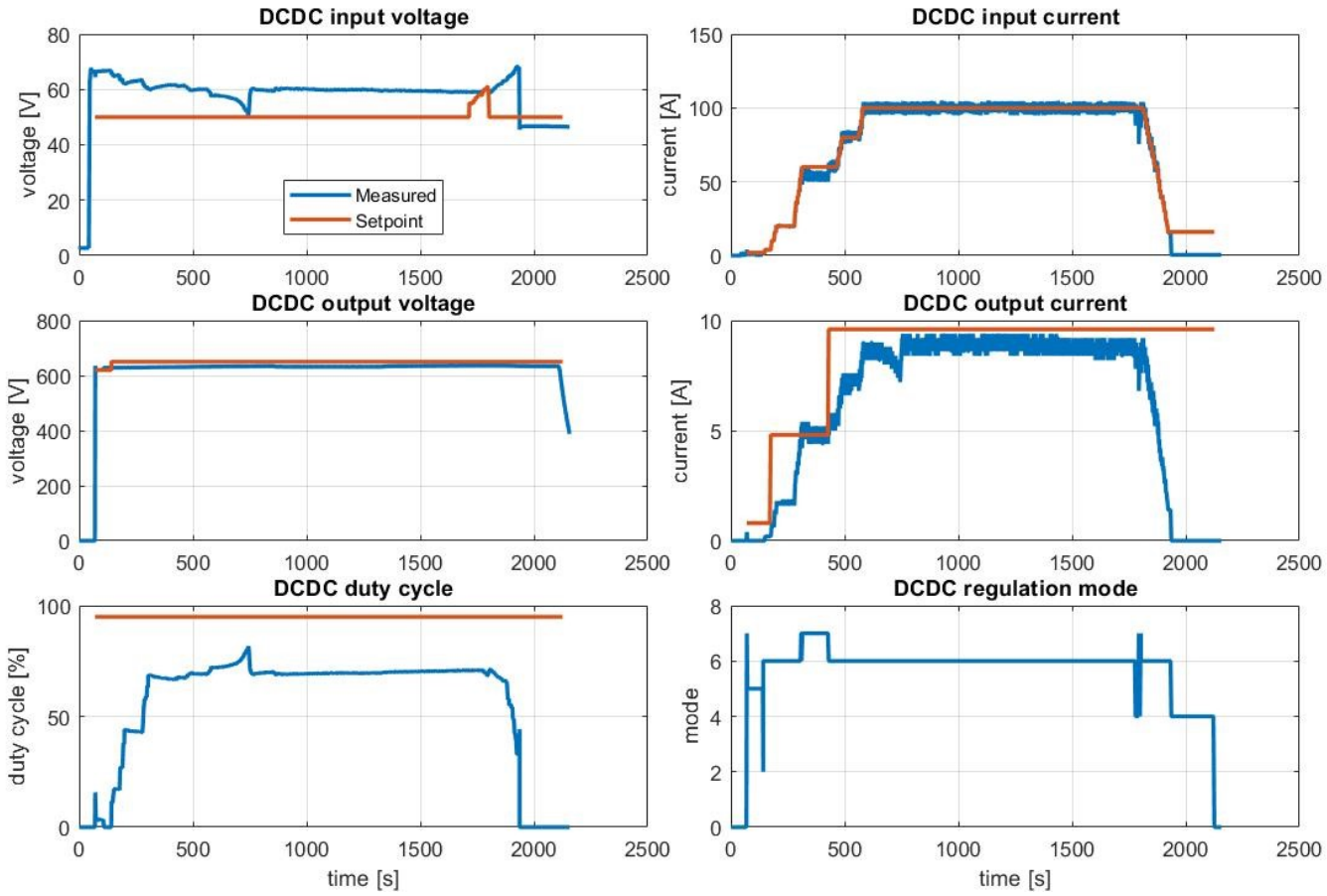

Figure 79. DCDC converter setpoints and measurements

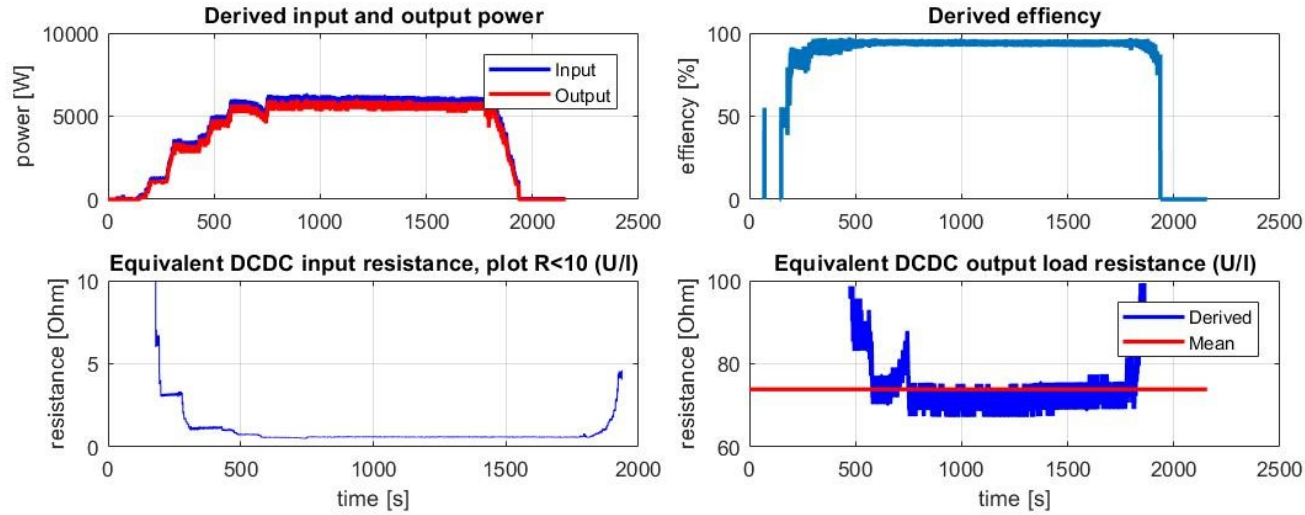

Figure 80. DCDC converter derived values: equivalent input and output load resistance, power and efficiency derived from measured values

Appendix 9. Range extender in bus, integration test results, rippel test attempt

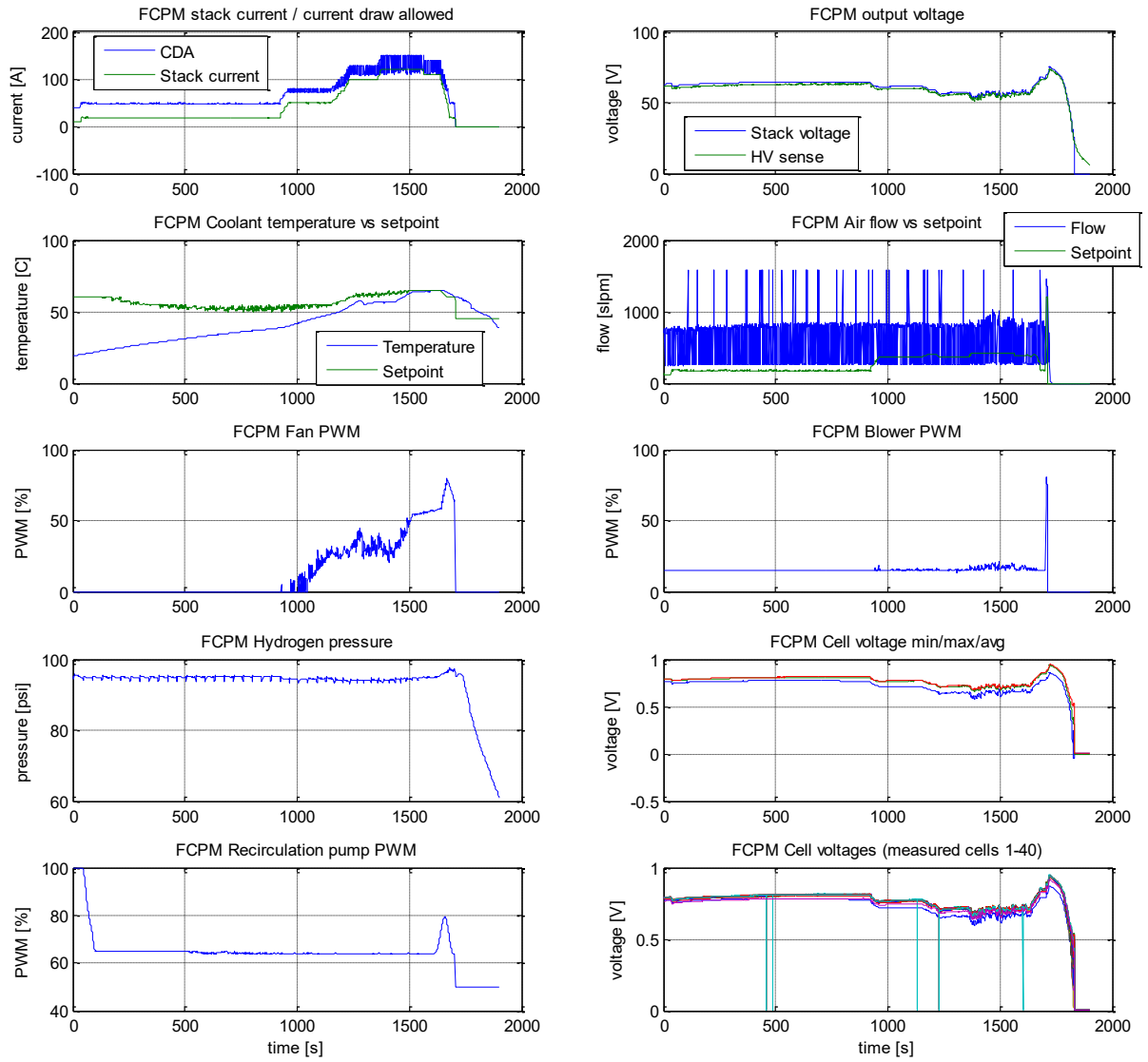

Figure 81. FCPM status data plotted, data gathered from HyPMview CSV log, 1 second logging interval

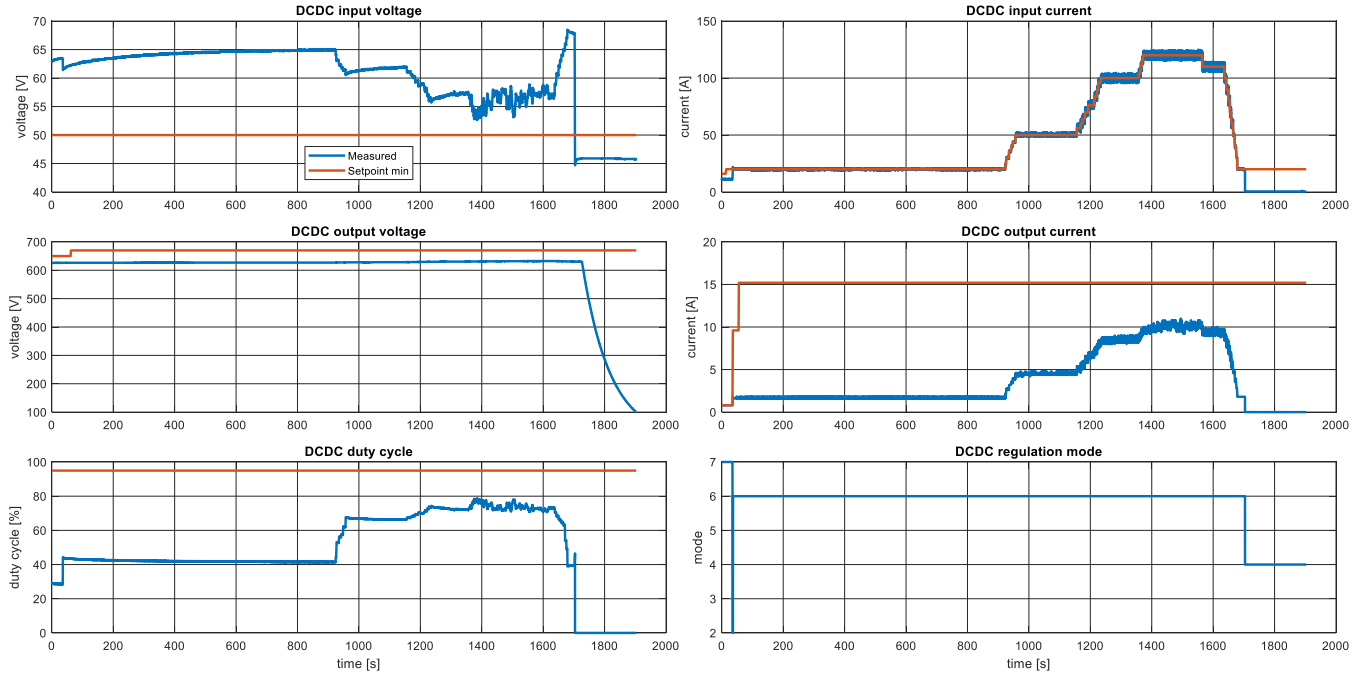

Figure 82. DCDC converter setpoints and measurements

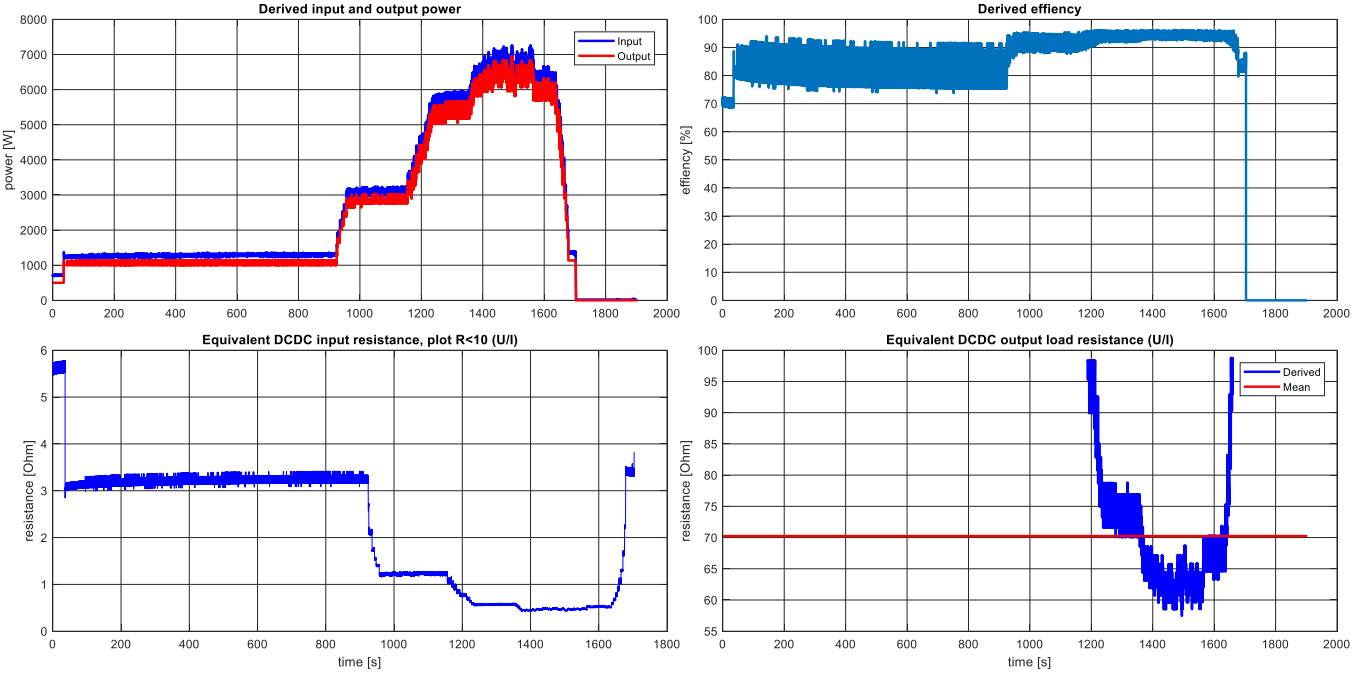

Figure 83. DCDC converter derived values: equivalent input and output load resistance, power and efficiency derived from measured values

Appendix 10. Matlab code for analyzing results

```
%% Stove test
clear all
close all
tic
[canlog,candata]=readcanoptimize('C:\data\CANtrace\LogFileFcDcdc.txt');
toc
tic
[istdata]=parseistoptimize(candata);
toc
tic
[solldata]=parsesolloptimize(candata);
toc
save('C:\data\CANtrace\LogFileFcDcdc.mat','canlog','candata','istdata','solldata')
plotdcdcistsoll

%% Bus integration
clear all
close all
tic
%[canlog,candata]=readcanoptimize('C:\data\CANtrace\LogFileFcpmDcdcBatteryFuse.txt');
[canlog,candata]=readcanoptimize('C:\data\HyPM\F508-HD16-80-1042847-170524-01-CAN-20170913-125736-
fcdcdcbusfuse.asc');
toc
tic
[istdata]=parseistoptimize(candata);
toc
tic
[solldata]=parsesolloptimize(candata);
toc
save('C:\data\CANtrace\BusFuse.mat','canlog','candata','istdata','solldata')
plotdcdcistsoll
%% DCDC precharge and power transfer start, trim dataset start 0s, length 115 seconds
close all
load('C:\data\CANtrace\BusFuse.mat')
x=istdata(1,1)
istdatay=istdata(istdata(:,1)>x,:);
istdata=istdatay(istdatay(:,1)<x+150,:);

solldatay=solldata(solldata(:,1)>x,:);
solldata=solldatay(solldatay(:,1)<x+150,:);
plotdcdcistsoll
%% CV mode test plot, trim dataset start 1700s, length 115 seconds
close all
load('C:\data\CANtrace\BusFuse.mat')
x=istdata(1,1)+1700
istdatay=istdata(istdata(:,1)>x,:);
istdata=istdatay(istdatay(:,1)<x+115,:);
solldatay=solldata(solldata(:,1)>x,:);
solldata=solldatay(solldatay(:,1)<x+115,:);
plotdcdcistsoll
%% Bus integration, rippel test run
clear all
close all
tic
[canlog,candata]=readcanoptimize('C:\data\CANtrace\F508-HD16-80-1042847-170524-01-CAN-20170915-131723-Log-
FileRippel.asc');
toc
tic
[istdata]=parseistoptimize(candata);
toc
tic
[solldata]=parsesolloptimize(candata);
toc
save('C:\data\CANtrace\LogFileFcpmDcdcBusRippel.mat','canlog','candata','istdata','solldata')
plotdcdcistsoll
```

Listing 3. Thesis data plots (thesisplot.m)

```
function [ medata,candata ] = readcanoptimize(lfilu)
%READCANTRACELOG Summary of this function goes here
%   Detailed explanation goes here


if ~exist('lfilu','var')
    % (isempty(lfilu))
    pathpattern='C:\data\CANtrace\*.txt';
    [filename, pathname] = uigetfile(pathpattern, 'Choose logfile');
    lfilu = strcat(pathname,filename);
end
fid = fopen(lfilu,'r');
% print the file name
lfilu
medata = textscan(fid, '%s' ,- 1 , 'delimiter' , '\n' );
fclose(fid);

howmanylines = size(medata{ 1 },1);

count=0;

logdata=medata{1};
alldata=size(logdata,1)
%data2=data(contains(data,{'Tx','Rx','RxErr'}),:);
logdatax=logdata(~contains(logdata,{'RxErr'}),:);
logdata2=logdatax(contains(logdatax,{'Tx','Rx'}),:);
count=size(logdata2,1);

count
candata=zeros(count,15);

for i = 1:count
        rowx = strsplit(logdata2{ i });
        % if(size(rowx,2) == 15)
        ts=double(sscanf(char(rowx(1)),'%f'));
        ch=double(sscanf(char(rowx(2)),'%d'));
        id=double(sscanf(char(rowx(3)),'%x'));
        dir=0;
        % double(sscanf(char(rowx(4)),'%d'));
        dlc=double(sscanf(char(rowx(5)),'%x'));
        len=double(sscanf(char(rowx(6)),'%d'));
        data1=double(sscanf(char(rowx(7)),'%x'));  %  Hex conversion
        data2=0;
        data3=0;
        data4=0;
        data5=0;
        data6=0;
        data7=0;
        data8=0;
        if(len > 1)
            data2=double(sscanf(char(rowx(8)),'%x'));  % Hex conversion
        end
        if(len > 2)
            data3=double(sscanf(char(rowx(9)),'%x'));  % Hex conversion
        end
        if(len > 3)
            data4=double(sscanf(char(rowx(10)),'%x'));  % Hex conversion
        end
        if(len > 4)
            data5=double(sscanf(char(rowx(11)),'%x'));  % Hex conversion
        end
        if(len > 5)
            data6=double(sscanf(char(rowx(12)),'%x'));  % Hex conversion
        end
        if(len > 6)
            data7=double(sscanf(char(rowx(13)),'%x'));  % Hex conversion
        end
        if(len > 7)
            data8=double(sscanf(char(rowx(14)),'%x'));  % Hex conversion
        end
        row=[ i, ts, ch, id, 0, dlc, len, data1, data2, data3, data4, data5, data6, data7, data8 ];
        candata(i,:)=row;
        if(mod(i,10000) == 0)
            % update progress
            i
        end
end
```

Listing 4. CAN log read function (canreadoptimize.m)

```
function [ mydata,data,header ] = readhypmcsvlog( )
%READCANTRACELOG Summary of this function goes here
%   Detailed explanation goes here

pathpattern='C:\data\HyPM\*.CSV';
[filename, pathname] = uigetfile(pathpattern, 'Choose logfile');

lfilu = strcat(pathname,filename);
fid = fopen(lfilu,'r');
% print the file name
lfilu
mydata = textscan(fid, '%s' ,- 1 , 'delimiter' , '\n' );
fclose(fid);

howmanylines = size(mydata{ 1 },1);

count=0;
header = textscan(mydata{ 1 }{ 1 }, '%s' ,- 1 , 'delimiter' , ',' );

% numofcolumns=size(header{ 1 },1)
numofcolumns=93
data=zeros(howmanylines-1,numofcolumns);

%for i = 2:howmanylines
for i = 2:howmanylines
    rowx=mydata{ 1 }{ i };
    row=zeros(1,numofcolumns);
    % 2017/9/6
12:10:24.7,Standby,-,0.0000,1.0000,2.0000,11.0000,89665.3984,15.1205,1.0000,0.0000,0.0000,0.0000,0.0000,0.
0000,-
0.9000,0.0000,0.0000,20.9000,45.0000,0.0000,0.0000,3.0000,37.1000,0.0000,0.0000,0.0000,50.0000,0.0000,0.00
00,0.0000,0.0000,23.8000,5.0000,0.0000,0.0000,0.0000,0.0000,0.0000,0.0000,0.0000,0.0000,0.0000,0.0000,0.00
00,0.0000,3292.0000,0.0000,0.0010,0.0000,0.0010,0.0000,0.0000,,
    C = textscan(rowx,'%s','delimiter',',');
    row(1)=datenum(C{1}{1});
    state=-1;
    if(strcmp(C{1}{2},'Standby'))
        state=1;
    elseif (strcmp(C{1}{2},'Run'))
        state=2;
    end
    row(2)=state;
    for j=4:size(C{1},1)
        val=sscanf(C{1}{j},'%f');
        if(~isempty(val))
          row(j)=val;
        end
    end
    %size(row)
    %size(data)
    data(i-1,:)=row(1,:);
end
```

Listing 5. HyPM log read function (readhypmcvslog.m)

```
figure('units','normalized','outerposition',[0 0 1 1])
dz=istdata(1,1);
t=(istdata(:,1)-dz);
ts=(solldata(:,1)-dz);
subplot_tight(3,1,1,.05)
plot(t,istdata(:,4:8))
grid on
subplot_tight(3,1,2,0.05)
plot(t,istdata(:,4).*istdata(:,6),'b','linewidth', 2)
hold
plot(t,istdata(:,5).*istdata(:,7),'r','linewidth', 2)
grid on
subplot_tight(3,1,3,.05)
powera=istdata(:,4).*istdata(:,6);
powerb=istdata(:,5).*istdata(:,7);
powerc=powerb./powera;
% Data sanitation
powerc(powerc>1)=NaN;
plot(t,powerc,'linewidth', 2)
grid on

figure('units','normalized','outerposition',[0 0 1 1])
subplot_tight(3,2,1,[0.07 0.04])
plot(t,istdata(:,4),ts, solldata(:,3),'linewidth', 2)
title('DCDC input voltage');
ylabel('voltage [V]')
legend('Measured','Setpoint min','Location','South');
grid on
subplot_tight(3,2,2,[0.07 0.04])
plot(t,istdata(:,6),ts, solldata(:,5),'linewidth', 2)
title('DCDC input current');
ylabel('current [A]')
%legend('Measured','Setpoint max');
grid on
subplot_tight(3,2,3,[0.07 0.04])
plot(t,istdata(:,5),ts, solldata(:,4),'linewidth', 2)
title('DCDC output voltage');
%legend('Measured','Setpoint max');
ylabel('voltage [V]')
grid on
subplot_tight(3,2,4,[0.07 0.04])
plot(t,istdata(:,7),ts, solldata(:,6),'linewidth', 2)
title('DCDC output current');
%legend('Measured','Setpoint max');
ylabel('current [A]')
grid on
subplot_tight(3,2,5,[0.07 0.04])
plot(t,istdata(:,8),ts, solldata(:,7),'linewidth', 2)
title('DCDC duty cycle');
ylabel('duty cycle [%]');
xlabel('time [s]');
%legend('Measured','Setpoint max');
grid on
subplot_tight(3,2,6,[0.07 0.04])
plot(t,istdata(:,3),'linewidth', 2)
title('DCDC regulation mode');
ylabel('mode')
xlabel('time [s]')
%legend('Measured','Setpoint max');
grid on

figure('units','normalized','outerposition',[0 0 1 1])
subplot_tight(2,2,1,[0.07 0.04])
plot(t,istdata(:,4).*istdata(:,6),'b',t,istdata(:,5).*istdata(:,7),'r','linewidth', 2)
% hold
% plot()
grid on
title('Derived input and output power');
legend('Input','Output');
ylabel('power [W]');

subplot_tight(2,2,2,[0.07 0.04])
powera=istdata(:,4).*istdata(:,6);
powerb=istdata(:,5).*istdata(:,7);
powerc=powerb./powera;
% Data sanitation
powerc(powerc>1)=NaN;
plot(t,powerc*100,'linewidth', 2)
title('Derived effiency');
ylabel('effiency [%]');
```

```
grid on
subplot_tight(2,2,3,[0.07 0.04])
%plot(istdata(:,1),istdata(:,4).*istdata(:,6),'b')
%hold
%plot(istdata(:,1),istdata(:,5).*istdata(:,7),'r')
r=istdata(:,4)./istdata(:,6);
% Data sanitation
r(r>10)=NaN;
r2=r;
% Data sanitation
r2(isnan(r2))=[];
r2(isinf(r2))=[];
%rmean=mean(r2);
plot(t,r,'b')
title('Equivalent DCDC input resistance, plot R<10 (U/I)');
ylabel('resistance [Ohm]')
%legend('Derived','Mean');
grid on
xlabel('time [s]')
subplot_tight(2,2,4,[0.07 0.04])
%plot(istdata(:,1),istdata(:,4).*istdata(:,6),'b')
%hold
%plot(istdata(:,1),istdata(:,5).*istdata(:,7),'r')
r=istdata(:,5)./istdata(:,7);
% Data sanitation
r(r<50)=NaN;
r(r>100)=NaN;
r2=r;
% Data sanitation
r2(isnan(r2))=[];
r2(isinf(r2))=[];
rmean=mean(r2);
plot(t,r,'b',t,ones(size(istdata,1),1)*rmean,'r','linewidth', 2)
title('Equivalent DCDC output load resistance (U/I)');
ylabel('resistance [Ohm]')
legend('Derived','Mean');
grid on
xlabel('time [s]')
```

Listing 6. DCDC converter data plot code (plotdcdcistsoll.m)

```
figure
% Normalize time series to seconds from start
dz=data(1,1);
t=(data(:,1)-dz)*60*60*24;
subplot(5,2,1)
%
plot(t,data(:,15:16))
grid on
title('FCPM stack current / current draw allowed');
ylabel('current [A]')
legend('CDA','Stack current');
subplot(5,2,2)
%
plot(t,data(:,17),t,data(:,23))
grid on
title('FCPM output voltage');
ylabel('voltage [V]')
legend('Stack voltage','HV sense');
subplot(5,2,3)
plot(t,data(:,54:93))
axis([min(data(:,1)) max(data(:,1)) 0.60 0.97])
grid on
title('FCPM Cell voltage on different cells');
ylabel('voltage [V]')
grid on
subplot(5,2,3)
plot(t,data(:,19:20));
grid on
title('FCPM Coolant temperature vs setpoint');
ylabel('temperature [C]')
legend('Temperature','Setpoint');
grid on
subplot(5,2,4)
plot(t,data(:,21:22))
title('FCPM Air flow vs setpoint');
legend('Flow','Setpoint');
ylabel('flow [slpm]')
grid on
subplot(5,2,5)
plot(t,data(:,25))
title('FCPM Fan PWM');
ylabel('PWM [%]');
grid on
subplot(5,2,6)
plot(t,data(:,27))
title('FCPM Blower PWM');
ylabel('PWM [%]');
grid on
subplot(5,2,7)
plot(t,data(:,24))
title('FCPM Hydrogen pressure');
ylabel('pressure [psi]')
grid on
subplot(5,2,8)
plot(t,data(:,49:51))
title('FCPM Cell voltage min/max/avg');
ylabel('voltage [V]')
grid on
subplot(5,2,9)
plot(t,data(:,28))
title('FCPM Recirculation pump PWM');
ylabel('PWM [%]');
xlabel('time [s]')
grid on
subplot(5,2,10)
plot(t,data(:,54:93))
xlabel('time [s]')
ylabel('voltage [V]')
title('FCPM Cell voltages (measured cells 1-40)');
grid on
```

Listing 7. FCPM data plot code (plotfcpm.m)